CANADIAN THESES

THÈSES CANADIENNES

NOTICE

The quality of this microfiche is heavily dependent upon the quality of the original thesis submitted for microfilming. Every effort has been made to ensure the highest quality of reproduction possible.

If pages are missing, contact the university which granted the degree.

Some pages may have indistinct print especially if the original pages were typed with a poor typewriter ribbon or if the university sent us an inferior photocopy.

Previously copyrighted materials (journal articles, published tests, etc.) are not filmed.

Reproduction in full or in part of this film is governed by the Canadian Copyright Act, R.S.C. 1970, c. C-30.

AVIS

La qualité de cette microfiche dépend grandement de la qualité de la thèse soumise au microfilmage. Nous avons tout fait pour assurer une qualité supérieure de reproduction.

S'il manque des pages, veuillez communiquer avec l'université qui a conféré le grade.

La qualité d'impression de certaines pages peut laisser à désirer, surtout si les pages originales ont été dactylographiées à l'aide d'un ruban usé ou si l'université nous a fait parvenir une photocopie de qualité inférieure.

Les documents qui font déjà l'objet d'un droit d'auteur (articles de revue, examens publiés, etc.) ne sont pas microfilmés.

La reproduction, même partielle, de ce microfilm est soumise à la Loi canadienne sur le droit d'auteur, SRC 1970, c. C-30.

THIS DISSERTATION HAS BEEN MICROFILMED EXACTLY AS RECEIVED

LA THÈSE A ÉTÉ MICROFILMÉE TELLE QUE NOUS L'AVONS REÇUE

KINETICS AND MECHANISM OF INHIBITION OF *RABBIT MUSCLE* PHOSPHOGLUCOMUTASE BY VANADATE ION

by

Kevin Doherty

B.Sc., Essex University, 1982

THESIS SUBMITTED IN PARTIAL FULFILLMENT OF

THE REQUIREMENTS FOR THE DEGREE OF

MASTER OF SCIENCE

in the Department

of

Chemistry

SIMON FRASER UNIVERSITY

APRIL, 1987

ISBN 0-315-36246-4

APPROVAL

Name: Kevin Doherty

Degree: MASTER OF SCIENCE

Title of thesis: Kinetics and Mechanism of Inhibition of *Rabbit Muscle* Phosphoglucomutase by Vanadate Ion

Examining Committee:

Chairman: Dr. F. W. B. Einstein

Dr. M. J. Gresser
Senior Supervisor

Dr. B. M. Hicks

Dr. E. C. Pearce

Dr. A. J. Davison
Internal Examiner, Department of Kinesiology
Simon Fraser University

Date Approved: April 16th, 1987

PARTIAL COPYRIGHT LICENSE

I hereby grant to Simon Fraser University the right to lend my thesis, project or extended essay (the title of which is shown below) to users of the Simon Fraser University Library, and to make partial or single copies only for such users or in response to a request from the library of any other university, or other educational institution, on its own behalf or for one of its users. I further agree that permission for multiple copying of this work for scholarly purposes may be granted by me or the Dean of Graduate Studies. It is understood that copying or publication of this work for financial gain shall not be allowed without my written permission.

Title of Thesis/Project/Extended Essay

[illegible]

Author: [illegible]
(signature)

[illegible]
(name)

April 16th 1984
(date)

ABSTRACT

The inhibition of *Rabbit muscle* phosphoglucomutase (E.C. .2.7.5.1.) by inorganic vanadate was investigated. It has been concluded that two mechanisms of competitive inhibition occur; a rapid inhibition due to free, non-esterified vanadate and a much slower, time dependent inhibition due to a tight binding glucose 1-phosphate 6-vanadate mixed diester, both inhibitors binding to the free dephosphorylated enzyme. From the analysis of steady state kinetic data, two values of K_i were obtained for the two competitive (vs. glucose-diphosphate) inhibitors. Free vanadate had a value K_v = 36.0 ±4.9 x 10^{-6} M and glucose 1-phosphate 6-vanadate was found to have a value K_{vp} = 2.7 ±0.4 x 10^{-11} M. The results of presteady-state studies were interpreted in terms of the rate limiting binding of the mixed diester to the free dephosphorylated form of the enzyme, competitive with glucose diphosphate. In the presence of inhibitor the approach to steady-state followed first order kinetics. The observed first order rate constant increased with inhibitor concentration to a limiting value. These observations were interpreted in terms of a change in rate-limiting step from binding of inhibitor to free dephosphorylated enzyme, to formation of free dephosphorylated enzyme by dissociation of the intermediate glucose 1,6-diphosphate. In terms of this model, glucose 1,6-diphosphate was found to dissociate from the enzyme once in every 1.3 x 10^4 catalytic turnovers.

Added glucose was found to enhance the competitive inhibition due to vanadate, and this behavior was attributed to binding of glucose 6-vanadate to the free dephosphorylated enzyme, with an inhibition constant K_{gv} = 3.9 ±0.4 x 10^{-9} M. An additional noncompetitive (vs. glucose-diphosphate) inhibition was found to occur, which was rationalized in terms of binding of glucose 6-vanadate to the phosphoform of the enzyme with a value for the inhibition constant K_{gv*} = 2.4 ±0.3 x 10^{-9} M. The generation of tightly bound mixed diester on the dephosphoenzyme as product of the reaction of glucose 6-vanadate with the phosphoform of phosphoglucomutase was the rational used to account for the observed noncompetitive inhibition.

DEDICATION

To my dear Mother and Father, Dale, Sandra and Mr. Adrian P. Harris.

QUOTATION

"Thought is not a trick, or a game, or a series of dodges,
Thought is a man in his wholeness wholly attending."

D. H. Lawrence

ACKNOWLEDGMENTS

I would like to thank Dr. Michael J. Gresser for the opportunity to have been a member of his laboratory group. Thanks also are due to Dr. S. Beharry and Dr. P. Stankiewicz for the friendship that has grown from our work and many discussions together. Last but not least Marcia M. Craig for her kindness and consideration. I shall remember you all, always.

TABLE OF CONTENTS

LIST OF TABLES

LIST OF FIGURES

INTRODUCTION

Vanadium has been proposed as an essential element required in trace amounts for the normal function of living organisms (1,2,3). Typically vanadium compounds present in living tissue fall in the micromolar range of concentration; e.g.: 0.34 μM in blood plasma, 0.52 μM in erythrocytes, 0.3–1.0 μM in rabbit and equine muscle (1). Whether vanadium performs an essential chemical role or not is debatable. Nevertheless, the use of vanadium compounds as therapeutic agents in the treatment of chronic disease and the toxic effects linked to occupational exposure (tempering of steel) (1) must be consequences of some fundamental effect on cellular activity that represents an expression of the chemical properties of this first series transition metal.

The availability on vanadium of low lying partially filled 3d orbitals confers on the metal centre the capacity to extend its covalency through the use of appropriate hybrid orbitals (4,5). This property is enhanced by the larger covalent radii and intrinsically weaker nature of the bonds formed to vanadium relative to phosphorus, the result of vanadium having higher energy valence orbitals. Usually V–O bond lengths fall in the range of 0.3–0.7 angstroms greater than the corresponding bonds on phosphorus and sulphur which similarly can utilize their vacant higher lying 3d orbitals (4,6,7). Molecules containing longer bonds are more susceptible to the close approach of groups on other molecules capable of donating lone pair electron density and are inherently activated towards cleavage in exchange reactions. The properties of vanadium described above are also shared by phosphorus and sulphur and form the chemical basis for the physiological role of these two third period elements in group transfer reactions. For this reason vanadium should also be suited for interaction at this same level in living systems.

The physiologically relevant oxidation states of vanadium are +4 and +5 (also +3) represented by their thermally stable oxides with electronic configurations of $3d^1$ and $3d^0$ respectively (5). The presence of this single d electron accounts for quite a significant difference in the aqueous behavior of these two oxidation states. At low pH vanadium (V) is a relatively strong oxidizing agent. Solutions at higher

pH, however, are characterized by more stable covalent species which are better able to express the electrophilic properties of vanadium. Mononuclear tetrahedral vanadates, VO_4^{3-} predominate (8) at concentrations of vanadium < 10^{-4} M, over the pH range 13.0 down to approximately 3.0, protonated as dictated by the pK of the basic sites on the anion (pK, 3.4, pK, 8.3, pK, 13.0), corresponding values for phosphoric acid are pK, 2.6, pK, 7.2, pK, 12.0 (9). Hence the forms of vanadate appearing at physiological pH in aqueous solution (7.0–8.0) will be the mono and dibasic species $H_2VO_4^-$ and HVO_4^{2-}, which are structurally similar to the forms of phosphate present in this interval. In aqueous solution at lower pH the electrophilic behavior of vanadium will be seen in the reactions of the more stable vanadyl (IV) oxide. However, vanadyl tends to hydrate above pH 3.0, followed by dimerization and eventually, owing to the low solubility of its hydroxide $VO(OH)_2$ (K_{sp} = 1.08 x 10^{-22} M^3), precipitation from solution occurs at around pH 5.0. At physiological pH vanadyl species are very susceptible to air oxidation. Because of its aqueous behavior vanadyl might not be expected to form a significant contribution to the physiological effects ascribed to vanadium present in living tissue.

Evidence obtained from electron spin resonance studies shows, however, that vanadium (IV) exists in living cells (10). The accumulation of vanadate by erythrocytes and yeast cells, when followed by e.s.r., shows up as the characteristic spectrum of the paramagnetic VO^{2+} (vanadyl) species (11,12,13). Intracellular reducing agents, such as glutathione in erythrocytes, have been identified as being responsible for vanadate reduction. Conditions in the cytoplasm may be sufficiently reducing for the vanadyl product of such redox behavior to be stabilized with respect to oxidation. The low solubility of $VO(OH)_2$ will be offset by the tendency of vanadyl to complex with intermediary metabolites and proteins, e.g., ATP and haemoglobin (11,14). Although these results point to vanadyl being the only form of vanadium oxide in living tissue, evidence exists to show that vanadate is also active. Vanadate in incubation media has been shown to gain access more readily to erythrocytes and yeast cells (13) than vanadyl, which shows an initial lag in the rate of its cellular association followed by a more rapid phase of uptake (15). It

has been suggested that this initial lag seen for vanadyl uptake by erythrocytes is linked to a slow phase of oxidation in the blood plasma to the more membrane permeable vanadate species. The anionic transport mechanism of yeast plasma membrane exhibits Km values for vanadyl and vanadate of 1.0 x 10^{-3} M and 0.3 x 10^{-3} M respectively (13), showing the selective uptake of these anions. It is considered that dissolved oxygen at a partial pressure of 40 mmHg, may be sufficient to oxidize vanadyl faster than its tendency to complex with transferrin and other agents; eg., serum albumin of the blood plasma (15). From *in vivo* studies with canine blood it has been found that injection of ^{48}V labelled vanadate or vanadyl both eventually give rise to a similar cell/plasma ratio of vanadium distribution, that remains constant despite removal of vanadium from the blood through excretion (15). The sensitivity of this ratio to changes in plasma vanadium levels could be the result of an equilibrium distribution of vanadate across the erythrocyte membrane. The erythrocyte transmembrane ion pump the Na^+–K^+ ATPase, which is strongly inhibited by vanadate (K_i of 40 μM) (1) but not vanadyl, was found to have an *in vivo* activity that represents 1/100th of its isolated activity. The lower intracellular activity of the Na^+–K^+ ATPase may be a consequence of intracellular vanadate being present (2,11). Hence it is possible that vanadium oxides of both oxidation states can be present together in living tissue.

Some of the physiological effects that have been ascribed to the presence of vanadium include its behavior as a diuretic and natriuretic, enhanced contractile ability of heart muscular tissue and increased blood oxygen tensions (1). A common feature of these effects is that the processes concerned either directly or indirectly are linked to the activity of proteins that catalyze phosphoryl group transfer, where in some instances the protein becomes phosphorylated in an intermediate step.

Vanadate has been shown *in vitro* studies to behave electrophilically, readily accepting lone pair electron density from hydroxyl groups on molecules to form labile vanadate esters. The oxidation of glucose by β-$NADP^+$, catalyzed by glucose 6-phosphate dehydrogenase, is activated in the presence of vanadate. This effect was rationalized in terms of a labile vanadate ester of glucose serving as a better

substrate than the non phosphorylated molecule (16). The rate constant for the formation of glucose 6-vanadate as the activating complex was estimated (16) to be 35.0 M^{-1} s^{-1} (cf. values of 9 x 10^{-11} and 1 x 10^{-6} M^{-1} s^{-1}, for glucose 6-phosphate and glucose 6-arsenate formation respectively (17,18)). ^{51}V NMR studies have also yielded an estimate for the value of the pseudo first order rate constant for ethyl vanadate hydrolysis of 1.21 x 10^{3} s^{-1} (19). This value far exceeds those observed for glucose 6-phosphate and glucose 6-arsenate hydrolysis, which are 10^{-1} and 10^{-4} s^{-1} respectively (17,18). Earlier studies had shown that arsenate like vanadate, could also form esters capable of acting as substrates in the phosphoglucomutase reaction (18). Vanadate has also been found to activate transfer of ^{32}P from labeled phosphoglucomutase to glucose (20). Hence vanadate esters are formed rapidly enough to serve as substrates of enzymes that catalyse the reactions of the analagous phosphate esters. The most pronounced effects of vanadate, however, from *in vitro* studies, occur at enzymes catalyzing phosphoryl transfer reactions that involve a phosphoprotein intermediate (21,22,23). Vanadate when present at only micromolar concentration is a very potent competitive inhibitor of such enzymes; e.g., of phosphoglucomutase (human erythrocyte) K_i = 1.0 μM, and of phosphoglycerate mutuase (human erythrocyte) K_i = 2.5 μM (21). Interference in a phosphoryl transfer step to a specific active site residue could be what confers upon these enzymes their sensitivity to the presence of vanadate and/or vanadate esters. The readiness with which vanadate esters form and hydrolyse (16,19) (cf. corresponding phosphate or arsenate esters), is the result of a lower free energy of activation for these reactions. This would favor the attainment of the pentacoordinate, trigonal bipyramidal geometry that characterizes the transition state of a phosphoryl transfer step to the enzyme (24). Perhaps in this way low concentrations of vanadate ester analogues arising at micromolar levels of free vanadate could mimic the normal phosphate ester substrates. The vanadate ester, which may be a factor of 10^{6} lower in concentration than the substrate, is able to act competitively by virtue of being stabilized as a transition state analogue at the enzyme active site.

To test the hypothesis, the mechanism of vanadate inhibition of *Rabbit muscle* phosphoglucomutase was investigated in this study.

EXPERIMENTAL PROCEDURES

Reagents used and the preparation of stock solutions

Concentrated stock solutions of the reagents were prepared in 20mM Tris-Cl⁻ (Sigma, reagent grade) buffer pH 7.6. Appropriately sized aliquots of these stocks were then used to generate the desired final assay concentration. The reagent stock solutions used and the commercial source of the reagents were as follows: 0.1M $MgCl_2 \cdot 6H_2O$ (Anachem, reagent grade), 12mM β-$NADP^+$ (Boehringer-Mannheim), 27mM EDTA (Fischer Scientific Co.), 2.9mM α-D-glucose 1,6 diphosphate (Boehringer-Mannheim), 5.3mM α-D-glucose 1-phosphate (essentially free of α-D-glucose diphosphate, Sigma, grade V), 0.13M D-glucose (Sigma, reagent grade), sodium orthovanadate ($Na_3VO_4 \cdot 10H_2O$, Fischer Scientific Co.). Since the hydration number of sodium vanadate was not known, the formula weight had to be determined from the absorbance at 260nm of a dilute solution of sodium vanadate at pH 10.5. The predominant form of vanadate present at pH 10.5 is the dianion HVO_4^{2-} with a molar extinction coefficient of 3.55×10^3 $M^{-1}cm^{-1}$ (28). Care was taken in preparing vanadate stock solutions not to make them to acidic thereby avoiding the formation of decavanadate, which hydrolyses slowly at neutral pH and is detected as a yellow colouration in solution. The concentrations of vanadate stock solutions used were: 0.5mM (in 20mM Tris-Cl⁻ pH 7.6) in the steady-state kinetic studies and 10mM (in 20mM Tris-Cl⁻ pH 7.6) for the progress curve studies. Careful attention was paid to the pH of all the reagent stock solutions, which were corrected to pH 7.6 using a combination of acidic (pH 3.0) and basic (pH 11.0) solutions of 20mM Tris-Cl⁻. The volume of these solutions at the correct pH was then adjusted with Tris-Cl⁻ buffer pH 7.6 using a volumetric flask to the desired final concentration.

Enzyme Preparation

Phosphoglucomutase (Boehringer-Mannheim, from rabbit muscle, 200 Umg^{-1} at 25°C, pH 7.5, 10mg ml^{-1} suspended in $(NH_4)_2SO_4$) and D-Glucose 6-phosphate dehydrogenase (Boehringer-Mannheim, from bakers yeast 350 Umg^{-1} at 25°C pH 7.5, 15mg $3ml^{-1}$ suspended in $(NH_4)_2SO_4$) were the enzymes used in this study.

Concentrated stock solutions of the enzymes were prepared by centrifuging the commercial ammonium sulphate suspension at 15000 r.p.m. for 15 minutes. After this period the ammonium sulphate supernatent was removed using a fine capilliary tube, being careful not to disturb the protein pellet. The pellet was then dissolved in Tris-Cl^- buffer (20mM pH 7.6). The concentrated stock enzyme solutions were used without further purification and always diluted prior to use in the kinetic assays. The approximate dilution factor of the pellet in the reaction mixture was 10^4, this enables an estimate of the $(NH_4)_2SO_4$ concentration in the reaction mixture to be obtained of 0.3 mM. The protein concentration of the enzyme solutions was determined using the method of Lowry et.al.(29).

Rate Measurement

The phosphoglucomutase reaction was followed in the thermodynamically favourable direction, i.e., α-D-glucose 1-phosphate (A) --> α-D-glucose 6-phosphate (C), by coupling the appearence of the mutase product to the activity of D-glucose 6-phosphate dehydrogenase. Rates were measured spectrophotometrically at 340 nm by monitoring the increase in absorbance due to β-NADPH appearing as product of the coupled reaction, using the extinction coefficient at this wavelength of 6.23×10^3 $M^{-1}cm^{-1}$ for NADPH. All measurements were carried out on a Varian spectrophotometer, Model 634, equipped with a thermostated sample compartment set at 25°C. All reagent stock solutions were temperature equilibriated to 25°C using a temperature regulated water bath, prior to their use. For standard initial velocity measurements the enzyme was assayed in a total volume of 1.0 ml containing appropriate concentrations of substrates and inhibitor in 20mM Tris-Cl^- buffer, pH 7.6. The enzyme assay was generally initiated by the addition of substrate, usually α-D-glucose 1-phosphate to a preincubation mixture of the enzyme and the remaining reagents. Progress curves that showed the time course of vanadate inhibition were obtained by initiating the reaction with substrate, glucose 1-phosphate, followed by the addition of vanadate.

The details of pH, temperature and reagent concentrations used in the individual experiments of this study and the special considerations that apply to the

design of certain experiments, including the analysis of data, are described throughout the text of the Results and Discussion section of this thesis and listed in the relevant figure legends.

Statistical analysis of data

In order to obtain a statistical analysis of double reciprocal plots a weighted least squares treatment was carried out. In this treatment an error of ±5% was assumed in velocity (v) measurements and error bars were calculated based on the upper and lower limits of reciprocal velocity (1/v). The slope and intercept values were obtained from a least squares analysis, the standard deviation of the slopes and intercepts was calculated using the upper and lower limits of uncertainty in each data point. For non-weighted data a least squares line was calculated for all the data points from which the values of the slope, intercept and standard deviation could be calculated. Also an additional 'N' least squares lines were calculated containing (N-1) data points, this generated a family of 'N' least squares lines of 'N' different slopes and 'N' different intercepts which were used to calculate a mean value and standard deviation for all the values of slope and intercept. Where insufficient data points were collected to apply a meaningful statistical analysis a standard deviation of at least ±50% was assumed for the parameter being determined.

RESULTS AND DISCUSSION

Preliminaries

Phosphoglucomutase, Mwt.62000, catalyses the interconversion of α-D-glucose 1-phosphate and α-D-glucose 6-phosphate (Keq of 17.2 at 25°C, pH 7.0 in the presence of 25 mM Mg^{2+}) (25) *via* an intermolecular mechanism involving a phosphorylated enzyme intermediate. That such a pathway operates is suggested by the results of equilibrium isotope exchange studies (26) and experiments using chiral phosphate esters (27). As a consequence of this transfer reaction, the enzyme exists in both phosphorylated and dephosphorylated forms on the reaction pathway. The added requirement that glucose diphosphate, as the intermediate of this transfer reaction from active phosphoenzyme to bound glucose monophosphate (25,30), be present in catalytic quantities suggests that the free dephosphoenzyme can appear off the reaction pathway, though this is considered to be an infrequent event (30,31).

Figure 1 shows the model proposed to account for the kinetics of the phosphoglucomutase reaction in the absence of inhibitors. In this scheme the active phosphoenzyme represented by (EP) reacts with the glucose monophosphates (A and C) but not with glucose 1,6-diphosphate (B). The reverse situation applies to the reaction of the catalytically inactive free dephosphoenzyme (E). The free dephosphoenzyme (E) and glucose 1,6-diphosphate (B) are not considered obligatory intermediates of this reaction path. Their infrequent dissociation (30,31), however, is responsible for the pattern of parallel line double reciprocal plots seen for phosphoglucomutase and characteristic of a Ping-Pong mechanism. A Ping-Pong mechanism is defined as one in which a product is released between binding of two substrates (32), in the model of Figure 1 free glucose 1,6-diphosphate (B) is considered as a first product and second substrate of the reaction. Using the "King-Altman method" (32) a rate equation was derived for the model in Figure 1

Figure 1

Kinetic model describing the Ping-Pong mechanism of *Rabbit Muscle* Phosphoglucomutase in the absence of inhibitors. The k's denote specific rate constants of the steps in the mechanism. In the model, E = free dephosphoenzyme (inactive), B = glucose diphosphate, C = glucose 6-phosphate, A = glucose 1-phosphate, EB = complex of dephosphoenzyme with glucose diphosphate, EP = free phosphoenzyme (active), EPA, EPC = complexes of the phosphoenzyme with A and C (defined above) respectively.

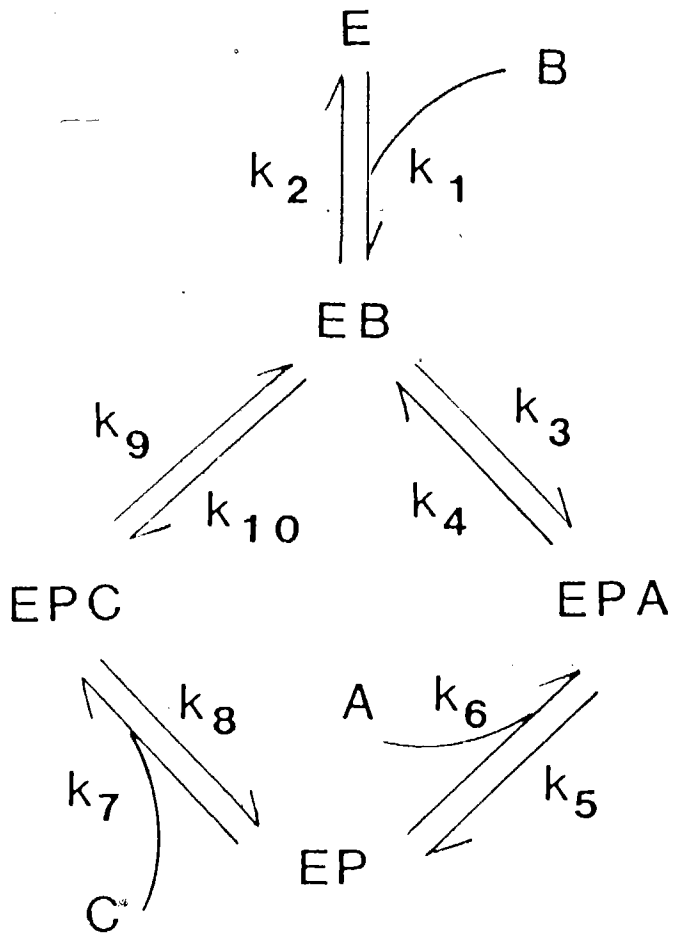
E
B
k_2
k_1
EB
k_9
k_{10}
k_3
k_4
EPC
EPA
k_8
A
k_6
k_7
k_5
C
EP

(see Appendix I) that accounts for the kinetics of the phosphoglucomutase reaction. The rate equation predicted by the model in the form of the double reciprocal (Lineweaver-Burke) plot is as follows:

$$1/v = Kmb/Vm \cdot 1/[B] + (\beta + Kma/[A]) \cdot 1/Vm \qquad \text{Eq. 1}$$

where:

v = initial velocity

Vm = maximum velocity

[B] = concentration of glucose 1,6-diphosphate

[A] = concentration of glucose 1-phosphate

Kmb = Michaelis constant of glucose 1,6-diphosphate for the free dephosphoenzyme (E)

Kma = Michaelis constant of glucose 1-phosphate for the active, phosphoenzyme (EP)

The equation as written above is appropriate for the conditions under which the kinetic assays of this study were conducted, namely with glucose 1,6-diphosphate (B) serving as the varied substrate and glucose 1-phosphate (A) held at different, constant concentrations. A plot of 1/v against 1/[B] is predicted to have a constant slope of Kmb/Vm and a vertical intercept of $1/Vm\ (\beta + Kma/[A])$, that would change with the concentration of glucose 1-phosphate used in the assay.

Figure 2 shows the parallel line pattern of double reciprocal plots obtained at three different glucose 1-phosphate concentrations. Analysis of the experiment of Figure 2 in terms of Equation 1 allows the kinetic parameters of the mutase reaction to be determined. These are listed in Table I. The values recorded are greater than those reported in the literature, eg, the Km values of glucose 1-phosphate and glucose 1,6-diphosphate are reported at 5×10^{-6} M and 4×10^{-6} M respectively in the presence of 0.4 mM Mg^{2+} ion at pH 7.4 and 30°C (33). A possible explanation could be the formation of inactive magnesium complexes of the substrates at the $MgCl_2$ concentration used in the assays of this

Figure 2

Parallel line pattern of plots showing reciprocal rate against reciprocal glucose-diphosphate concentration observed for the uninhibited phosphoglucomutase reaction and characteristic of a Ping-Pong mechanism. The double reciprocal plots were obtained at three concentrations of glucose 1-phosphate: 25 μM (●), 50 μM (▲) and 125 μM (■), over the indicated range of glucose-diphosphate concentration. Experimental conditions are listed in footnote b of Table I.

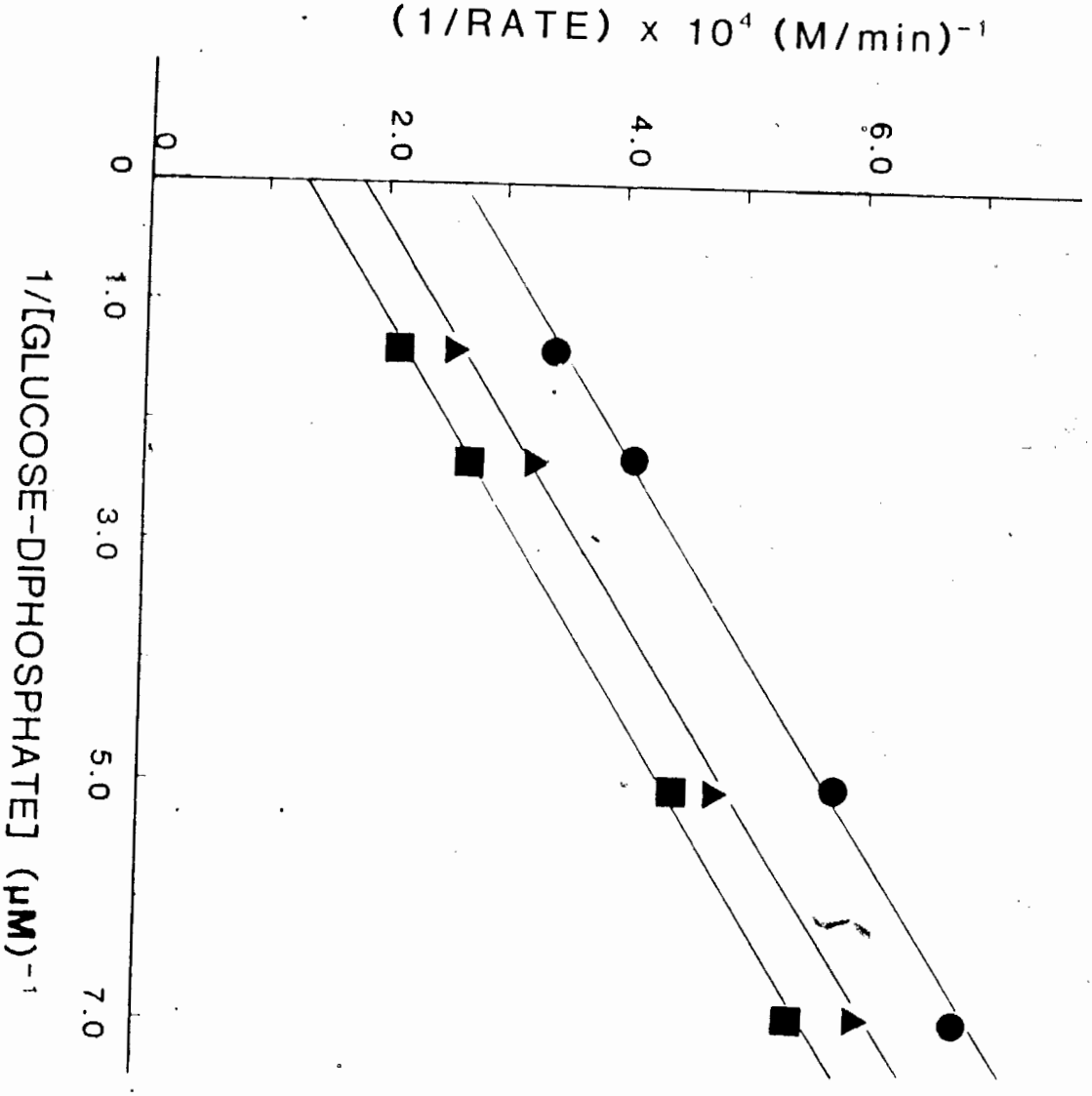
(1/RATE) x 10⁴ (M/min)⁻¹
0
2.0
4.0
6.0
0
1.0
3.0
5.0
7.0
1/[GLUCOSE-DIPHOSPHATE] (μM)⁻¹

study (2mM), plus the effects of the anions Cl^- and SO_4^{2-} as competitive inhibitors of substrate binding. However, since conditions in the assays generally, and especially in Mg^{2+} ion concentration, were kept constant throughout this work, the analysis of vanadate inhibition of phosphoglucomutase was not complicated by taking into account the above effects which were assumed to be constant.

TABLE I: Km values for the phosphoglucomutase reaction, determined for the experimental conditions used in this study:

SUBSTRATE	Km (M)
α-D-glucose 1,6-diphosphate	70 ± 3.3 x 10^{-4}
α-D-glucose 1-phosphate	35 ± 1.5 x 10^{-4}

a. α-D-glucose 1-phosphate is a competitive inhibitor with respect to glucose diphosphate binding at the free dephosphoenzyme having a K_i = 4.5 ± 0.3 x 10^{-3} M. The conditions used in the experiment to determine the K_i of glucose 1-phosphate were the same as those described in footnote b of this table except that the range of glucose 1-phosphate concentrations considered were: 2.6 mM, 10 mM and 15 mM. The K_i value was determined from the negative horizontal intercept of a replot of slope of the 1/v against 1/[B] plots against glucose 1-phosphate concentration.

b. Reactions contained: 0.05 U phosphoglucomutase, 0.27 U glucose 6-phosphate dehydrogenase, 2 mM $MgCl_2$, 0.8 mM EDTA, 0.48 mM β-$NADP^+$, 20 mM Tris-Cl buffer pH 7.6 at 25°C in a total volume of 1.0 ml. Double reciprocal plots were obtained at fixed concentrations of glucose 1-phosphate of 25 μM, 50 μM and 125 μM over a range of glucose diphosphate concentration spanning 0.73 μM to 0.06 μM.

c. kcat = 1.5 ±0.2 x 10^{1} s^{-1}, determined for a V_{max} of 420 x 10^{-4} M/mgmin, with phosphoglucomutase (Mwt.62000) present at 2.7 x 10^{-4}mg/ml

Vanadate Inhibition of Phosphoglucomutase

The time dependent nature of the inhibition

Figure 3 shows the effect of different pre-incubation conditions on the time course of vanadate inhibition of phosphoglucomutase. The experiment was carried out under the conditions listed in the figure legend, with glucose 1-phosphate present in the assay at 530μM concentration.

Trace a represents the uninhibited mutase reaction initiated after 3 minutes pre-incubation at 25°C in the absence of vanadate with glucose 1-phosphate. In trace b the enzyme was added to a pre-incubation mixture of all the reactants except glucose 1-phosphate and vanadate. After a period of incubation the same as in a above, the reaction was initiated with glucose 1-phosphate, but this time was followed by the rapid addition of 4μl of a vanadate stock solution to give a final assay concentration of 40μM. Under these conditions the complete time course of vanadate inhibition of the enzyme, represented by the progress curve of Trace b can be visualized. Two distinct regions can be seen in this progress curve that correspond to different time separated components of vanadate inhibition. The first is a rapid inhibition by vanadate of the initial velocity which is seen not to be identical to that of the uninhibited reaction in Trace a. The second is a much slower inhibition that is responsible for the gradual decrease in the initial velocity and the establishment of a final steady state rate which is less than that observed in the absence of vanadate (16% of the uninhibited rate).

Trace c is the result of pre-incubating the enzyme in the presence of glucose 1-phosphate and vanadate for 2 minutes at 25°C in the presence of all the reactants except glucose-diphosphate which was used to initiate the reaction. Under these conditions the mutase rate started initially close to zero and then increased over a short period of time until an inhibited rate similar to that in the progress curve of trace b was reached. This result is consistent with the hypothesis that the onset of the slower time dependent vanadate inhibition occurs more rapidly in the absence of glucose-diphosphate, and that the site of the inhibition is the free dephosphoenzyme (E). In the progress curve of trace b glucose-diphosphate present

Figure 3

The time dependent nature of vanadate inhibition of phosphoglucomutase in the presence of high glucose 1-phosphate concentration. Reactions contained: 0.02 U phosphoglucomutase, 0.12 U glucose 6-phosphate dehydrogenase, 20 mM Tris-Cl at pH 7.6, 2 mM $MgCl_2$, 0.8 mM EDTA, 0.48 mM $NADP^+$, 0.53 mM glucose 1-phosphate, 0.2 μM glucose 1,6-diphosphate and 40 μM vanadate for b) and c) in a total assay volume of 1.0 ml at 25°C.

a. The reaction in the absence of vanadate was initiated after 3 minutes incubation by adding glucose 1-phosphate.

b. Vanadate 4μl, was added rapidly to the already initiated mutase reaction.

c. All the reactants with the exception of glucose-diphosphate were incubated for 2 minutes at 25°C, after which the reaction was initiated by adding the diphosphate to a final concentration of 0.2μM in the assay.

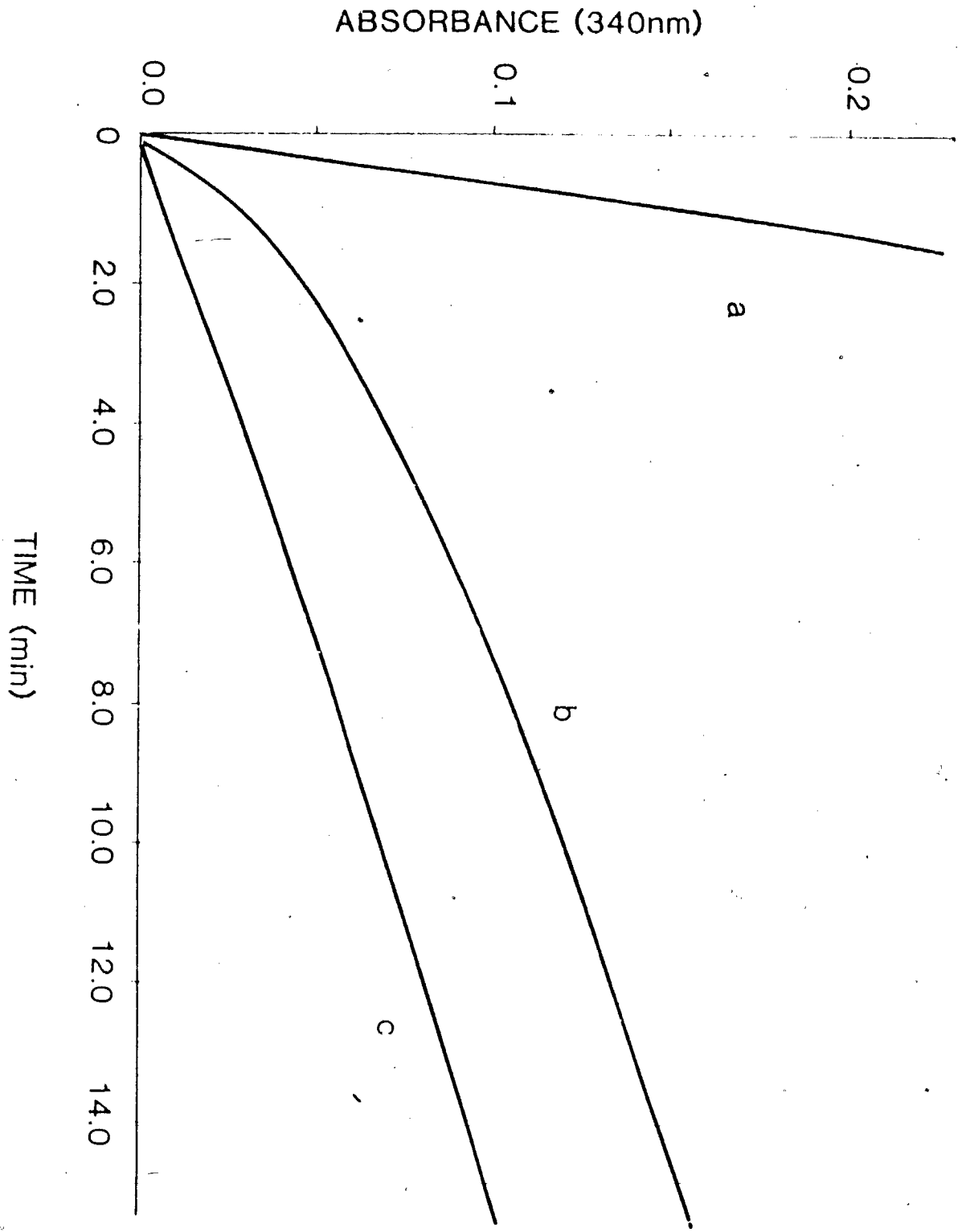
ABSORBANCE (340nm)
0.0
0.1
0.2
0
2.0
4.0
6.0
8.0
10.0
12.0
14.0
TIME (min)
a
b
c

competes with the slow vanadate inhibition, and is responsible in part for the time dependent behavior seen. It is also relevant to note that in the absence of glucose-diphosphate the enzyme present in its stable active phosphoform is capable of turning over glucose 1-phosphate albeit at a much reduced rate (30). The significance of this point will be appreciated later.

To date, all published studies of vanadate interaction with phosphoglucomutase have employed the same pre-incubation conditions used to generate trace c in Figure 3 (21,22,35). Clearly the above results show that under such conditions the complete time course of the inhibition would not be seen, so an accurate description of the inhibition mechanism would be difficult to obtain.

Analysis of the pre-steady state interval of the inhibition

The pre-steady state interval in the progress curve of trace b in Figure 3, is the time period following the initiation of the enzyme reaction and prior to the attainment of the inhibited steady state rate, during which the enzyme activity is seen to decrease with time. This was only observed when vanadate was added after the reaction had been initiated with glucose 1-phosphate.

The conditions in the assays used to generate progress curve data were such as to avoid effects arising from substrate depletion and product accumulation (36,37). Glucose 1-phosphate was kept at saturating concentration of at least 530μM. Substrate depletion was always observed to be less than 15% of this value for instance, over the range of glucose-diphosphate and at the vanadate concentrations used in the experiment of Figure 5. Even at 20% depletion of substrate of the above concentration, glucose 1-phosphate would be present at 10^5 times the concentration of total enzyme typically used or 12 times the Km value under these conditions. $NADP^+$ as cofactor of the coupling dehydrogenase was also kept at saturating concentrations to avoid effects arising from its depletion. Product of the mutase reaction was trapped by the coupling enzyme, glucose 6-phosphate dehydrogenase, so that product accumulation did not present a problem. Another important consideration is that of inhibitor depletion by the

enzyme. Vanadate is used at concentrations in the assays of at least 20μM (total inhibitor concentration greater than that of total enzyme present). However this may not be the concentration of the actual inhibitor. A small apparent first order rate constant for the reaction of a low concentration of an inhibitor capable of binding tightly to the dephosphoenzyme could cause the slow onset of inhibition seen. If the presence of a low equilibrium concentration of a glucose 1-phosphate 6-vanadate mixed diester as the product of the ability of vanadate to rapidly esterify hydroxyl groups, is responsible for the time dependent inhibition of phosphoglucomutase, its concentration would approach that of the enzyme (approximately nanomolar) and would be lowered through binding to the enzyme. However, rapid vanadate esterification at the high glucose 1-phosphate and vanadate concentrations used in these assays would serve to maintain the equilibrium concentration of the inhibitor. Hence, whether the true inhibitor is vanadate or a low concentration of a mixed vanadate-phosphate diester, inhibitor depletion should not occur.

The first order rate constant for approach to the steady state i.e. k_{obs}, was determined from an analysis of the progress curve as shown in Figure 4 (38). A line O.D. was drawn through t=0 of the absorbance (340nm) versus time plot parallel to the linear, steady state region of the progress curve. The absorbance change at time t (minutes), A_t, was measured as the distance between the line O.D. and the pre-steady state region of the progress curve, values of A_t were obtained at several reaction times. The total change in absorbance accompanying the attainment of the steady state rate i.e. A_∞, was measured as the distance between the linear region of the progress curve and the line O.D. which are now parallel. The natural logarithms of the differences between A_∞ and A_t were then plotted against time. The slopes of these were equal to $-k_{obs}$ as described in appendix III Eq.9b.

If all the conditions above are met, respecting substrate depletion, inhibitor depletion and product accumulation then the decrease in velocity during the pre-steady state interval can also be described by the analogous equation (Eq.2) which was derived by other workers (39):

Figure 4

Analysis of the pre-steady state interval of the slow inhibition. Determination of k_{obs}, the apparent first order rate constant for approach to the steady state.

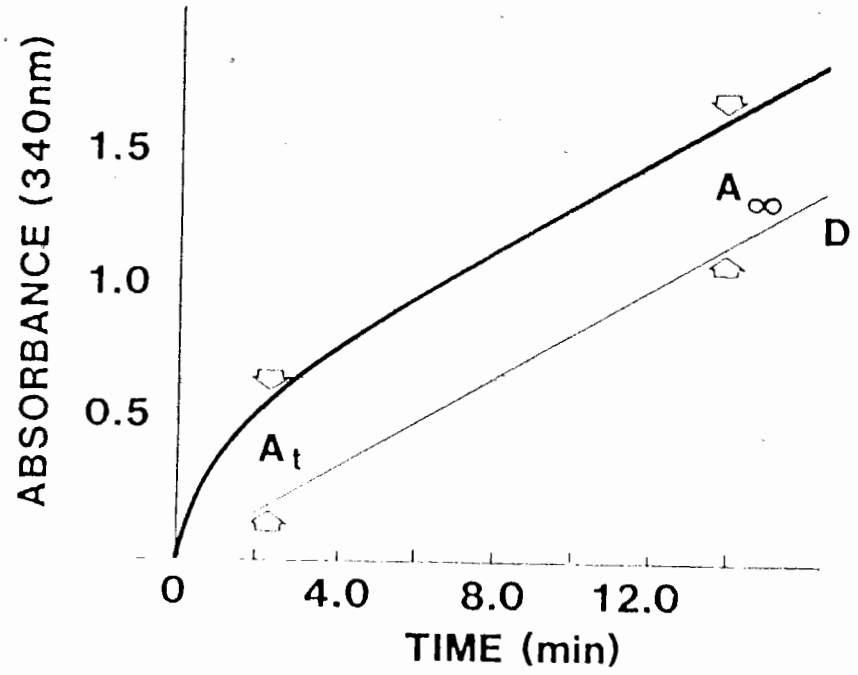
ABSORBANCE (340nm)
1.5
1.0
0.5
A_∞
D
A_t
0
4.0
8.0
12.0
TIME (min)

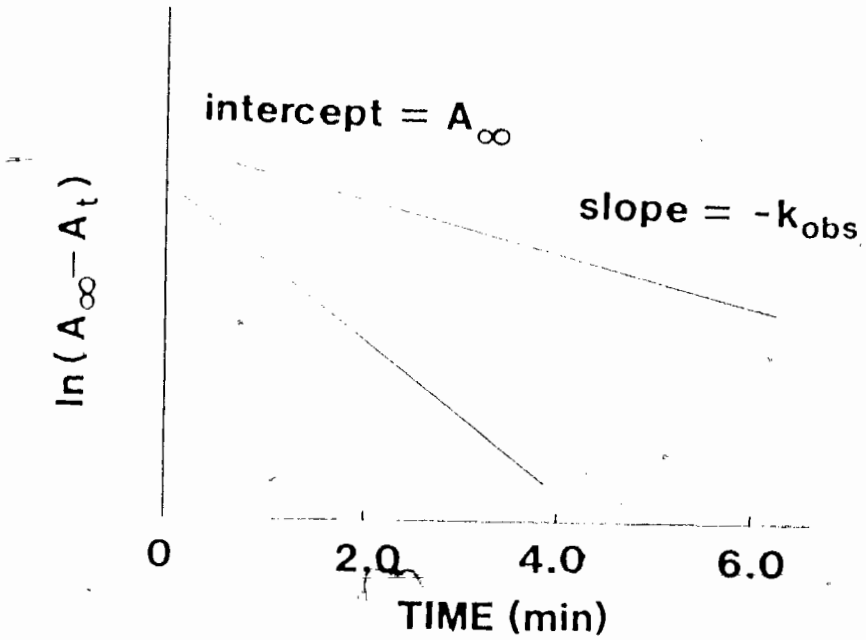
intercept = A_∞
slope = $-k_{obs}$
$\ln(A_\infty - A_t)$
0
2.0
4.0
6.0
TIME (min)

$$v = v_i + (v_o - v_i)\, e^{-kobs.t} \qquad \text{Eq. 2}$$

where:

v = velocity at any time t

v_i = velocity in the steady state

v_o = velocity at zero time

k_{obs} = the apparent first-order rate constant for the approach to the steady state.

Equation 2 predicts that a plot of $\ln(v - v_i)$ against time, should be linear with the slope equal to $-k_{obs}$.

The experiment of Figure 5 was conducted to determine the effect of varying glucose diphosphate concentration on the time dependent inhibition. The conditions of pH, temperature and reactant concentrations used in the assays of this experiment are listed in the figure legend. All the reactants except glucose 1-phosphate and vanadate were incubated at 25°C for 3 minutes after which the reaction was initiated by adding 100 μl of the glucose 1-phosphate stock solution to a final concentration of 530μM. After the almost instantaneous establishment of a steady-state rate, 2, 4 or 8μl of a vanadate stock solution (10 mM, in 20 mM Tris-Cl pH 7.6) was added rapidly, to a final reaction volume of 1.0 ml.

Progress curves showing the time course of vanadate inhibition were obtained over a range of glucose-diphosphate concentration. The reactions were followed until a new inhibited steady-state rate had been established, judged as a linear region in the progress curve lasting at least 5 minutes. The glucose diphosphate concentrations used were: 0.2, 0.44, 0.73, 1.16 and 1.45μM respectively. Figure 6 shows semi-logarithmic plots of the pre-steady state data in an experiment of the type shown in Figure 5, from which it can be seen that the onset of inhibition follows first-order kinetics. The plots of $\ln (A_\infty - A_t)$ against time (sec) are linear over at least three half-lives, which is considered a sufficient length of time for a reaction to have demonstrated first-order kinetics (40). The values of the apparent first-order rate constants (k_{obs}) determined from the slopes of the semi-log plots

Figure 5

The effect of varying glucose diphosphate concentration on the time-dependent inhibition of phosphoglucomutase caused by vanadate at constant high glucose 1-phosphate concentration. Reaction mixtures contained: 0.021 U phosphoglucomutase, 0.12 U glucose 6-phosphate dehydrogenase, 2.0 mM $MgCl_2$, 0.8 mM EDTA, 0.48 mM βNADP$^+$, 0.53 mM α-D-glucose 1-phosphate , 20 mM Tris-Cl$^-$ buffer pH 7.6 at 25°C, in a total assay volume of 1.0 ml. The experiment was carried out at three vanadate concentrations, 20μM, 40μM and 80μM over a range of α-D-glucose diphosphate concentration. The figure shows representative progress curves obtained at 40μM vanadate, in the presence of 0.44μM (●) and 0.73μM (▲) glucose diphosphate.

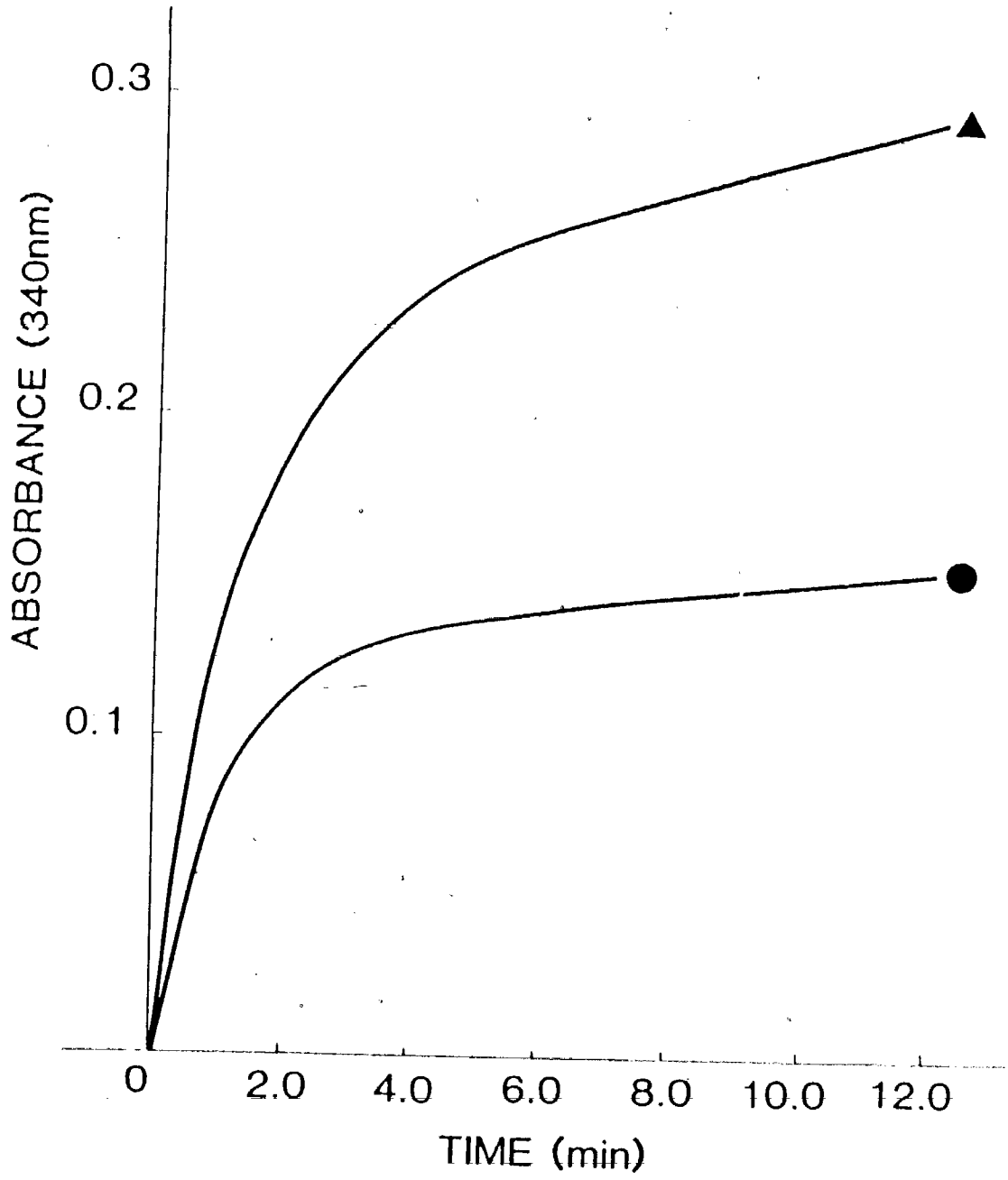
0.3
0.2
0.1
ABSORBANCE (340nm)
0
2.0
4.0
6.0
8.0
10.0
12.0
TIME (min)

are listed in Table II, and in Figure 7 the values determined at vanadate concentrations of 20μM and 40μM are plotted against glucose-diphosphate concentration. From Table II and the plot of Figure 7 it is seen that the rate constant for approach to the steady state decreases with increasing concentration of glucose diphosphate. At higher vanadate concentrations more glucose diphosphate is required to reverse the inhibition, i.e. to decrease k_{obs}. The above results are consistent with the hypothesis that the time dependent inhibition is occurring at the site of the free dephospho form of phosphoglucomutase, competitive with the binding of glucose-diphosphate. It should also be appreciated that the range of reaction half times ($t_{1/2}$), that correspond to the values of k_{obs} listed in Table II are within reach of the approximate value expected for inhibition due to a low concentration of a glucose vanadate-phosphate, mixed diester, interacting in a diffusion rate-limited step with the free dephosphoenzyme. The equilibrium constant for formation of the vanadate ester with the 6-hydroxyl group on glucose, has been determined elsewhere (16) as Keq = 0.084 M^{-1}. At 530 μM glucose 1-phosphate and 20 μM vanadate in the assay the concentration of glucose 1-phosphate 6-vanadate [gP-V] will be 9×10^{-10} M. The forward reaction rate (v_f) for the binding of the mixed diester inhibitor to the free dephosphoenzyme (E) in the absence of glucose diphosphate is as follows:

$$v_f = k_{on}[gP - V]\ [E]$$

Since the concentration of the inhibitor (gP-V) remains constant, as discussed earlier, the reaction will be first-order with respect to the free dephosphoenzyme (E) and have an apparent first-order rate constant of, $k_{on}[gP-V]$ sec^{-1}. If the binding step is diffusion controlled with $k_{on} = 1 \times 10^{7}$ M^{-1} s^{-1} (41) the binding of inhibitor to the dephosphoenzyme will have an apparent first-order rate constant of 9×10^{-2} s^{-1} and thus a half time ($t_{1/2}$) of 8 seconds. This represents only a guideline value, an upper limit under the above conditions, for the half time corresponding to k_{obs} for approach to steady-state since, as seen above in the plot of Figure 7 and the results in Table II, the observed first-order rate constant varies with the concentrations of vanadate and glucose-diphosphate present in the

Figure 6

Analysis of the progress curve data of the experiment of Figure 5. The figure shows semi-logarithmic plots of ln $(A_\infty - A_t)$ against time from the analysis of the presteady-state interval of progress curves obtained at 20μM and 40 μM vanadate over a range of glucose diphosphate concentration in the assays. Glucose diphosphate concentrations used were: 0.2μM (○), 0.44μM (●), 0.73 μM (▲), 1.16μM (△), 1.45μM (■).

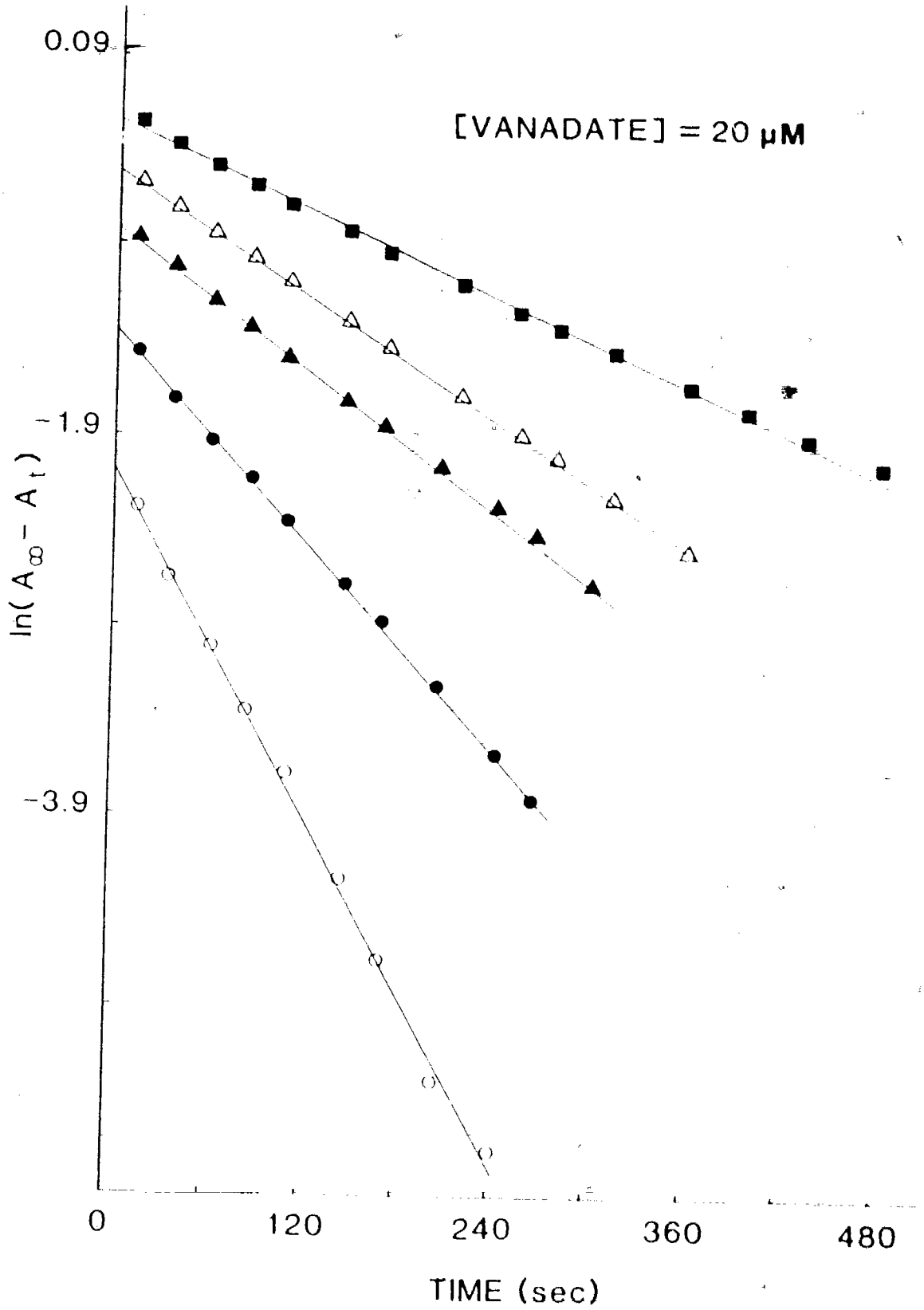
[VANADATE] = 20 μM
0.09
-1.9
-3.9
ln(A∞ - At)
0
120
240
360
480
TIME (sec)

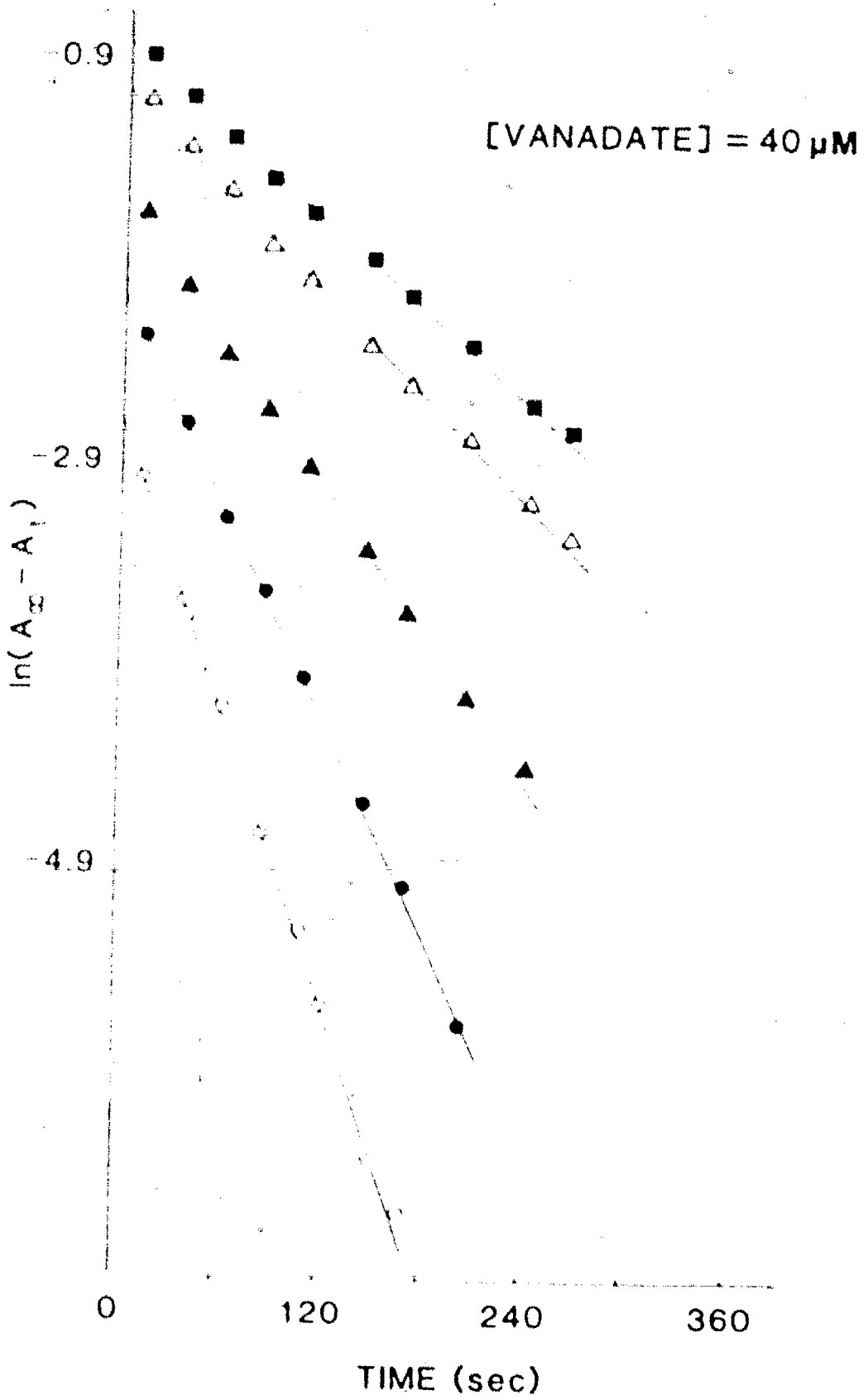
[VANADATE] = 40 μM
-0.9
-2.9
-4.9
ln(A∞ - At)
0
120
240
360
TIME (sec)

TABLE II: Values for k_{obs} of phosphoglucomutase inhibition derived from the slopes of the semi-log plots shown in Figure 6 obtained at 20 and 40μM vanadate, as a function of varying glucose diphosphate concentration.

[g 1,6-P] μM	k_{obs} ±6% (s^{-1}) 20μM vanadate, 530μM [g-1-P]	k_{obs} ±6% (s^{-1}) 40μM vanadate, 530μM [g-1-P]
0.20	0.0150	0.0239
0.44	0.0092	0.0175
0.73	0.0061	0.0119
1.16	0.0055	0.0085
1.45	0.0038	0.0073

a. k_{obs} is the apparent first-order rate constant of the reaction governing the time dependent inhibition of phosphoglucomutase activity.

b. [g-1-P] represents concentration of glucose 1-phosphate in the assay.

c. [g 1,6-P_2] represents concentration of glucose diphosphate in the assay.

Figure 7

A plot of the k_{obs} values from Table II obtained at 20 and 40μM vanadate, against glucose diphosphate concentration. The k_{obs} values were obtained from the slopes of the plots shown in Figure 6. The lines drawn represent the calculated fit to the data points obtained at 20μM (○) and 40μM (●) vanadate, using Equation 6 derived later.

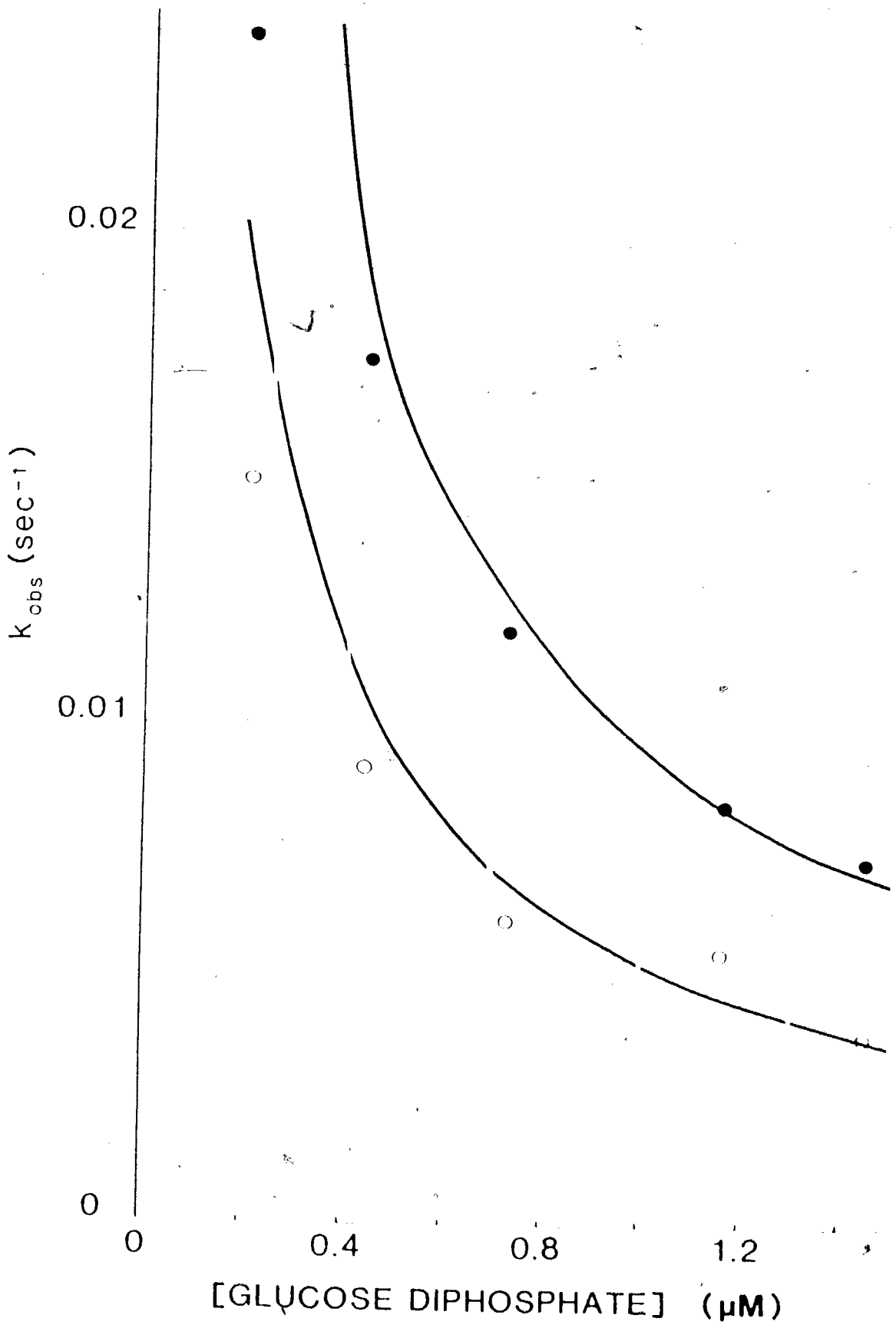
0.02
0.01
0
k_{obs} (sec^{-1})
0
0.4
0.8
1.2
[GLUCOSE DIPHOSPHATE] (μM)

assay. The previous results also provide an explanation for the initial velocity of the mutase reaction starting almost completely inhibited in trace c) of Figure 3. Here the pre-incubation was carried out in the absence of glucose-diphosphate but in the presence of glucose 1-phosphate and vanadate. Clearly under these conditions the observed first-order rate constant will be large and therefore the onset of the inhibition should be fast. The above considerations show that the pre-steady state data in the experiment of Figure 5 can be interpreted in terms of the reaction of a low concentration of an inhibitor, which must be capable of binding tightly to the enzyme, giving rise to a small apparent first-order rate constant that governs the onset of the inhibition. Here the inhibitor is the putative, glucose 1-phosphate 6-vanadate, which acts competitively with respect to glucose diphosphate binding to the free dephosphoenzyme.

Steady state analysis of the two time separated components of vanadate inhibition of phosphoglucomutase

To recapitulate, the time separated components as pointed out earlier in the examination of Figure 3, are:

1. a rapid inhibition seen as the effect of vanadate on the initial slope of the progress curve, and
2. a slower time dependent inhibition that results in a final steady-state rate much slower than that seen in the absence of vanadate, and represented by the linear region in the progress curve.

In Figure 8 the model proposed to account for the steady-state behavior of the phosphoglucomutase reaction in the presence of vanadate is shown. The scheme is the same as that described for the mutase reaction in the model of Figure 1, except that here vanadate is included as a competitive inhibitor acting at the level of the free dephosphoenzyme (Ė). The model of Figure 8 shows vanadate inhibition to develop in two possible ways: *via* a) the reaction of a low equilibrium concentration of glucose 1-phosphate 6-vanadate (AI), mixed diester with the free dephosphoenzyme (E) and, b) a sequential route that involves free vanadate (I) reacting with the dephosphoenzyme (E), followed by glucose 1-phosphate (A)

binding to the resulting complex of the dephosphoenzyme with vanadate (EI). This route will be associated with the formation of the mixed diester on the enzyme.

Again using the "King-Altman method" (32) a rate equation was derived for the model in Figure 8 (see Appendix II) in terms of which the steady-state behavior of phosphoglucomutase in the presence of vanadate could be adequately explained. The rate equation predicted by the model in the form of the double reciprocal (Lineweaver-Burke) plot showing reciprocal rate against reciprocal glucose diphosphate concentration is as follows:

$$\frac{1}{v} = \frac{Kmb}{Vm} \cdot \left(1 + \frac{[I]}{Kv} + \frac{[AI]}{Kvp} \right) \cdot \frac{1}{[B]} + \left(\frac{Kma}{[A]} + \beta \right) \cdot \frac{1}{Vm} \qquad \text{Eq. 3}$$

where:

v = initial velocity

Vm = maximum velocity

[B] = concentration glucose diphosphate

[A] = concentration of glucose 1-phosphate

Kmb = Michaelis constant of glucose diphosphate for the free dephosphoenzyme (E)

Kma = Michaelis constant of glucose 1-phosphate for the active, phosphoenzyme (EP)

[I] = concentration of free vanadate, taken to be the total concentration in the assay

K_v = inhibition constant for free vanadate as a competitive inhibitor vs. glucose-diphosphate

[AI] = concentration of glucose 1-phosphate 6-vanadate

K_{vp} = inhibition constant for the mixed diester as a competitive inhibitor vs. glucose-diphosphate

Equation 3 shows that competitive inhibition due to vanadate acting at the free dephosphoenzyme (E) will appear as an increase in the slope of a plot of

Figure 8

Kinetic model proposed to account for the inhibition of phosphoglucomutase activity by vanadate. The k's, denote specific rate constants of the steps in the mechanism. In the model, B = glucose diphosphate, A = glucose 1-phosphate, C = glucose 6-phosphate, I = vanadate (oxyanion), AI = glucose 1-phosphate 6-vanadate, EP = phosphoenzyme (active), EB = complex of the dephosphoenzyme with glucose diphosphate, E = free dephosphoenzyme (inactive), EI = inhibited complex of the dephosphoenzyme with vanadate, EAI = inhibited complex of the dephosphoenzyme with glucose 1-phosphate 6-vanadate (mixed diester), EPA,EPC = complexes of the active phosphoenzyme with the glucose monophosphates (A and C) defined above.

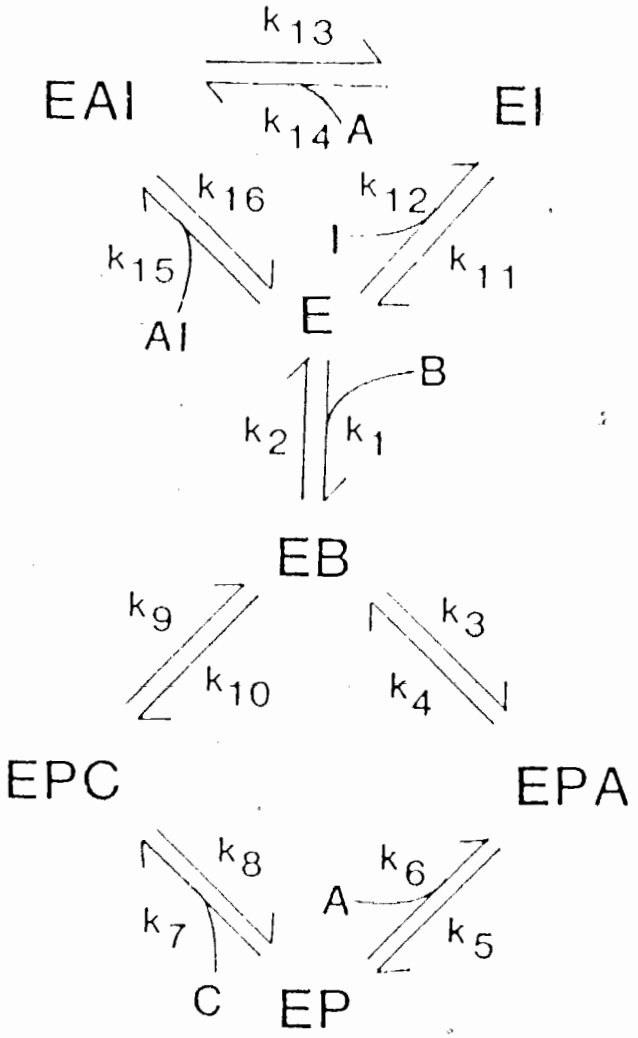
k13
EAI
k14
A
EI
k16
k12
I
k15
k11
AI
E
B
k2
k1
EB
k9
k3
k10
k4
EPC
EPA
k8
k6
A
k7
k5
C
EP

1/v against 1/[B]. Hence at different vanadate and constant glucose 1-phosphate concentrations in the assay the expected pattern of the double reciprocal plots will be a series of lines of varying slope converging to a common vertical intercept of,

$$-\left(\frac{Kma}{[A]} + \beta\right) \cdot \frac{1}{Vm}$$

The slope of the double reciprocal plot of Equation 3 is given by,

$$\frac{Kmb}{Vm}\left(1 + \frac{[I]}{Kv} + \frac{[AI]}{Kvp}\right)$$

The value of [AI] in the brackets can be expressed in terms of the known concentrations of vanadate and glucose 1-phosphate and the equilibrium constant for formation of glucose 1-phosphate 6-vanadate, mixed diester, Keq = 0.084 M^{-1}. This gives,

$$\text{slope} = \frac{Kmb}{Vm}\left(1 + \frac{[I]}{Kv} + \frac{[I]\,[g\text{-}1\text{-}P]Keq}{Kvp}\right)$$

Summation of the terms common in vanadate concentration allows the expression for the slope of the double reciprocal plot to be abbreviated as shown below.

$$\text{slope} = \frac{Kmb}{Vm}\left(1 + \frac{[I]}{Kiapp}\right) \qquad \text{Eq. 4}$$

where:

[I] = concentration of free (non esterified) vanadate, taken as the total concentration present in the assay.

$$Kiapp = \frac{Kv \cdot Kvp}{Kvp + Kv \cdot Keq\,[g\text{-}1\text{-}P]}$$

and [g-1-P] = total concentration of glucose 1-phosphate present in the assay.

The slopes of double reciprocal plots of the form of Equation 3 obtained at different vanadate concentrations can be analyzed in terms of Equation 4 which predicts that a replot of slope against vanadate concentration will be linear and have a horizontal intercept of $-Ki_{app}$. As seen above Ki_{app} is an overall, apparent inhibition constant representing the sum of the competitive effects due to free vanadate and glucose 1-phosphate 6-vanadate present in the assay.

Figure 9 shows plots of reciprocal rate, obtained from the initial slopes of the progress curve data of the experiment in Figure 5 against reciprocal glucose diphosphate concentration. It is seen that the initial velocity of the mutase reaction is subject to a rapid reversible competitive inhibition that increases with increasing concentration of vanadate and which occurs at the level of the free dephosphoenzyme. The rapid inhibition seen here is probably due only to competitive effects arising from free (nonesterified) vanadate. Previous results suggest that no significant contribution due to mixed diester present would be expected to have developed in the short time interval subsequent to initiating the reaction and adding vanadate, during which inhibition of the initial velocity takes place. Also, experiments described later, Figure 12, show that the initial rate, before time-dependent inhibition has developed significantly, is independent of glucose 1-phosphate concentration near the concentration of glucose 1-phosphate used in these experiments. To generate progress curves the reaction was first initiated after an incubation period of 3 minutes at 25°C by adding glucose 1-phosphate to the reaction mixture in the absence of vanadate and replacing the cuvette in the spectrophotometer. Once steady state had been established the chart recorder was disengaged, the cuvette removed and an aliquot of a vanadate stock solution added. The cuvette contents were then mixed by inverting several times and finally the cuvette was replaced in the spectrophotometer. The chart recorder was immediately reengaged and data collection continued. On average the time that elapsed subsequent to adding vanadate before data collection could begin was 5 seconds. This represents the earliest opportunity that a rate could be measured, hence the rates recorded from the initial slope of the progress curves in this experiment correspond to those at t=5 seconds. The half-time ($t_{1/2}$) associated with the onset

Figure 9

A plot of reciprocal rate, obtained from the initial slope of the progress curves of the experiment of Figure 5, against reciprocal glucose diphosphate concentration. The figure shows the effect of vanadate on the initial velocity of the phosphoglucomutase reaction, concentrations of vanadate present were 20 μM (○) and 40μM (●). The inset shows a replot of slope of the above plot against vanadate concentration. From the negative horizontal intercept a value of K_i for vanadate as a competitive inhibitor can be obtained, K_v = 37 (±18)μM.

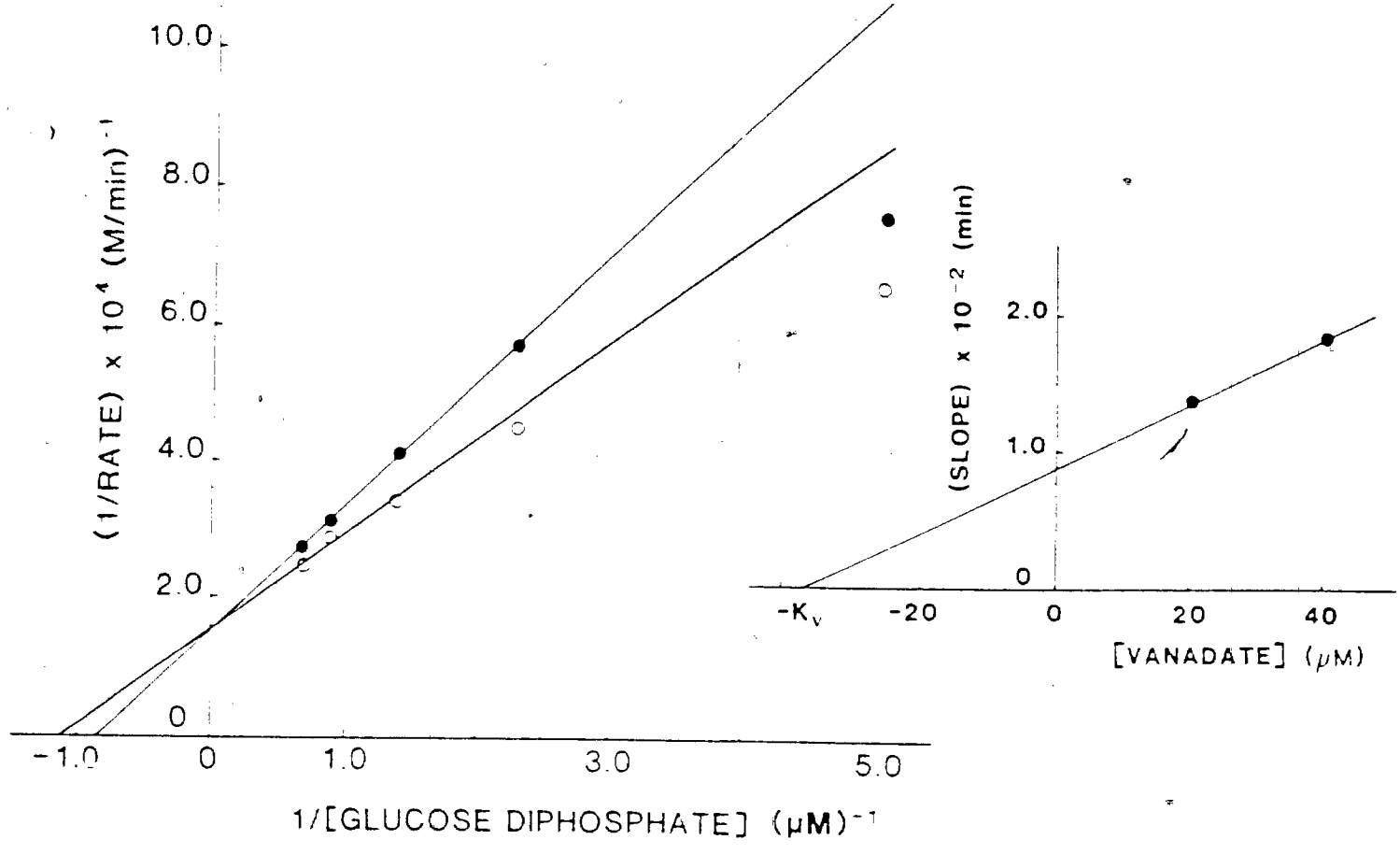
10.0
8.0
6.0
4.0
2.0
0
(1/RATE) x 10⁴ (M/min)⁻¹
-1.0
0
1.0
3.0
5.0
1/[GLUCOSE DIPHOSPHATE] (μM)⁻¹
2.0
1.0
0
(SLOPE) x 10⁻² (min)
-Kv
-20
0
20
40
[VANADATE] (μM)

of inhibition due to mixed diester at a concentration of 530μM glucose 1-phosphate in the presence of 40μM vanadate and at the lowest glucose-diphosphate concentration used in the plot of Figure 9 was calculated to be 40 seconds, determined from the data presented later in the plot of Figure 15 and the relationship $t_{1/2} = \ln 2 / k_{obs}$. A measure of the extent to which mixed diester inhibition had progressed in this 5 second interval toward steady state is provided by the percentage deviation of the rates recorded at t=5 seconds from the expected initial rate at t=0 calculated using Equation 2 given earlier and the half-time of 40 seconds. It is found that the rates differ by approximately 9% from that expected for the initial rate at t=0 seconds. Since the accepted limit of allowed experimental error in rate determinations is $\pm$5% it can be seen that the rates recorded at t=5 seconds vary by a margin of 4% outside this limit. However when constructing the lines in the plot of Figure 9 emphasis was placed on the points collected at the higher concentrations of glucose-diphosphate eg., at the next highest concentration of 0.73μM the $t_{1/2}$ for mixed diester inhibition under the conditions considered above becomes 77 seconds and the deviation of the rate recorded falls to only 4% of that expected at t=0 seconds. At lower vanadate concentration the $t_{1/2}$ becomes even longer. Thus inhibition due to mixed diester is not considered to have developed sufficiently in this interval of 5 seconds to form a contribution toward the rapid component of inhibition that expresses itself in this interval. For this reason the value of Ki_{app} obtained from the replot of slope against vanadate concentration shown in Figure 9 will be equal to K_v, the inhibition constant for the complex of the dephosphoenzyme with vanadate (EI) in the model of figure 8. The value of K_v determined from the replot was 37 $\pm$18μM. As considered earlier, the time dependent inhibition will progress further towards steady state over a given interval of time at low glucose-diphosphate concentration than will be the case at high glucose-diphosphate concentration. This implies that the points recorded at the lowest glucose-diphosphate concentrations in Figure 9 should deviate upward, not downward from the lines in the plot as seen. The downward deviation is rationalized in terms of contaminating glucose-diphosphate present in the commercial source of glucose 1-phosphate used in these studies. The effect of this contaminating glucose-diphosphate on the initial rate is more

profound over shorter time intervals than the inhibition due to the mixed diester, hence the trend in the rates recorded.

In Figure 10 are shown plots of reciprocal rate obtained from the slope of the linear, steady-state region of the progress curves generated in the experiment of figure 5 against reciprocal glucose diphosphate concentration. The rate measured in this region of the progress curve is the result of the slow component of vanadate inhibition, thought to be due to a tight binding complex of glucose 1-phosphate 6-vanadate.

The pattern seen for the double reciprocal plots of Figure 10 in the presence of varying vanadate is as predicted above for reversible, competitive inhibition arising at the free dephosphoenzyme (E). As shown in Figure 11 a replot of slope of the reciprocal plots of Figure 10 against vanadate concentration is linear, having a vertical intercept of

$$\frac{Kmb}{Vm},$$

and a slope of $$\frac{Kmb}{Vm}\left(\frac{1}{Kv} + \frac{Keq\ [g\text{-}1\text{-}P]}{Kvp}\right).$$

From the observed value of the replot intercept (Kmb/Vm) and the known values of K_v, Keq and the concentration of glucose 1-phosphate used in the assay it is possible to determine K_{vp}, the inhibition constant for the complex of the dephosphoenzyme with glucose 1-phosphate 6-vanadate mixed diester (EAI) in the model of Figure 8. The value of K_{vp} determined from the slope of the replot of Figure 11 was 2.7 $\pm$0.4 x 10^{-11} M. The value of $K_{I_{app}}$ obtained from the horizontal intercept of this replot was 0.6 $\pm$0.08 x 10^{-4} M. The ratio Kmb/Vm determined from the vertical intercept of this replot yields a value of Kmb the same as that obtained from the intercept of the corresponding plot in Figure 9.

Ninfalli et al. (21) had earlier obtained a value of 1.0 x 10^{-4} M from the horizontal intercept of a replot similar to that of Figure 11 which was taken to be the

Figure 10

A plot of reciprocal of the rate obtained from the slope of the linear, steady-state region of the progress curves of experiments of the type shown in Figure 5 against reciprocal glucose diphosphate concentration. The figure shows the effect of varying vanadate concentration on the rate of the phosphoglucomutase reaction in this region of the progress curve. Concentrations of vanadate considered were: 20μM (○), 40μM (●) and 80 μM (▲). Reaction mixtures contained: 0.021 U phosphoglucomutase, 0.12 U glucose 6-phosphate dehydrogenase, 2.0 mM $MgCl_2$, 0.8 mM EDTA, 0.48 mM β-$NADP^+$, 0.53 mM α-D-glucose 1-phosphate, 20 mM Tris-Cl buffer pH 7.6 at 25°C, in a total assay volume of 1.0 ml.

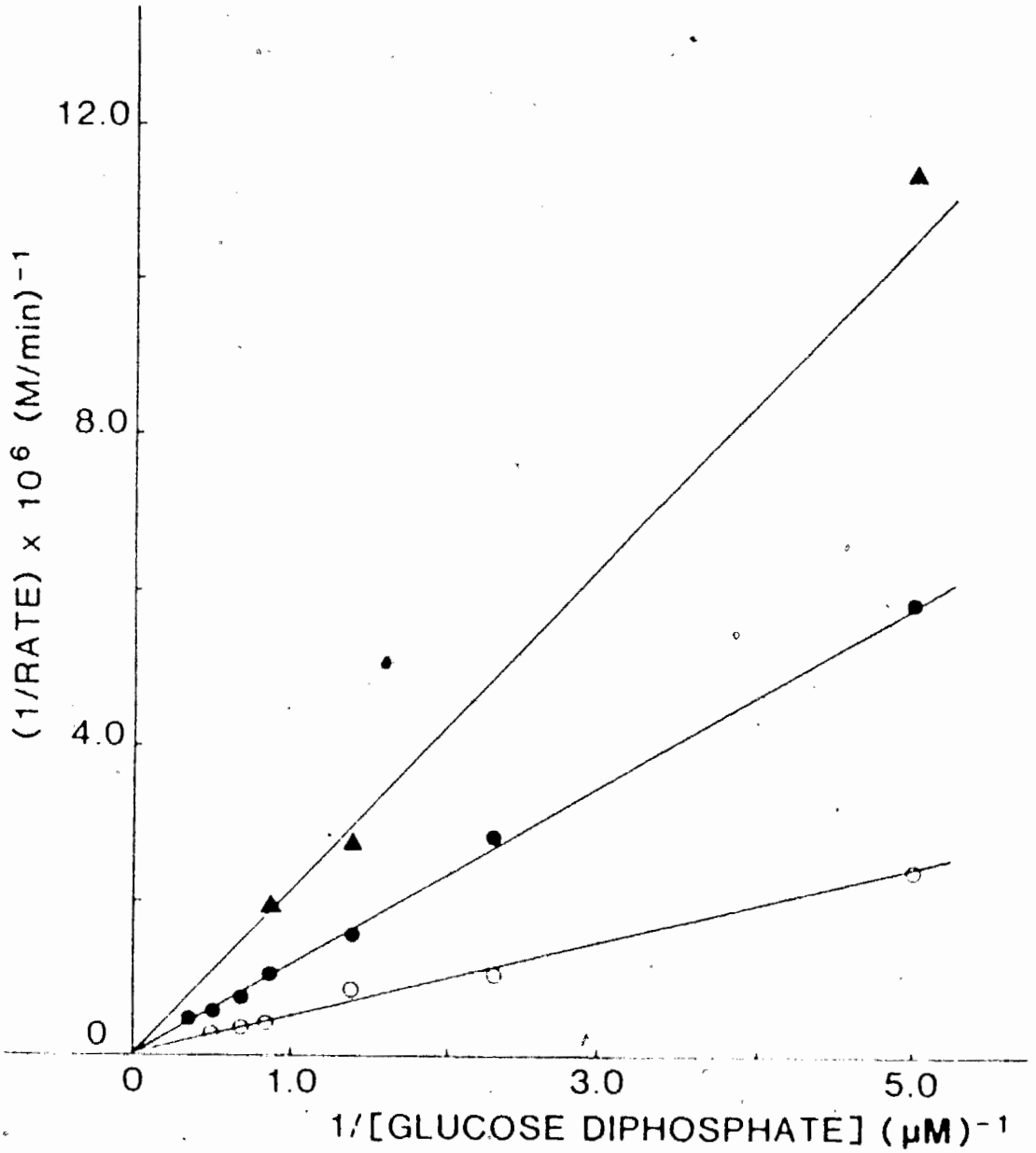
12.0
8.0
4.0
0
(1/RATE) x 10^6 (M/min)$^{-1}$
0
1.0
3.0
5.0
1/[GLUCOSE DIPHOSPHATE] (μM)$^{-1}$

Figure 11

A primary replot of the data in Figure 10 i.e., slope of the double reciprocal plot against vanadate concentration : 20μM, 40μM and 80μM. A linear regression technique was used to fit the line to the data points. From the slope of the replot a value of K_i, the inhibition constant of glucose 1-phosphate 6-vanadate as a competitive inhibitor of the dephosphoenzyme is obtained,

$K_{vp} = 2.7 \pm 0.4 \times 10^{-11}$ M.

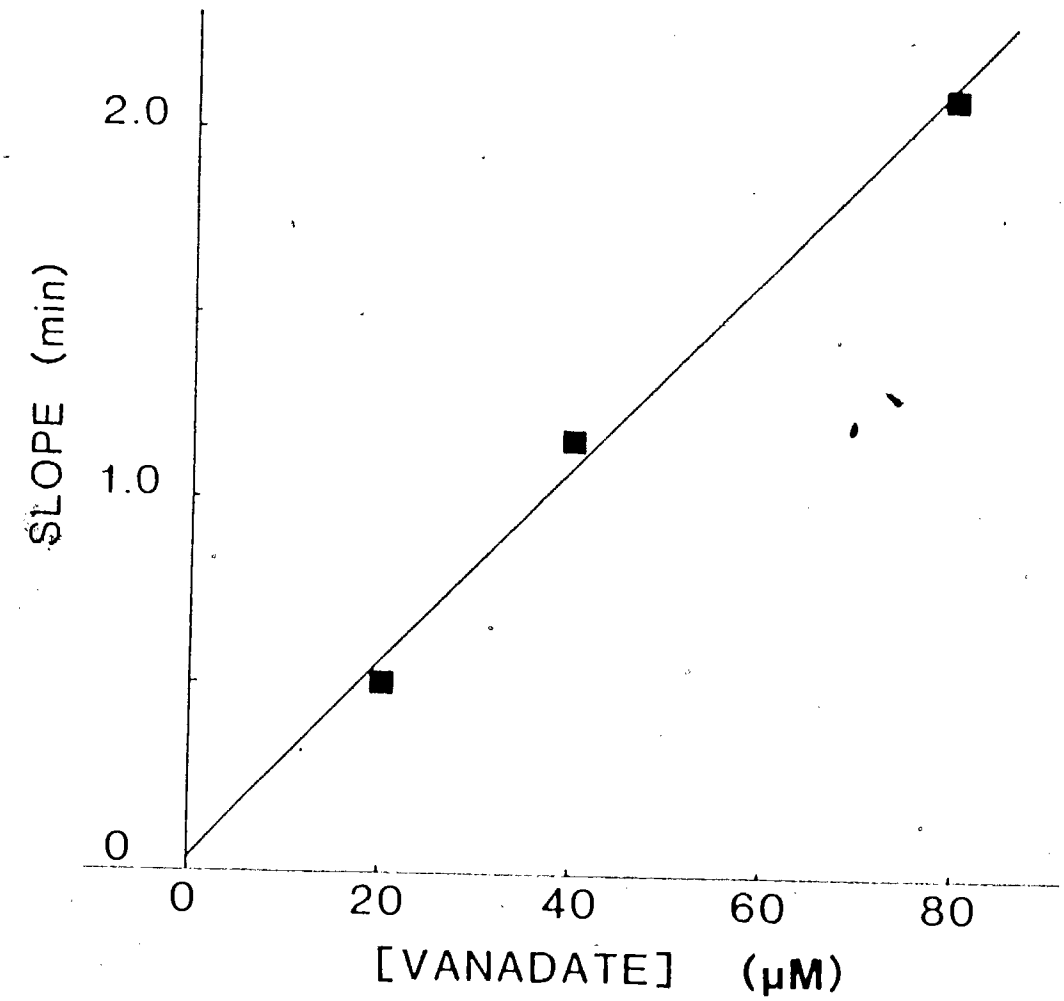
2.0
1.0
0
SLOPE (min)
0
20
40
60
80
[VANADATE] (μM)

inhibition constant for free vanadate as a competitive inhibitor of phosphoglucomutase (rabbit muscle). In Ninfalli's study (21) the enzyme had been pre-incubated with vanadate in the presence of 250μM glucose 1-phosphate. For this reason the full time course of inhibition was not appreciated (see trace c of Figure 3) and the value of 1×10^{-4} M obtained really represents the apparent inhibition constant Ki_{app}, as defined with Equation 4.

The relationship of the Ki_{app} values determined at these two concentrations of glucose 1-phosphate, provides support for the identity of the inhibitor responsible for the time dependent inhibition as an equilibrium concentration of glucose 1-phosphate 6-vanadate.

The value of Ki_{app} determined from the steady-state analysis of the linear portion of the progress curves at a given concentration of glucose 1-phosphate corresponds to the concentration of vanadate at which the equilibrium concentration of mixed diester approaches a value equal to K_{vp}. A comparison of the values determined above for K_v and K_{vp} shows that the complex of glucose 1-phosphate 6-vanadate is bound a factor of 10^6 times more tightly to the dephosphoenzyme than free (nonesterified) vanadate. As a result of the large difference in the magnitude of these inhibition constants the meaning of Ki_{app} in equation 4 will vary depending on which region of the progress curve is considered in the steady-state analysis.

The results obtained so far do not provide conclusive proof of the slow time dependent inhibition arising from the reaction of a low concentration of a tight binding inhibitor (mixed diester) with the free dephosphoenzyme. The inhibition could also arise from the rapid binding of the inhibitor components, i.e., vanadate and glucose 1-phosphate separately, as considered by the sequential pathway in the model of Figure 8. Once these components are bound, a rate determining conformational change in the dephosphoenzyme, resulting in a tighter association with the mixed diester may control the slow onset of inhibition. In this case it might be expected that the rapid inhibition seen as the effect on the initial velocity of changing vanadate concentration should also be sensitive to changes in the

concentration of glucose 1-phosphate.

The experiment of Figure 12 was conducted to test this possibility. The concentrations of reactants used are listed in the figure legend, experiments were carried out at concentrations of glucose 1-phosphate of 75μM and 150μM in the presence in each case of 20μM and 60μM vanadate. Initial rates were collected over a range of glucose diphosphate concentration as shown. All the assay components including vanadate but not glucose 1-phosphate were incubated for 3 minutes at 25°C prior to initiating the reaction with substrate. At the higher concentration of glucose 1-phosphate used in this experiment, in the presence of 40μM vanadate and 0.44μM glucose-diphosphate the half-time associated with the onset of inhibition due to mixed diester was 120 seconds. For this reason effects due to the slower component of inhibition on the initial rates measured from the spectrophotometric trace, were not considered to be significant in the interval of 10 seconds that elapsed before a rate measurement could be made. In this interval mixed diester inhibition would have advanced only 6% of the way toward steady state. The pattern seen for the double reciprocal plots in Figure 12, is again as predicted (see Equation 3) for reversible competitive inhibition occurring at the free dephosphoenzyme. The downward deviation of the rates recorded at low glucose-diphosphate concentration in the plots of Figure 12, is ascribed to the presence of contaminating glucose-diphosphate present in the commercial source of glucose 1-phosphate used in these studies as discussed earlier. In the absence of effects due to the slow inhibition, the slopes of the reciprocal plots of Figure 12 in the presence of rapid, competitive inhibition due to both glucose 1-phosphate and vanadate are described by analogy with Equation 3 above as follows:

$$\text{slope} = \frac{Kmb}{Vm}\left(1 + \frac{[I]}{Kv} + \frac{[g\text{-}1\text{-}P]}{Kg1p}\right) \qquad \text{Eq. 5}$$

The terms in Equation 5 are as defined earlier except for K_{g1p}, which is included in this analysis to represent the inhibition constant for glucose 1-phosphate reacting with the free dephosphoenzyme. Equation 5 predicts that the negative horizontal intercept of a replot of slope against [I] (vanadate concentration in the assay)

Figure 12

The effect of varying glucose 1-phosphate concentration on the rapid, initial component of vanadate inhibition of phosphoglucomutase. Reactions contained: 20 mM Tris-Cl pH 7.6 at 25°C, 0.034 U phosphoglucomutase, 0.20 U glucose 6-phosphate dehydrogenase, 2 mM $MgCl_2$, 0.49 mM β-NADP$^+$, and 0.81 mM EDTA in a final volume of 1.0 ml. The experiment was carried out at concentrations of glucose 1-phosphate of 75μM and 150μM. The figure shows plots of reciprocal rate against reciprocal glucose diphosphate concentration, obtained at the above two concentrations of glucose 1-phosphate in the absence of vanadate (○), and in the presence of vanadate at 20 μM (●) and 60 μM (▲).

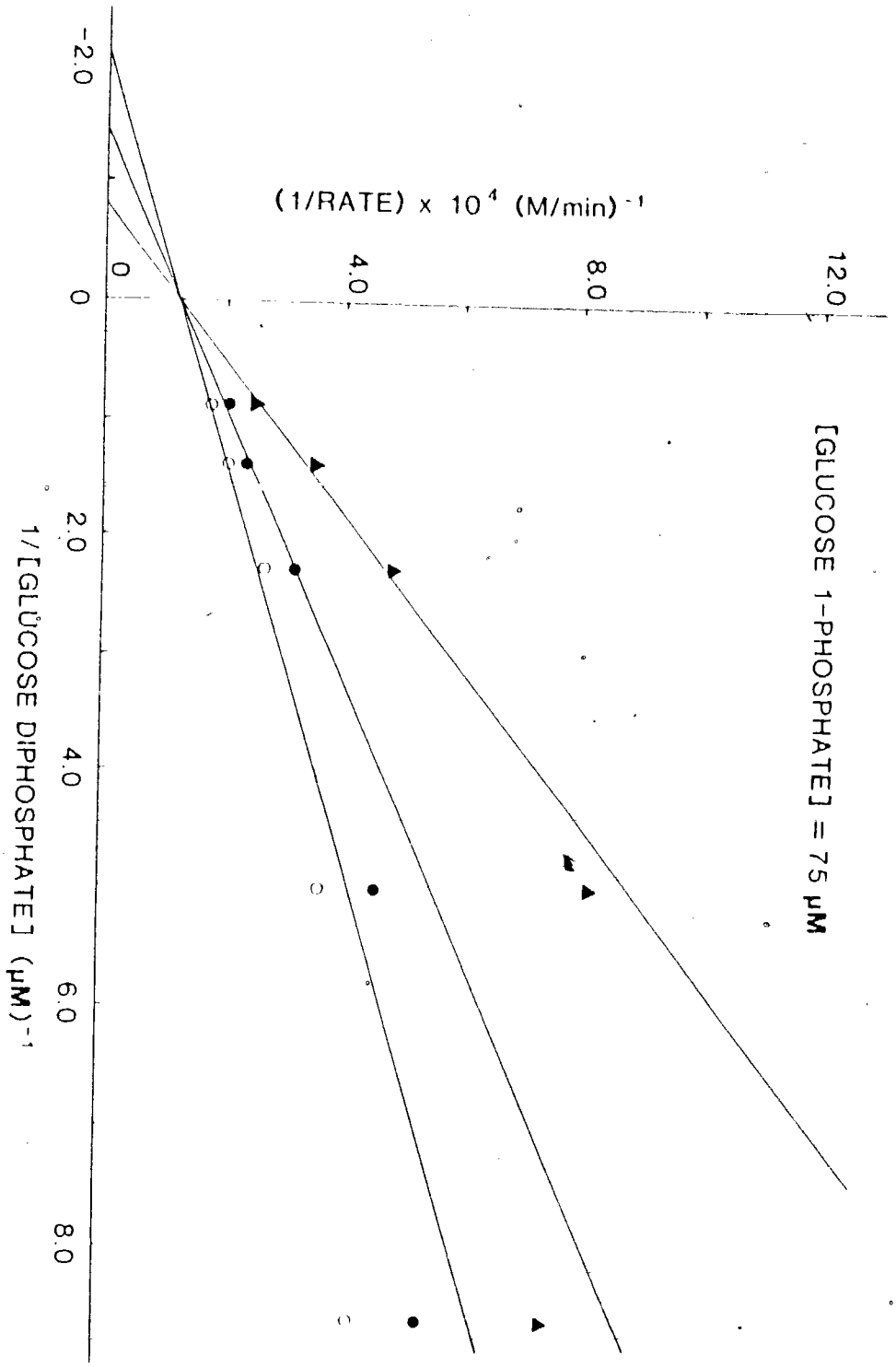
(1/RATE) x 10^4 (M/min)$^{-1}$
-2.0
0
4.0
8.0
12.0
2.0
4.0
6.0
8.0
1/[GLUCOSE DIPHOSPHATE] (μM)$^{-1}$
[GLUCOSE 1-PHOSPHATE] = 75 μM

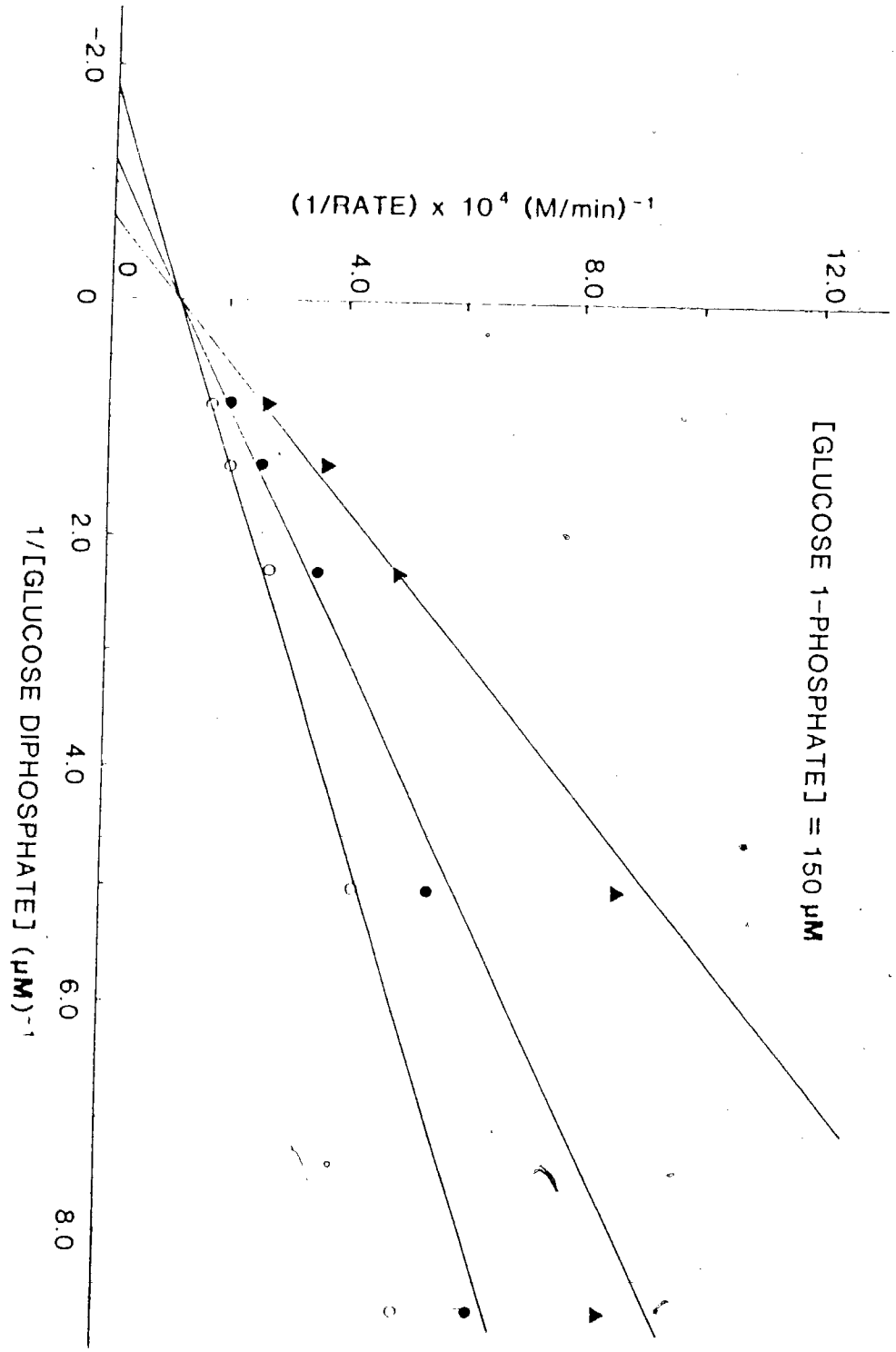
(1/RATE) x 10^4 (M/min)$^{-1}$
4.0
8.0
12.0
[GLUCOSE 1-PHOSPHATE] = 150 μM
-2.0
0
0
2.0
4.0
6.0
8.0
1/[GLUCOSE DIPHOSPHATE] (μM)$^{-1}$

Ki_{app} will be equal to,

$$Kv \left(1 + \frac{[g\text{-}1\text{-}P]}{Kg1p} \right) .$$

Hence Ki_{app} should become larger as the concentration of glucose 1-phosphate present increases. Clearly from the values obtained for this intercept from the replots shown in Figure 13 of 34.9 ±4.6 x 10^{-6} M and 37.3 ±1.9 x 10^{-6} M at 75μM and 150μM glucose 1-phosphate respectively, it can be seen that the effect on Ki_{app} of doubling the glucose 1-phosphate concentration was not significant. It is also important to note that these values of Ki_{app} are the same as that obtained earlier for K_v at 530 μM glucose 1-phosphate (p.43), from the intercept of the replot shown in Figure 9. The initial velocity of the mutase reaction from the results of the last experiment decreased with increasing concentration of vanadate but was independent of glucose 1-phosphate at the two concentrations used. Such a response of the initial velocity would not be expected for inhibition due to a low concentration of a tight binding, mixed vanadate-phosphate diester. Clearly this represents a separate, rapid component of inhibition due to free (nonesterified) vanadate acting competitively with respect to glucose diphosphate at the free dephosphoenzyme.

The experiment of Figure 14 was performed to determinethe effect of varying glucose 1-phosphate concentration on the observed first-order rate constant (k_{obs}) of the slow inhibition. Progress curves were obtained in the same manner, with reference to considerations of substrate and inhibitor depletion and also product accumulation and under the same experimental conditions of reactant concentration, pH and temperature as those of the experiment in Figure 5, except that here glucose 1-phosphate concentration was varied at constant vanadate concentration of 40 μM in the assay. The experiment was performed at two different concentrations of glucose diphosphate which were held constant in each case at 0.44 μM and 0.73 μM respectively. The analysis of the presteady-state interval as described in Figure 4 yielded the semi-logarithmic plots of ln $(A_\infty - A_t)$ against time shown in Figure 14. From Figure 14 it can again be seen that the observed rate of the slow

Figure 13

Primary replots of the data in Figure 12. The slopes of the double reciprocal plots obtained at the two concentrations of glucose 1-phosphate used of 75μM (●) and 150μM (▲), are plotted against vanadate concentration at 20μM and 60μM.

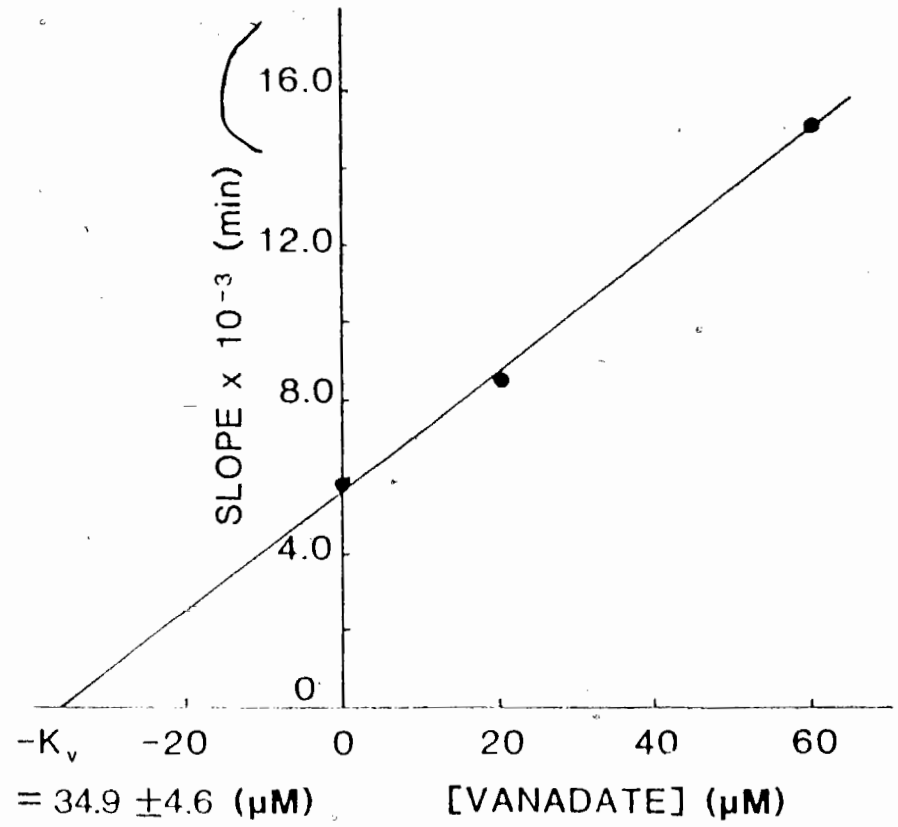
16.0
12.0
8.0
4.0
0
SLOPE x 10^{-3} (min)
$-K_v$
-20
0
20
40
60
= 34.9 ±4.6 (μM)
[VANADATE] (μM)

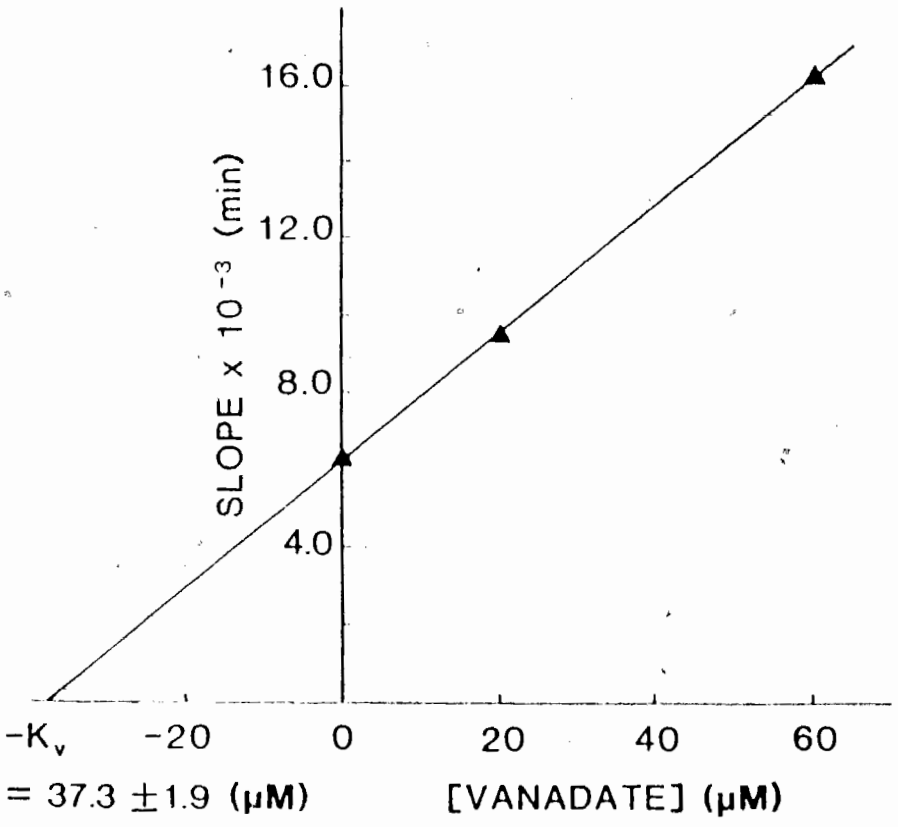
16.0
12.0
8.0
4.0
SLOPE x 10^{-3} (min)
$-K_v$
-20
0
20
40
60
= 37.3 ±1.9 (μM)
[VANADATE] (μM)

Figure 14

The effect of varying glucose 1-phosphate concentration on k_{obs}, i.e., the apparent first-order rate constant of the time dependent inhibition. Reaction mixtures contained: 0.02 U phosphoglucomutase, 0.12 U glucose 6-phosphate dehydrogenase, 2.0 mM $MgCl_2$, 0.8 mM EDTA, 0.48 mM β-$NADP^+$, 20 mM Tris-Cl pH 7.6 at 25°C, and the indicated concentrations of vanadate and glucose-diphosphate in a total volume of 1.0 ml. Concentrations of glucose 1-phosphate used were: 0.53 mM (●), 0.8 mM (△), 1.06 mM (▲), 1.48 mM (○), 2.12 mM (■), 2.38 mM (□) and 3.18 mM (◇). The figure shows the semi-log plots of $\ln(A_\infty - A_t)$ against time (sec) obtained at glucose-diphosphate concentrations of 0.44 μM and 0.73 μM respectively.

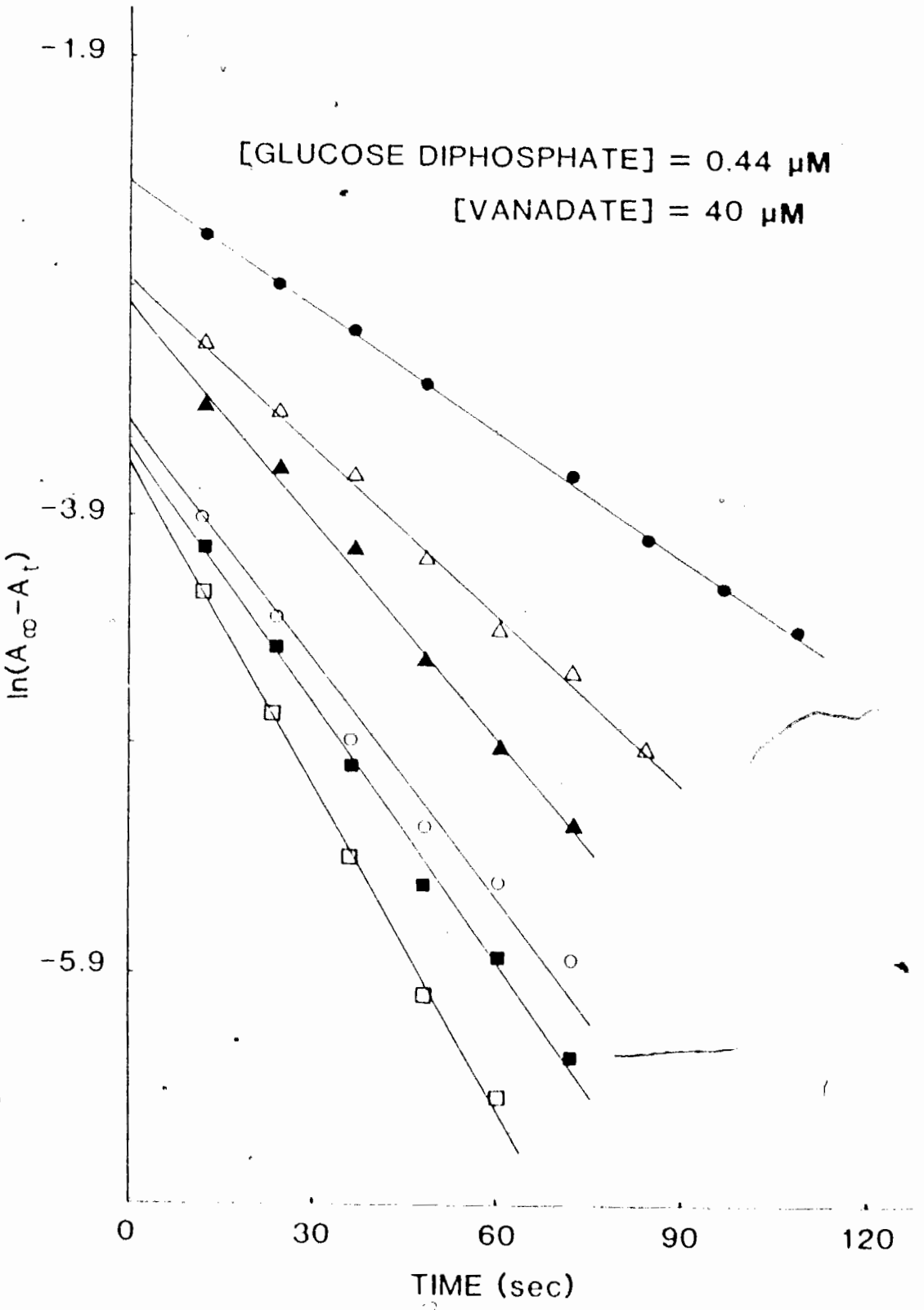
[GLUCOSE DIPHOSPHATE] = 0.44 μM
[VANADATE] = 40 μM
-1.9
-3.9
-5.9
ln(A∞-At)
0
30
60
90
120
TIME (sec)

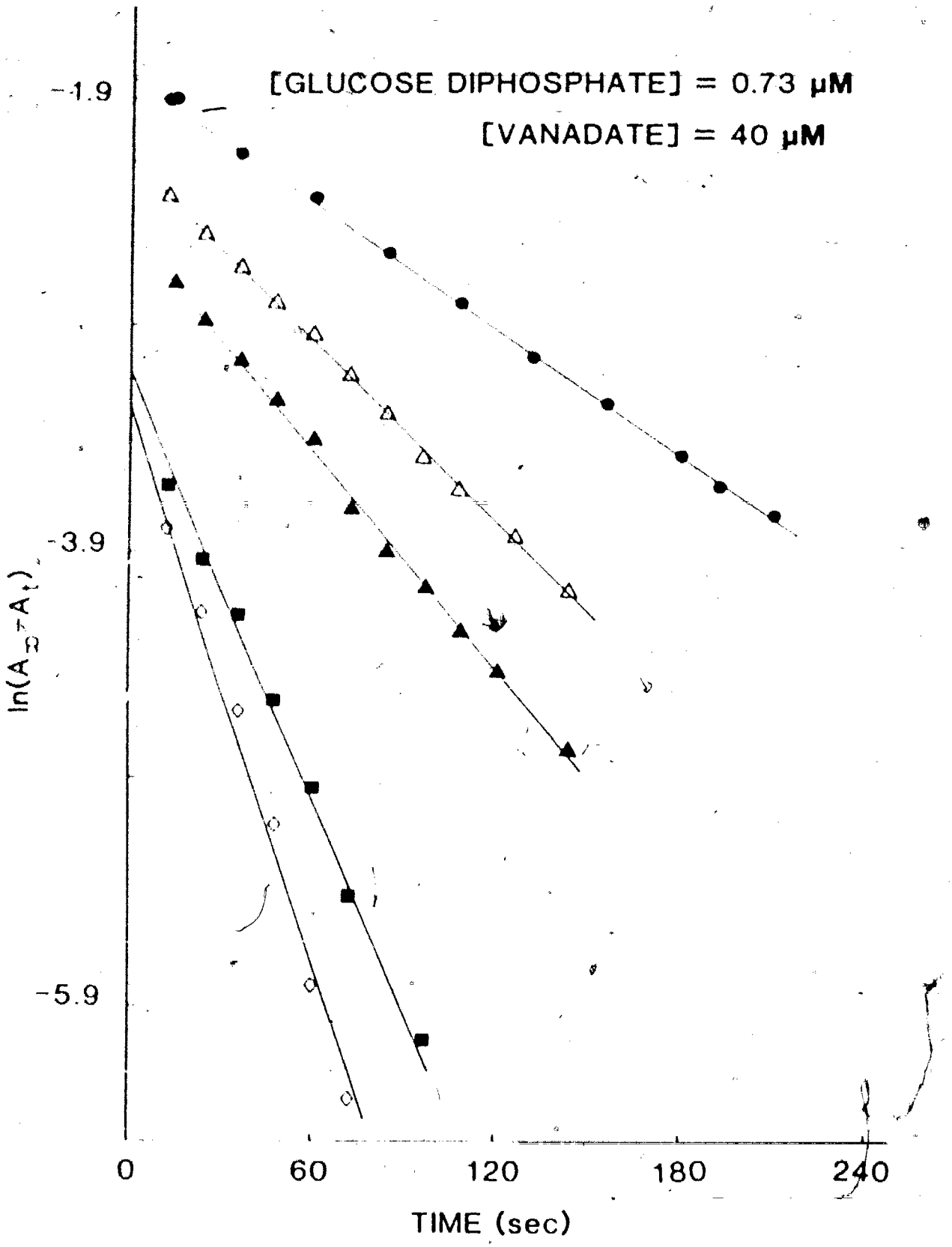
[GLUCOSE DIPHOSPHATE] = 0.73 µM
[VANADATE] = 40 µM
-1.9
-3.9
-5.9
ln(A∞-At)
0
60
120
180
240
TIME (sec)

inhibition follows first-order kinetics. The values of the apparent first-order rate constant (k_{obs}), obtained from the slopes of the semi-log plots, are listed in Table III. In Figure 15 the values of k_{obs} determined at 0.44 μM glucose-diphosphate and 40 μM vanadate are plotted against glucose 1-phosphate concentration.

Table III and the plot of Figure 15 show that the value of k_{obs} becomes larger as the concentration of glucose 1-phosphate in the assay is increased. It can also be seen that higher concentrations of glucose-diphosphate tend to decrease the value of k_{obs} i.e., oppose the onset of the slow inhibition. The dependence of k_{obs} on glucose 1-phosphate and vanadate concentration suggests that the time dependent inhibition is a product of both species acting together at the level of the free dephosphoenzyme (E). This supports the previous analysis of the steady-state data in the linear region of the progress curves, based on a model that accounts for the strong inhibition being due to a complex of glucose 1-phosphate 6-vanadate at the dephosphoenzyme.

To summarize the above observations; vanadate inhibition of the initial velocity of the mutase reaction occurs independently of glucose 1-phosphate concentration and yet, glucose 1-phosphate and vanadate together have an essential role in the time dependent inhibition . These results can be rationalized in terms of the reaction of a low equilibrium concentration of glucose 1-phosphate 6-vanadate, capable of binding tightly to the free dephosphoenzyme, being responsible for the slow onset of the strong inhibition as considered in the model of Figure 16.

Figure 15 also shows that k_{obs} approaches a limiting value at high concentrations of glucose 1-phosphate. In the absence of a particular feature of the mutase reaction i.e., the infrequent appearance of the free dephosphoenzyme and glucose diphosphate (30,31) such a trend in k_{obs} would not be expected for slow inhibition due to a low concentration of a tight binding glucose 1-phosphate 6-vanadate mixed diester. At the high concentrations of glucose 1-phosphate used in the experiment of Figure 14 the results are rationalized in terms of the inhibitor (mixed diester) binding to the dephosphoenzyme with an

TABLE III: Values for k_{obs} of phosphoglucomutase inhibition derived from the slope of the semi-log plots of Figure 14 obtained at 40μM vanadate in the presence of 0.44μM and 0.73μM glucose diphosphate, as a function of glucose 1-phosphate concentration.

[g-1-P] (mM)	k_{obs} ±6% (s^{-1}) 40μM vanadate, 0.44μM [g 1,6-P_2]	k_{obs} ±6% (s^{-1}) 40μM vanadate, 0.73μM [g 1,6-P_2]
0.27	0.007	-----
0.53	0.018	0.009
0.79	0.025	0.014
1.06	0.031	0.017
1.48	0.038	-----
2.12	0.041	0.029
2.38	0.047	-----
3.18	-----	0.042

a. [g-1-P] is the concentration of glucose 1-phosphate present in the assay.

b. [g 1,6-P_2] represents glucose diphosphate.

Figure 15

A plot of the k_{obs} values from Table III , obtained in the presence of 0.44μM glucose diphosphate and 40μM vanadate, against glucose 1-phosphate concentration. Data for this plot were obtained from the analysis of results of the experiment described in Figure 14.

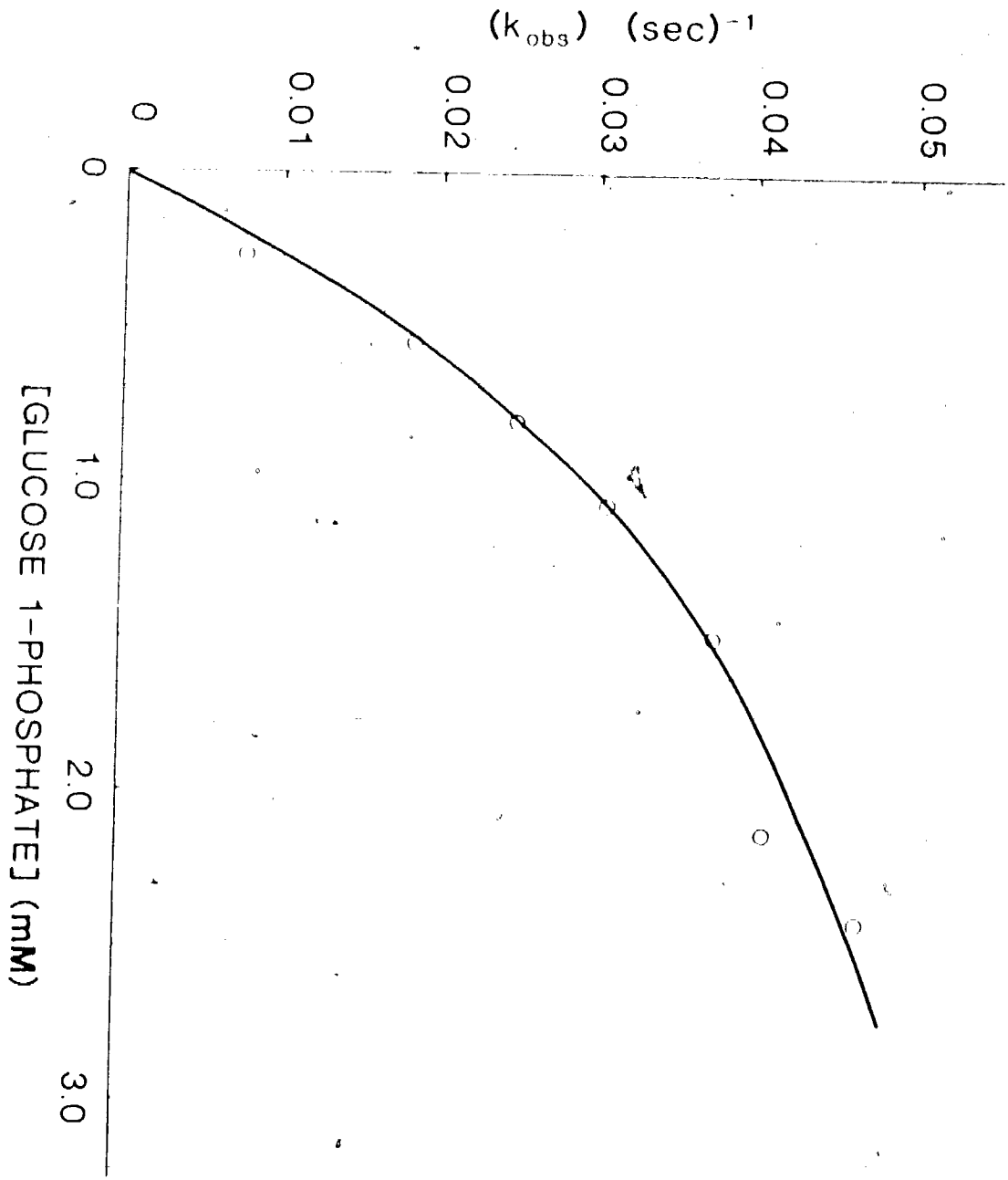
(k_{obs}) $(sec)^{-1}$
0
0.01
0.02
0.03
0.04
0.05
0
1.0
2.0
3.0
[GLUCOSE 1-PHOSPHATE] (mM)

apparent first order rate constant approaching closely that with which the free dephosphoenzyme appears off the main mutase reaction path. But for this feature of the mutase reaction k_{obs} would be expected to vary as a linear function of glucose 1-phosphate concentration.

In Figure 16 is shown the model proposed to account for the slow inhibition in terms of a low equilibrium concentration of glucose 1-phosphate 6-vanadate i.e., the rate limiting binding of inhibitor to the dephosphoenzyme . From this model an expression can be derived for k_{obs} that predicts the dependence of this apparent first order rate constant upon the concentration of glucose 1-phosphate, vanadate and glucose diphosphate present in the assay. The expression for k_{obs} is shown as follows (the derivation of the expression is given in Appendix III):

$$k_{obs} = \frac{\dfrac{k_3 \, Kds \, [T]}{[S]} + k_4}{1 + \dfrac{k_3[T]}{k_1[S]}} \qquad \text{Eq. 6}$$

where,

[T] = equilibrium concentration of glucose 1-phosphate 6-vanadate

[S] = concentration of glucose diphosphate, substrate of the free dephosphoenzyme

K_{ds} = taken as the Km for glucose diphosphate (using the value determined in this study).

k_3 = the bimolecular association rate constant for the mixed diester (T) binding to the free dephosphoenzyme (E).

k_4 = the unimolecular dissociation rate constant of the inhibited complex of dephosphoenzyme-glucose 1-phosphate 6-vanadate (ET).

k_1 = the bimolecular association rate constant for glucose diphosphate (S) binding to the dephosphoenzyme (E).

In the experiment of Figure 14 the effect of changing glucose 1-phosphate concentration on k_{obs} was examined. At the concentrations of glucose diphosphate

Figure 16

A proposed simple mechanism to account for the slow onset of inhibition of phosphoglucomutase , in terms of the reaction of a low, equilibrium concentration of glucose 1-phosphate 6-vanadate (T). In the figure, ES = complex of the dephosphoenzyme and glucose diphosphate. E = free dephosphoenzyme, ET = complex of dephosphoenzyme and tightly bound T, k = specific rate constants of the individual steps of the reaction, S = glucose diphosphate, substrate of the dephosphoenzyme.

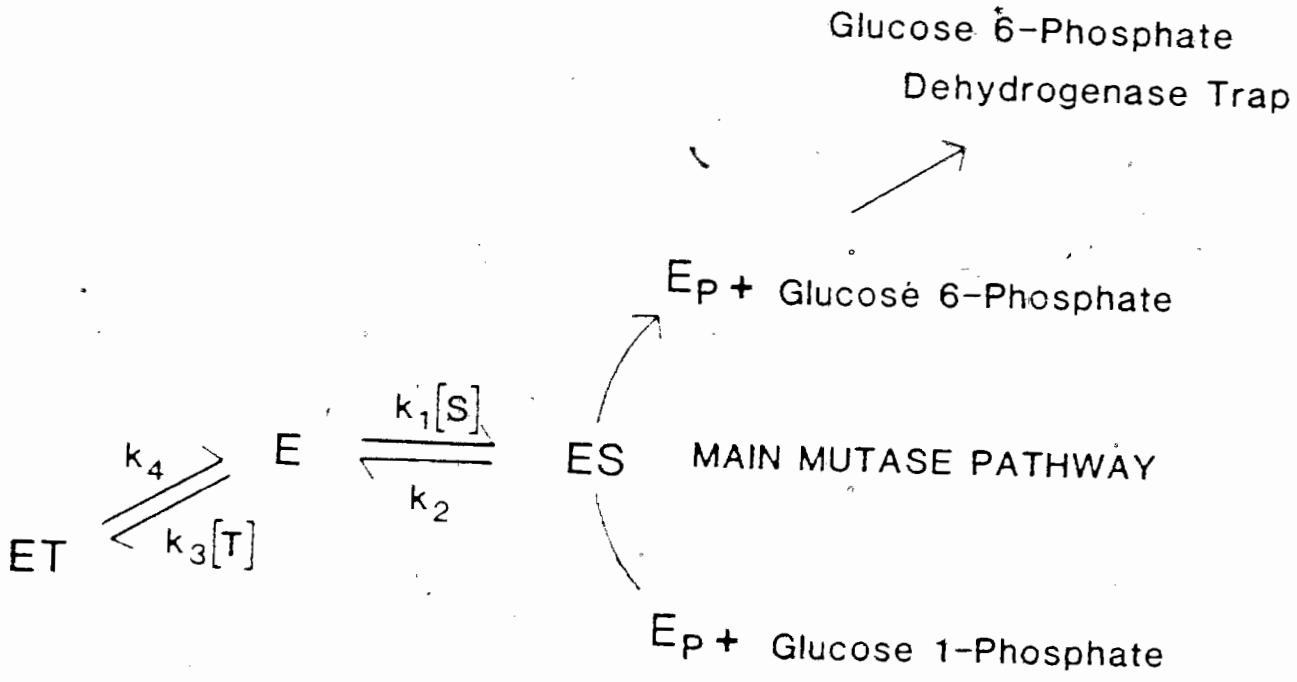
Glucose 6-Phosphate
Dehydrogenase Trap
E_P + Glucose 6-Phosphate
k_4
$k_3[T]$
ET
E
$k_1[S]$
k_2
ES
MAIN MUTASE PATHWAY
E_P + Glucose 1-Phosphate

employed ≤ Kmb, the apparent first-order rate constant (k_{obs}) is expected to be largely a function of the inhibitor binding steps shown in Figure 16. As the concentration of glucose 1-phosphate is increased so will the concentration of the mixed diester inhibitor (T). Hence the pseudo first-order rate constant k_3 [T] for the association step becomes large with respect to k_4 (k_4 must be by necessity small to account for tight binding) and is assumed to form the major contribution overall to k_{obs}. For this reason, in Equation 6 k_4 is dropped and the equation used to analyze the data of this experiment becomes,

$$\frac{1}{k_{obs}} = \frac{[S]}{k_3\ Kds\ [T]} + \frac{1}{k_2} \qquad \text{Eq. 7}$$

The terms in Equation 7 are as defined before except for k_2 which is the specific rate constant for the step in the model of Figure 16 that involves dissociation of glucose diphosphate and the free dephosphoenzyme off the main mutase pathway. Equation 7 predicts that under the above experimental conditions and taking account of the assumptions made, that a plot of $(k_{obs})^{-1}$ against $[T]^{-1}$ will be linear having a slope of:

$$\frac{[S]}{k_3\ Kds}$$

and a vertical intercept of,

$$\frac{1}{k_2}$$

In Figure 17 is shown a plot of $(k_{obs})^{-1}$ against [glucose 1-phosphate]$^{-1}$ obtained from the analysis of the data generated in the experiment of Figure 14 in terms of Equation 7, except that here the slope of the plot is given by

$$\frac{[S]}{k_3\ Kds\ Keq\ [I]}$$

where:

Keq = the equilibrium constant for vanadate ester formation at the 6-hydroxyl group on glucose 1-phosphate

[I] = concentration of free vanadate in the assay, which is taken to be the total concentration present.

The slope of the plot increases at higher glucose-diphosphate concentration as predicted by Equation 7. From the measured value of k_1 the slope of this plot and the known values for [S], K_{ds}, Keq and [I] all as defined earlier, a value for k_3 the association rate constant for the inhibitor binding step in the model of Figure 16, can be calculated.

The values determined from the slope of the plots in Figure 17 obtained at concentrations of 0.44 and 0.73 μM glucose-diphosphate were: $8.3 \pm 0.9 \times 10^6\ M^{-1}\ s^{-1}$ and $6.2 \pm 0.7 \times 10^6\ M^{-1}\ s^{-1}$ respectively. As can be seen both values are close enough to almost be within a single standard deviation of each other, hence the average of these values is taken as the closest estimate of the association constant k_3 and is equal to $7.3 \pm 1.2 \times 10^6\ M^{-1}\ s^{-1}$.

From the vertical intercept of the same plot a value for k_2 (defined above) was obtained equal to $7.9 \pm 0.5 \times 10^{-2}\ s^{-1}$. The half-time that corresponds to k_2, for the dissociation of glucose-diphosphate from the dephosphoenzyme is 8.7 seconds. Since phosphoglucomutase has a turnover number (k_{cat} value) of $10^3\ s^{-1}$, it can be seen that the free dephosphoenzyme will appear with a frequency of $1 \times 10^3\ s^{-1} / 7.9 \times 10^{-2}\ s^{-1} = 1.3 \times 10^4$ turnovers per dissociation. The above results support the previous explanation for the trend in k_{obs} values seen in the plot of Figure 15 as a function of glucose 1-phosphate concentration i.e., a change of the rate limiting step, from the binding of inhibitor to the free dephosphoenzyme to the rate limiting dissociation of glucose-diphosphate from the dephosphoenzyme at high inhibitor concentration. At the concentrations of mixed diester attained in this experiment the pseudo first order rate constant for the inhibitor association step can approach values close to that of k_3 above (see later).

Figure 17

A plot of $(k_{obs})^{-1}$ against $[g\text{-}1\text{-}P]^{-1}$ obtained from the analysis of data of the experiment in Figure 14, in terms of Equation 7 in the text. The figure shows the plots obtained at 0.44μM (●) and 0.73μM (▲) glucose diphosphate.

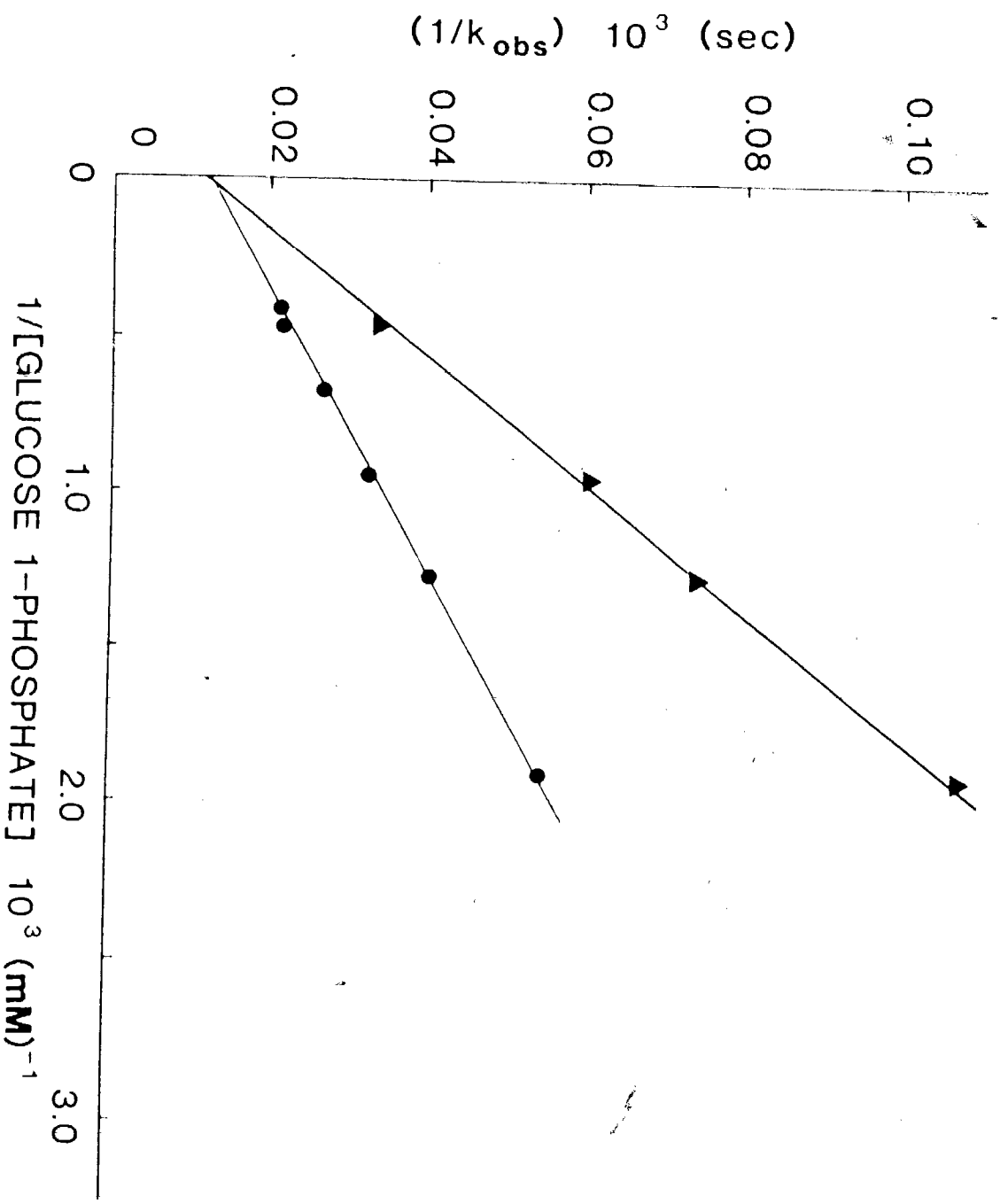
$(1/k_{obs})$ 10^3 (sec)
0.02
0.04
0.06
0.08
0.10
0
0
1.0
2.0
3.0
1/[GLUCOSE 1-PHOSPHATE] 10^3 $(mM)^{-1}$

The value for k_4, the rate constant of the inhibitor dissociation step can be calculated from progress curve data obtained in this study using a previously established relationship (42,43) in which the slope of the linear, steady-state region is given by,

$$vi = \frac{v_0 \, k_4}{kobs}$$

rearranging

$$k_4 = \frac{vi \; kobs}{v_0} \qquad \text{Eq.8}$$

where,

v_i = inhibited velocity in the steady state

v_o = initial velocity in the absence here, of effects due to the mixed diester inhibitor

k_{obs} = the observed first order rate constant for the approach to the inhibited steady state.

Using Equation 8 and the values determined for v_o, v_i and k_{obs} from the progress curves generated under the conditions of the experiment described in the legend to Figure 14, a value for k_4 was obtained equal to 3.3 $\pm$0.6 x 10^{-4} s^{-1}. The ratio of this k_4 value, to that determined for k_3 above gives the dissociation constant K_{vp} for the inhibited complex of the dephosphoenzyme with glucose 1-phosphate 6-vanadate. From the ratio k_4/k_3 a value of 4.5 $\pm$1.1 x 10^{-11} M was obtained for K_{vp} which is close to the value determined earlier from the steady state analysis of the data in Figure 10 where K_{vp} was found to equal 2.7 $\pm$0.4 x 10^{-11} M. The values determined for the rate constants k_3 and k_4 using the data from the experiment described in the legend to Figure 6 and the plot obtained in the presence of 20μM vanadate and 530μM glucose 1-phosphate were; k_3 = 7.9 $\pm$0.7 x 10^6 M^{-1} s^{-1} and k_4 = 4.9 $\pm$1.7 x 10^{-4} s^{-1}. The ratio of these two values k_4/k_3 gives an estimate of K_{vp} equal to 6.2 $\pm$2.2 x 10^{-11} M. At 530 μM glucose 1-phosphate, 40 μM vanadate and 0.44 μM glucose-diphosphate, and taking

K_{ds} as equal to K_{mb} (defined previously) the k_3 term in the numerator of Equation 6 on p.63, $k_3K_{ds}[T]/[S] = 2 \times 10^{-2}\ s^{-1}$, is a factor of 10^2 greater than the value of k_4 determined above. This calculation shows that dropping k_4 from Equation 6 in analysing the results of the experiment of Figure 14 was justified. Under the above conditions, the pseudo first-order rate constant of the inhibitor association step in the model of Figure 16 approaches closely the value of k_2 (defined earlier) equal to $7.9 \pm 0.5 \times 10^{-2}\ s^{-1}$.

The effect of glucose on vanadate inhibition

The experiment of Figure 18 was carried out to determine the effect of added glucose on vanadate inhibition of phosphoglucomutase. Conditions of reactant concentration, temperature and pH used in the experiment are detailed in the figure legend. The experiment was carried out at three different glucose concentrations of 1.3, 2.6 and 5.3 mM respectively in the presence of 40μM vanadate which was held constant throughout. Rates were collected over a range of glucose diphosphate concentration ~~as shown~~. All the reactants except glucose 1-phosphate were incubated for 3 minutes at 25° C prior to initiating the reaction with the substrate which was held constant at 100 μM. Control reactions were carried out to determine the extent of vanadate activated glucose oxidation catalyzed by the coupling dehydrogenase of the assay system. Only at the highest glucose concentration, i.e. 5.3 mM was an additional background rate seen. This activity represented approximately 2% of the recorded mutase rate, at the lowest concentration of glucose diphosphate used. Since the additional activity falls within the accepted limit of allowed experimental error (±5%) it could be safely ignored.

The double reciprocal plots of Figure 18 show a mixed pattern of competitive and noncompetitive inhibition. Increasing glucose concentration in the presence of constant vanadate caused enhanced competitive inhibition at the level of the free dephosphoenzyme as indicated by the increased slope of the 1/v against 1/[B] plots. The non-competitive component has its effect on the vertical intercept of these plots which becomes larger as the concentration of glucose in the reaction mixture increases and is considered to be the result of inhibition occurring at the

Figure 18

The effect of added glucose on vanadate inhibition of phosphoglucomutase. Reactions contained: 2 mM $MgCl_2$, 0.49 mM β-NADP$^+$, 0.80 mM EDTA, 0.048 U phosphoglucomutase, 0.26 U glucose 6-phosphate dehydrogenase, 20 mM Tris-Cl pH 7.6 at 25°C in a total volume of 1.0 ml. The figure shows a plot of reciprocal rate against reciprocal glucose-diphosphate concentration obtained in the presence of 40μM vanadate and at three concentrations of glucose, 1.3 (●), 2.6 (▲), 5.3 (△) mM respectively. An uninhibited line obtained in the absence of glucose and vanadate is also shown (○).

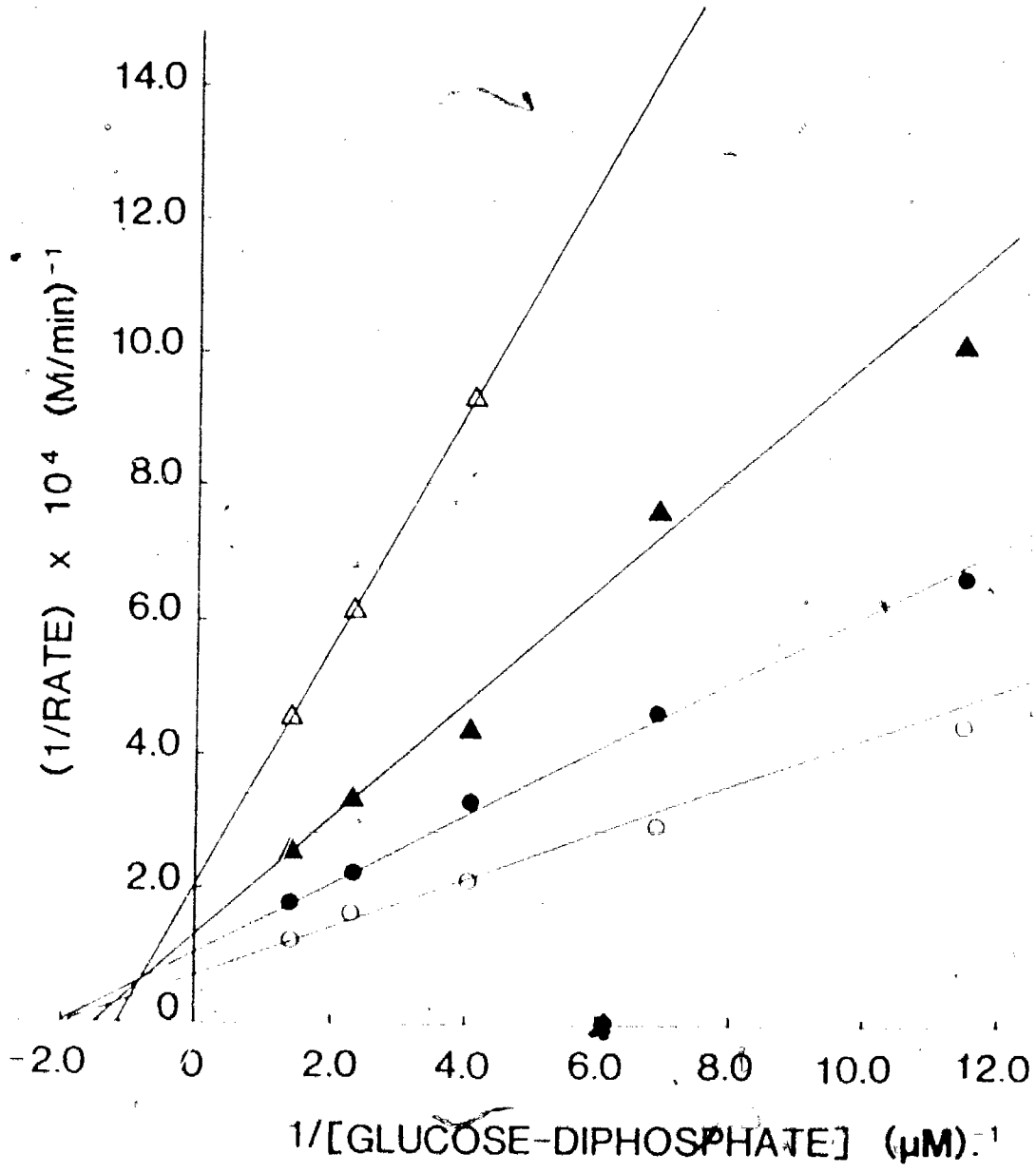
14.0
12.0
10.0
8.0
6.0
4.0
2.0
0
(1/RATE) x 10^4 (M/min)$^{-1}$
-2.0
0
2.0
4.0
6.0
8.0
10.0
12.0
1/[GLUCOSE-DIPHOSPHATE] (μM)$^{-1}$

active phosphoenzyme.

No presteady-state phase was observed in these experiments. It was therefore concluded that binding of glucose 1-phosphate 6-vanadate to the dephosphoenzyme did not contribute significantly to the inhibition observed in these experiments. The half-time ($t_{1/2}$) associated with the onset of inhibition ascribed to binding of glucose 1-phosphate 6-vanadate to the dephosphoenzyme at the concentration of glucose 1-phosphate used here, in the presence of 40μM vanadate and 0.44μM glucose diphosphate is 198.0 seconds determined from the data presented in the plot of Figure 15 and the relationship $t_{1/2} = \ln 2/k_{obs}$. Rate measurements on average were made 15 seconds after initiation of the reaction, in addition to mixing time this interval includes that taken for steady-state to be reached and represents the earliest opportunity that a rate could be measured from the spectrophotometric trace. The percentage deviation of the rates recorded at t=15 seconds from the expected initial rate at t=0 calculated for a halftime under the above conditions of 198.0 seconds using Equation 2 earlier, provides a measure of the extent to which mixed diester inhibition has progressed in this interval towards steady-state. It was found that the rates recorded at t=15 seconds differ by approximately 7% from the value calculated for the initial rate at t=0 seconds. Since the accepted limit of allowed experimental error in rate determinations is ±5% the recorded rates are seen not to vary significantly from the calculated initial rate. Hence inhibition due to mixed diester under the conditions used here is considered not to have developed sufficiently in this interval of 15 seconds to form a contribution toward the component of inhibition that has its effect on the slope of the plots in Figure 18 and which expresses itself during this time. The enhancement of vanadate inhibition by glucose at the dephosphoenzyme was rationalized in terms of an additional rapid component arising from vanadate esterification of glucose producing a glucose-vanadate ester. Though both the glucose 1-vanadate and glucose 6-vanadate esters will be present, the analysis of these results is considered only in terms of the more favoured glucose 6-vanadate ester (cf. Keq of 17.2 at 25°C, pH 7.0 in the presence of 25mM Mg^{2+} for α-D-glucose 6-phosphate/α-D-glucose 1-phosphate (25).There is no documented evidence that phosphate esters at the 2, 3

and 4 positions on glucose act as substrates or inhibitors of the enzyme and as such the behaviour of the corresponding vanadate esters, which are also likely to be present is uncertain.

Previous studies (18,20) have shown that both arsenate and vanadate esters of glucose are capable of acting as substrates in the phosphoglucomutase reaction. The noncompetitive inhibition detected in the vertical intercepts of the plots shown in Figure 18 was rationalized in terms of the ability of glucose 6-vanadate to serve as substrate for the active phosphoenzyme (EP), resulting ultimately in the formation of the inhibited complex of the dephosphoenzyme and tightly bound glucose 1-phosphate 6-vanadate. In the absence of effects arising from the slow inhibition due to mixed diester acting at the free dephosphoenzyme, the reaction of glucose 6-vanadate with the phosphoenzyme (EP) is considered to represent the only path under these experimental conditions by which the complex of the dephosphoenzyme and tightly bound mixed diester is generated. Figure 19 shows the model proposed to account for the steady-state behavior of the phosphoglucomutase reaction in the presence of glucose and vanadate. In the model inhibition is considered to occur at two levels:

a. at the free dephosphoenzyme (E) where the rapid components of inhibition due to free vanadate (I) and glucose 6-vanadate (D) take place competitive with the binding of glucose-diphosphate (B), and

b. at the active phosphoenzyme (EP) where the reaction of glucose 6-vanadate (D) competitive with the glucose monophosphate substrates (A or C), results in the formation of the inhibited complex of the dephosphoenzyme with glucose 1-phosphate 6-vanadate (mixed diester), (EAI) in the model.

Using the "King-Altman method" (32) a rate equation was derived for the model in Figure 19 (see appendix IV) in terms of which the steady-state behavior of phosphoglucomutase in the presence of inhibition due to vanadate and glucose 6-vanadate could be explained. The rate equation predicted by the model expressed in the form of the double reciprocal (Lineweaver-Burke) plot, showing reciprocal rate against reciprocal glucose-diphosphate concentration [B] is as follows:

Figure 19

Kinetic model proposed to account for the effect of glucose upon the inhibition of phosphoglucomutase activity by vanadate. The k's denote specific rate constants of the steps in the mechanism. In the model, B = glucose diphosphate, A = glucose 1-phosphate, C = glucose 6-phosphate, I = vanadate, D = glucose 6-vanadate, EP = phosphoenzyme, EB = complex of the dephosphoenzyme with glucose diphosphate, E = free dephosphoenzyme, EI = inhibited complex of the dephosphoenzyme with vanadate, ED = inhibited complex of the dephosphoenzyme with glucose 6-vanadate, EAI = inhibited complex of the dephosphoenzyme with glucose 1-phosphate 6-vanadate arising from the reaction of glucose 6-vanadate (D) at the phosphoenzyme (EP), EPA, EPC = complexes of the active phosphoenzyme with the glucose monophosphates (A and C) defined above.

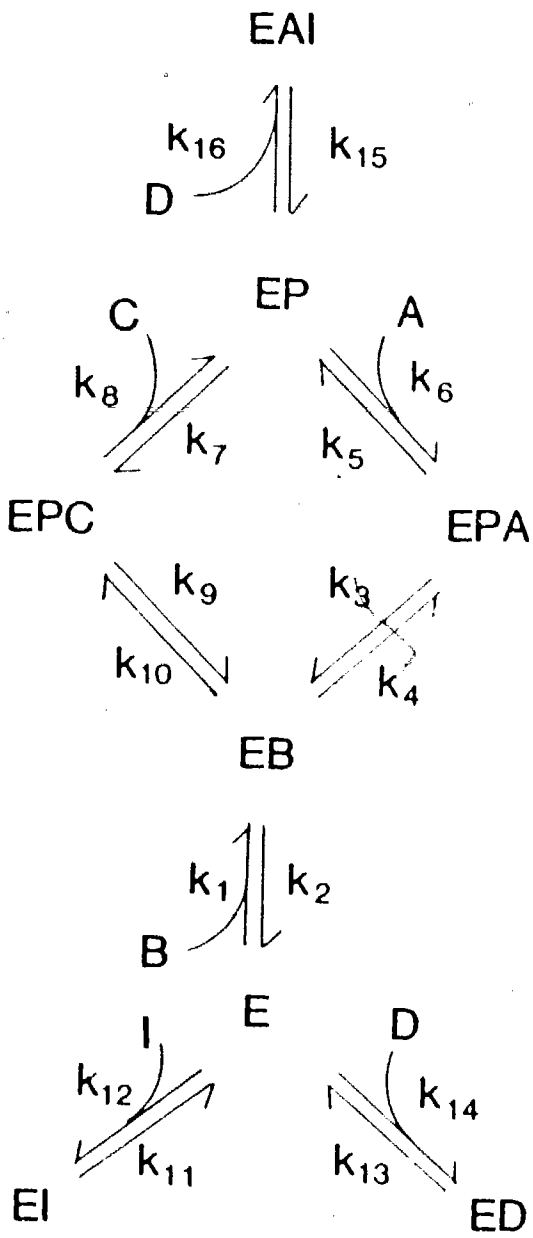
EAI
k16
k15
D
EP
C
A
k8
k6
k7
k5
EPC
EPA
k9
k3
k10
k4
EB
k1
k2
B
E
I
D
k12
k14
k11
k13
EI
ED

$$\frac{1}{v} = \left[\frac{Kma}{[A]} \left(1 + \frac{[glu][I]Keq}{Kgv^{\bullet}} \right) + \beta \right] . \frac{1}{Vm} + \frac{Kmb}{Vm} \left(1 + \frac{[I]}{Kv} + \frac{[D]}{Kgv} \right) . \frac{1}{[B]}$$

The terms in Equation 9 above are as defined previously except for:

[glu] = concentration of glucose present in the assay

Keq = the equilibrium constant for formation of glucose 6-vanadate

[D] = the equilibrium concentration of glucose 6-vanadate, at the concentrations of glucose and vanadate used in the assay and is given by [glu][I]Keq

$Kgv^{\bullet}$ = inhibition constant (i.e. Ki) for glucose 6-vanadate as a competitive inhibitor of the phosphoenzyme (EP)

Kgv = inhibition constant for glucose 6-vanadate as a competitive inhibitor at the level of the free dephosphoenzyme (E)

In the absence of effects arising from the slow inhibition as considered earlier, Equation 9 shows that the slopes of reciprocal 1/v against 1/[B] plots such as those of Figure 18, in the presence of competitive inhibition due to vanadate (I) and glucose 6-vanadate (D) acting at the free dephosphoenzyme (E) will increase with higher glucose and vanadate concentrations as follows:

$$\text{slope} = \frac{Kmb}{Vm} \left(1 + \frac{[I]}{Kv} + \frac{[glu][I]Keq}{Kgv} \right) \qquad \text{Eq. 10}$$

Rearranging, Equation 10 becomes,

$$\text{slope} = \frac{Kmb}{Vm}\left(1 + \frac{[I]}{Kv}\right) + \frac{Kmb\ Keq[I][glu]}{Vm\ Kgv} \qquad \text{Eq. 11}$$

As shown in Figure 20 and predicted by Equation 11 a replot of slope of the reciprocal plots of Figure 18 against glucose concentration at constant vanadate is linear having a slope of:

$$\frac{Kmb}{Vm} \cdot \frac{Keq[I]}{Kgv}$$

and a vertical intercept of:

$$\frac{Kmb}{Vm}\left(1 + \frac{[I]}{Kv}\right)$$

Kmb/Vm, can be obtained from the slope of the reciprocal plot in Figure 18 seen in the absence of inhibition due to vanadate and glucose 6-vanadate, with this value and that for Keq = 0.084 M^{-1} and the known concentration of vanadate used in the assay [I], K_{gv} can be found from the slope of the replot. The value for K_{gv} i.e., the inhibition constant for the complex of dephosphoenzyme with glucose 6-vanadate, (ED) in the model, was calculated to be 3.9 $\pm$0.4 x 10^{-6} M. From the replot intercept the value of K_v was determined to be 46 $\pm$7 x 10^{-6} M. It can be seen from these results that the added presence of glucose enables vanadate in the form of its glucose 6-vanadate ester to bind to the free dephosphoenzyme a factor of 10^4 times more tightly than nonesterified vanadate. Large apparent first order rate constants for the inhibitor association step at the concentrations of glucose 6-vanadate likely to appear at the values of glucose concentration used in this experiment plus a larger off rate constant would account for the faster onset of inhibition and the absence of slow time dependent effects. Hence the sensitivity which is seen in the response of the initial velocity of the mutase reaction to changes in the glucose concentration.

Figure 20

A primary replot of the data in Figure 18 i.e., slope of the double reciprocal plots against glucose concentration: 1.3mM, 2.6mM and 5.3mM . A linear regression technique was used to fit the line to the data points. From the slope of the replot a value of K_i i.e., the inhibition constant for glucose 6-vanadate as a competitive inhibitor of the free dephosphoenzyme is obtained,

$K_{gv} = 3.9 \pm 0.4 \times 10^{-9}$ M.

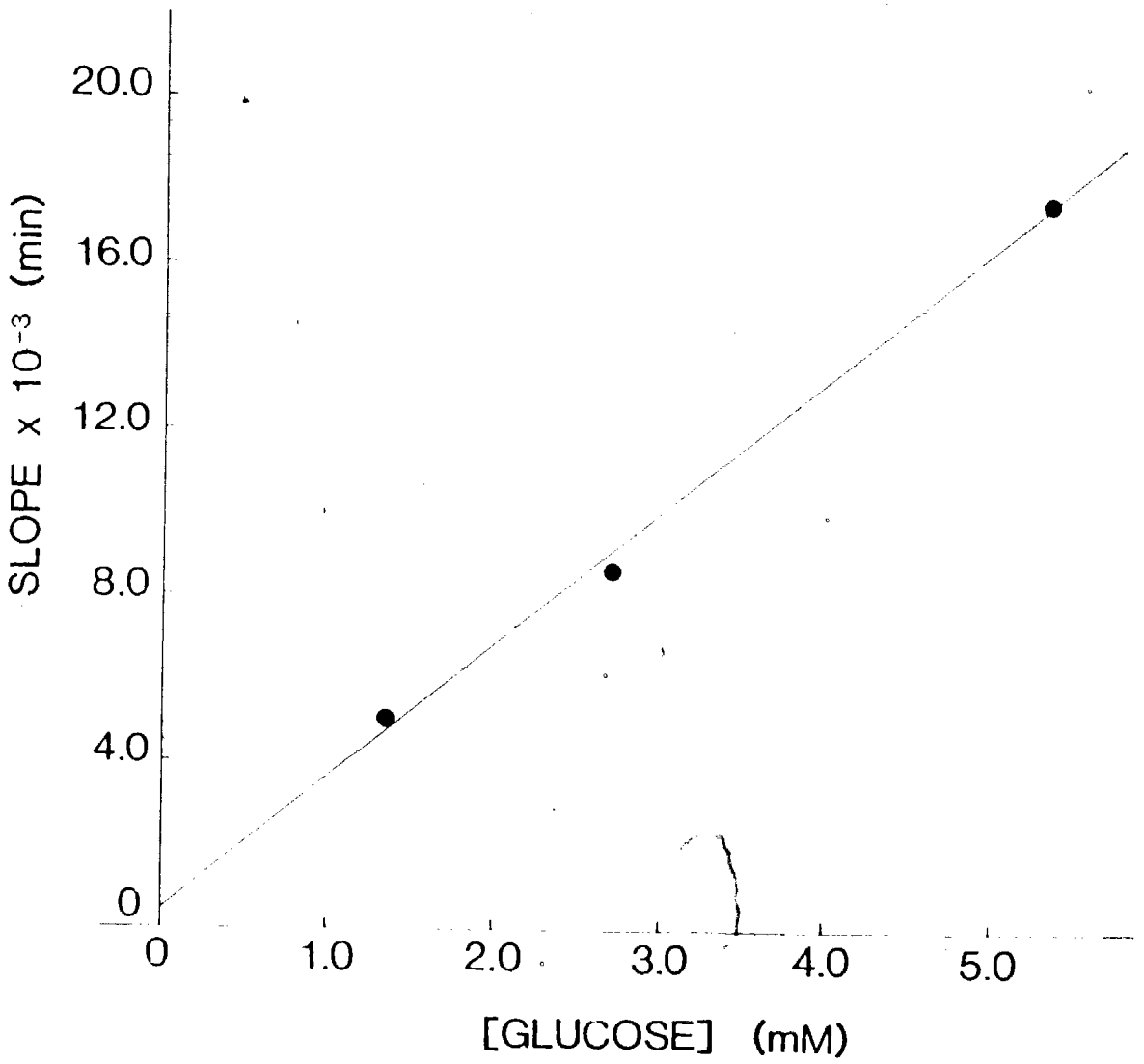
20.0
16.0
12.0
8.0
4.0
0
SLOPE x 10⁻³ (min)
0
1.0
2.0
3.0
4.0
5.0
[GLUCOSE] (mM)

In terms of the model shown in Figure 19, binding of glucose 6-vanadate to the phosphoenzyme (noncompetitive vs. glucose-diphosphate) is predicted to be manifested as an intercept effect in the plots shown in Figure 18. From Equation 9 given earlier, this effect can be analysed quantitatively in terms of Equation 12 for the vertical intercept of a plot of 1/v against 1/[B].

$$\text{intercept} = \left[\frac{Kma}{[A]} \left(1 + \frac{[glu][I]Keq}{Kgv^*} \right) + \beta \right] . \frac{1}{Vm} \qquad \text{Eq. 12}$$

Equation 12 shows that at constant vanadate and non-saturating glucose 1-phosphate concentrations, the effect of increasing glucose concentration will be to increase the value of the vertical intercept. Rearranging, Equation 12 becomes:

$$\text{intercept} = \left(\frac{Kma}{[A]} + \beta \right) . \frac{1}{Vm} + \frac{Kma\ Keq\ [I][glu]}{[A]\ Vm\ Kgv^*} \qquad \text{Eq. 13}$$

As shown in Figure 21 and predicted by Equation 13, a replot of intercept against glucose concentration, at constant vanadate and non-saturating glucose 1-phosphate concentrations, is linear having a slope of:

$$\frac{Kma\ Keq\ [I]}{[A]\ Vm\ Kgv^*}$$

and a vertical intercept of,

$$\left(\frac{Kma}{[A]} + \beta \right) . \frac{1}{Vm}$$

Vm, can be obtained from the replot intercept and the known values of Kma and the concentration of glucose 1-phosphate ([A]) used in the experiment. With these values and that for Keq = 0.084 M^{-1} and the known concentration of vanadate [I], K_{gv^*} can be found from the slope of the replot. The value of K_{gv^*} the inhibition constant for glucose 6-vanadate as a competitive inhibitor of the active

Figure 21

A primary replot of the data in Figure 18 i.e., intercept of the double reciprocal plots against glucose concentration: 1.3mM, 2.6mM and 5.3mM. A linear regression technique was used to fit the line to the data points. From the slope of the replot a value of K_i, the inhibition constant for glucose 6-vanadate as a competitive inhibitor of the phosphoenzyme is obtained

$K_{gv*} = 2.4 \pm 0.3 \times 10^{-3}$ M.

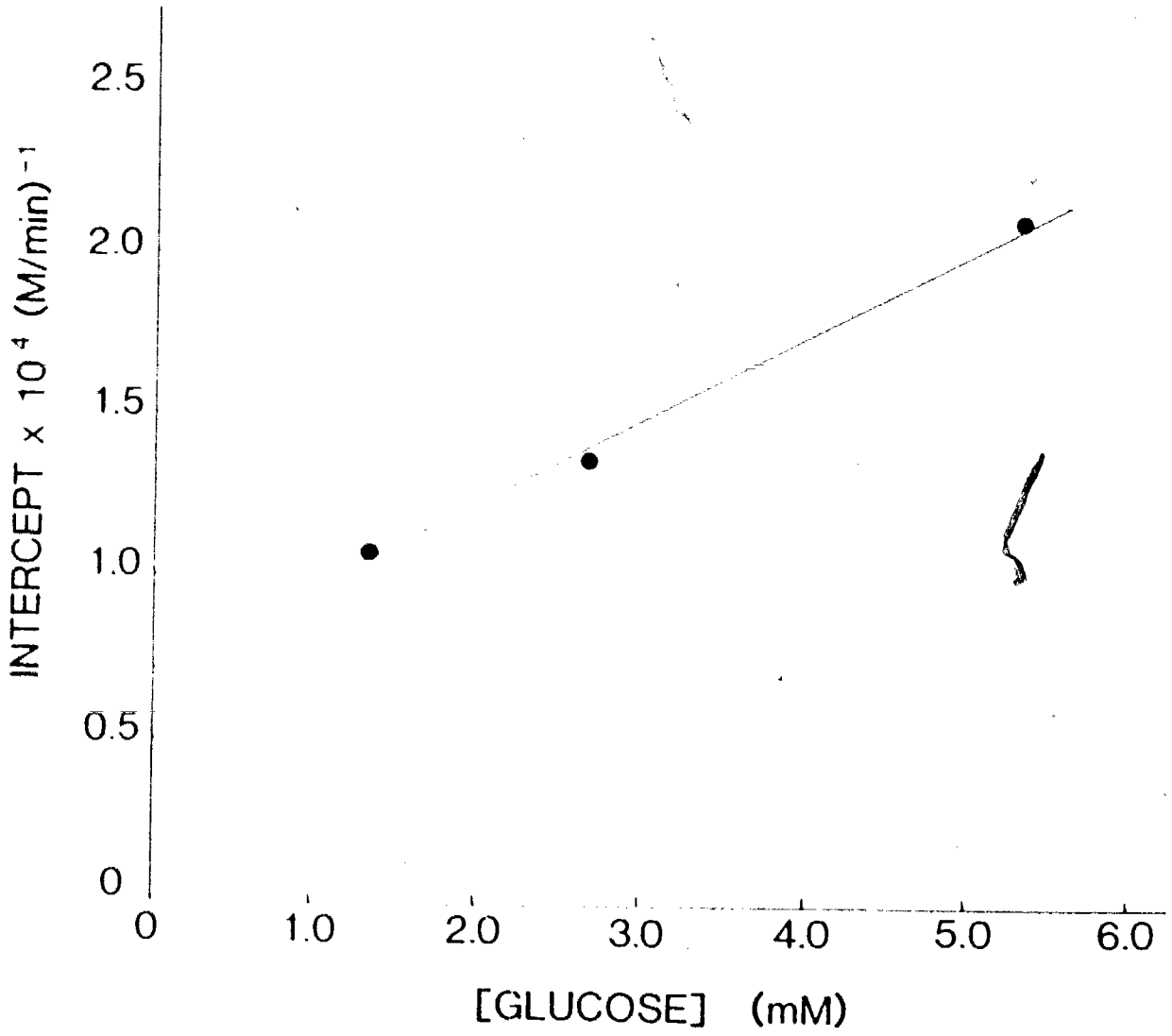
INTERCEPT x 10^4 (M/min)$^{-1}$
2.5
2.0
1.5
1.0
0.5
0
0
1.0
2.0
3.0
4.0
5.0
6.0
[GLUCOSE] (mM)

phosphoenzyme was calculated to be 2.4 ±0.3 x 10^{-9} M.

The favourable thermodynamic pull of the reaction that leads to the generation of tightly bound mixed diester on the dephosphoenzyme is considered to be what enables glucose 6-vanadate to act competitively with respect to glucose 1-phosphate binding at the phosphoenzyme. The meaning of the value determined for K_{gv*} and what it implies about the catalytic mechanism of the normal mutase reaction (i.e. the feature that enables glucose 6-vanadate inhibition at EP) can be obtained from a consideration of the thermodynamic scheme presented in Figure 22, and what is known about the substrate binding site of the dephosphoenzyme.

Figure 22 shows the thermodynamic box used to interpret the value of K_{gv*} in terms of the mechanism proposed for glucose 6-vanadate as a competitive inhibitor of the phosphoenzyme (EP). The top line and right-hand side of the box show the reaction of glucose 6-vanadate with EP leading to the formation of the inhibited complex of the dephosphoenzyme and tightly bound mixed diester (ED*.g1P,6V). The bottom line of the box shows the reaction involved in the inhibition caused by binding of glucose 1-phosphate 6-vanadate to the dephosphoenzyme to yield the same dead-end complex. The left-hand side of the box completes the thermodynamic cycle, and makes it possible to determine whether the K_i values corresponding to the two modes of inhibition are consistent with the value of K_3, which can be estimated as described below. The standard free energy of hydrolysis of EP has been estimated at -1.0 kcal mol^{-1} at pH 7.5 and 25°C (44), and under the same conditions the standard free energy of glucose 1-phosphate formation from glucose and phosphate has been estimated at +4.2 kcal mol^{-1} (45). If it is assumed that the standard free energy of formation of glucose 1-phosphate 6-vanadate from glucose 6-vanadate and phosphate is also +4.2 kcal mol^{-1}, then the standard free energy corresponding to K_1 is -3.2 kcal mol^{-1}, and $K_1 = 2.3 \times 10^2$. In terms of the models shown in Figures 8 and 19, $K_{gv*} = K_1 \cdot K_2 = 2.4 \pm 0.3 \times 10^{-9}$ M, and $K_{vp} = K_4 = 2.7 \pm 0.4 \times 10^{-11}$ M. The thermodynamic cycle shown in Figure 22 requires that $K_3 = K_1 K_2 / K_4 = 0.89 \times 10^2$. This value is reasonably close to the value for K_3 calculated as described above from published values of the free energies of hydrolysis of the phosphoenzyme and glucose 1-phosphate. This

Figure 22

Thermodynamic box used to interpret the value of K_{gv^*} in terms of a possible mechanism for glucose 6-vanadate as a competitive inhibitor of the phosphoform of phosphoglucomutase. In the scheme, EP = phosphoenzyme, V = vanadate, g6-V= glucose 6-vanadate, g1P,6V = glucose 1-phosphate 6-vanadate, E = dephosphoenzyme, ED.g1P,6V and ED*.g1P,6V represent isomerizing complexes of the dephosphoenzyme with bound mixed diester, the latter complex the one in which mixed diester is bound tightly, stabilized as a transition state analogue.

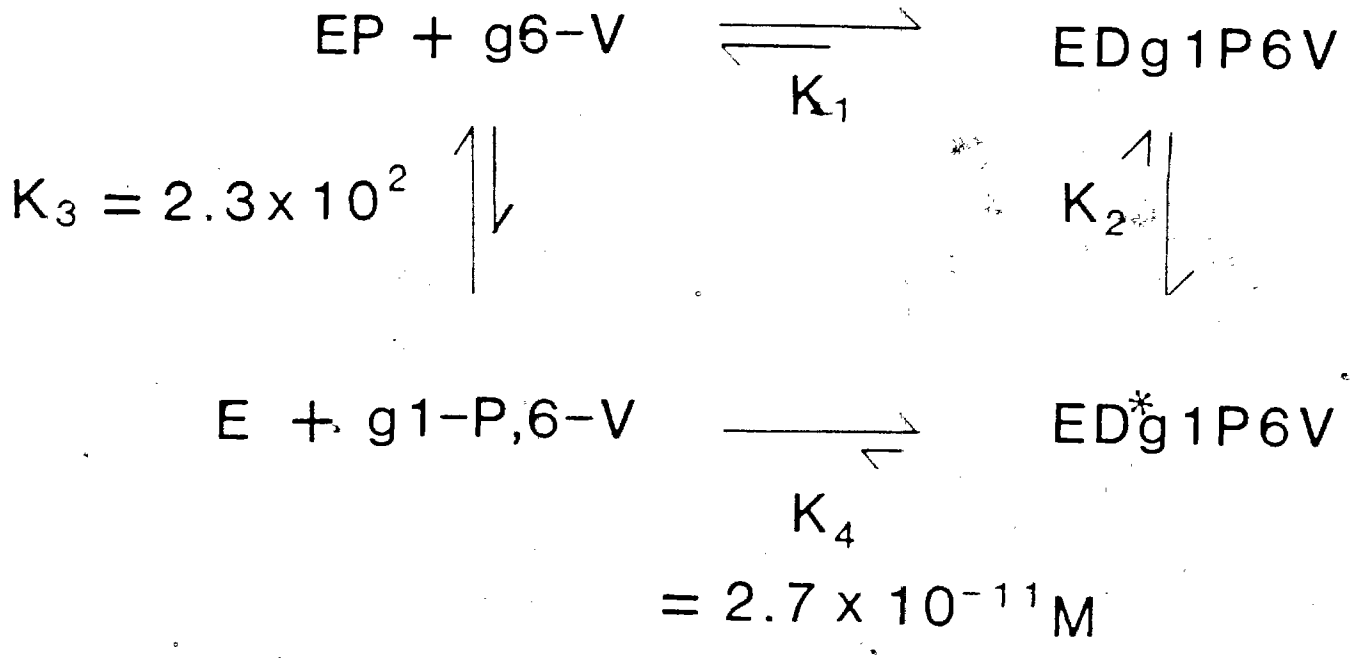
EP + g6-V
EDg1P6V
K1
K3 = 2.3x10^2
K2
E + g1-P,6-V
ED*g1P6V
K4
= 2.7 x 10^-11 M

agreement is about as close as can reasonably be expected for a comparison of this sort, and it supports the model used to rationalize the results of the inhibition studies reported here.

Evidence from earlier studies had pointed toward the existence of two intrinsically different phosphoryl group binding subsites being present on the dephosphoenzyme. Published results have shown that a single strong phosphate binding subsite is common to both the phospho and dephosphoforms of phosphoglucomutase with an additional substantially weaker phosphate binding subsite present on the dephosphoenzyme considered to be the site at which phosphoryl transfer takes place (46,47). The presence of two phosphoryl group binding subsites, only one of which has the ability to transfer a phosphoryl group to the enzyme, supports the earlier proposed "Exchange" hypothesis in which two different complexes of the dephosphoenzyme with glucose 1,6-diphosphate appear on the reaction pathway. In one of these complexes transfer of the 6-phosphoryl group of glucose-diphosphate to the dephosphoenzyme could occur while in the other transfer of the 1-phosphoryl group would be possible. Interconversion of the two complexes would require an exchange of position or reorientation of the two phosphoryl groups of the substrate relative to the phosphate binding subsites on the dephosphoenzyme, and would have to occur *via* a process that involved only a partial dissociation of glucose-diphosphate.

In terms of the "Exchange" hypothesis and the presence of two different phosphoryl group binding subsites it is possible to arrive at an explanation for the feature of the catalytic mechanism of the mutase reaction, specifically the nature of the step on the dephosphoenzyme, that leads to the inhibited complex of the dephosphoenzyme and tightly bound mixed diester (ED•g1P,6V) in Figure 22. Figure 23 shows a schematic representation of the substrate binding site on the dephosphoenzyme, in which the reorientation of glucose 1-phosphate 6-vanadate (mixed diester) with respect to the weak and strong phosphoryl group binding subsites is regarded as the step that supplies the 'driving force' behind glucose 6-vanadate inhibition at the phosphoenzyme. In the complex of the dephosphoenzyme with mixed diester (ED.g1P,6V) produced initially, the 1-phosphoryl

Figure 23

Schematic representation of the substrate binding site on the dephosphoenzyme. The diagram shows the reorientation of glucose 1-phosphate 6-vanadate (mixed diester) with respect to the weak and strong phosphoryl group binding subsites as the step providing the 'driving force' behind glucose 6-vanadate inhibition at the phosphoenzyme (EP).

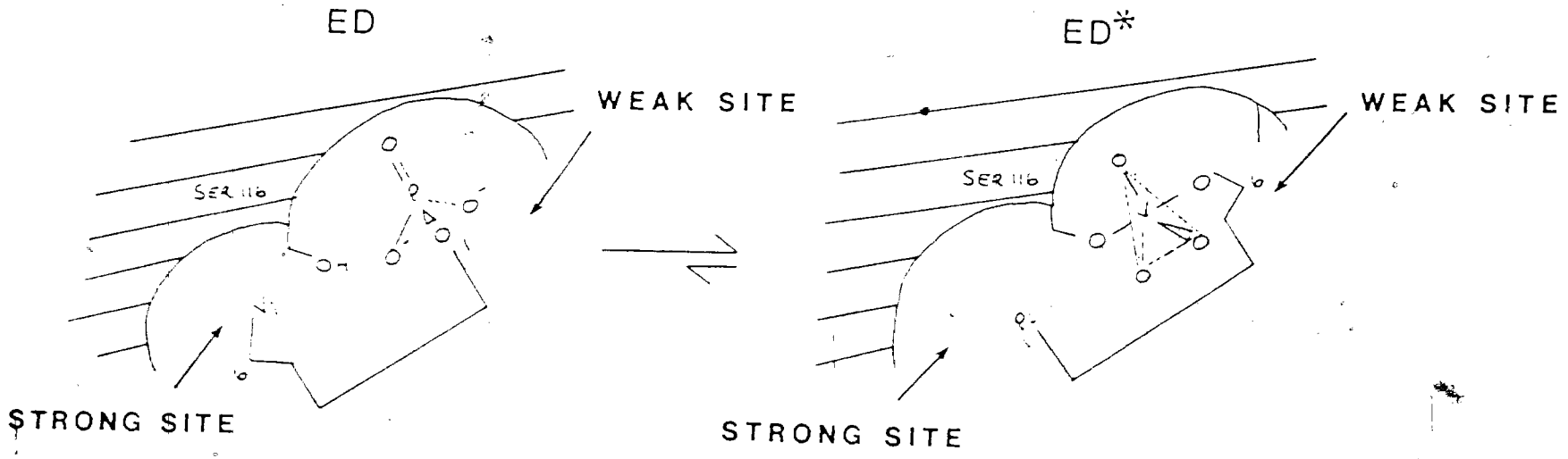
ED
WEAK SITE
SER 116
STRONG SITE
ED*
WEAK SITE
SER 116
STRONG SITE

group is at the weak site with the 6-vanadate group located at the strong site where its ability to readily assume a five-coordinate structure will not result in tight binding, because the strong site provides no special stabilization of this structure. Inorder for inhibition to develop, the next step has to involve a rearrangement of the mixed diester on the dephosphoenzyme. This enables the 1-phosphoryl and 6-vanadate groups of the substrate to exchange positions relative to the weak and strong phosphate binding subsites. In this way the 6-vanadate group could then occupy the weak site where it readily adopts the penta-coordinate, trigonal bipyramidal geometry characteristic of the transition state for a phosphoryl transfer step to the enzyme (24). What these results suggest is that partial dissociation and rearrangement of the glucose-diphosphate molecule on the dephosphoenzyme as proposed by the "Exchange" hypothesis is a feature of the catalytic mechanism of the normal mutase reaction. The phosphoryl group which is transferred to the enzyme is determined by the positioning of the glucose-diphosphate molecule with respect to weak (high transfer potential) and strong (low transfer potential) phosphoryl group binding subsites. The outcome of such a rearrangement in the mechanism of glucose 6-vanadate inhibition at EP is the stabilization of the mixed diester as a transition state analogue at the active site of the enzyme which gives rise to the inhibited complex of the dephosphoenzyme with tightly bound mixed diester (ED•g1P,6V).

CONCLUSION

The strong inhibition of *Rabbit muscle* phosphoglucomutase seen in the presence of vanadate results from the ability of this anion to form labile esters with hydroxyl groups on physiological substrates; in this case, resulting in the formation of a glucose 1-phosphate 6-vanadate, mixed diester. Despite being present at low concentration, in the range of 10^{-10} - 10^{-11} M at micromolar levels of vanadate, it can act as a competitive inhibitor by virtue of binding more tightly to the free dephosphoenzyme than the normal substrate which it mimics structurally. The tight binding results from the ease with which the vanadate ester adopts the pentacoordinate, trigonal bipyramidal geometry characteristic of the transition state for a phosphoryl transfer step to the protein (24). The rapid component of inhibition seen can reasonably be ascribed to direct esterification by vanadate from solution of the serine 116 hydroxyl group on the dephosphoenzyme. The tight binding develops because of the stabilization of the mixed diester as a transition state analogue at the enzyme active site (48). The normal criterion of transition state analogue behavior is binding constants that fall in the range 10^{2} - 10^{4} times greater than that of the normal substrate (41). The results reported here show that glucose 1-phosphate 6-vanadate binds a factor of at least 10^{3} times more tightly to the dephosphorylated form of phosphoglucomutase than does the glucose diphosphate substrate. The gradual increase in the binding affinity of free vanadate, glucose vanadate and glucose 1-phosphate 6-vanadate seen, arises from the additional binding contribution afforded by the larger leaving group (H_2O --> glucose --> glucose 1-phosphate) towards stabilization of the vanadate ester on the enzyme.

That the strong inhibition of phosphoglucomutase is due to a low concentration of a tight binding mixed diester, reacting with the free dephosphoenzyme in a step that has a large second order rate constant, is suggested by the observed first order kinetics which govern the approach to the inhibited steady state. The apparent first order rate constant was found to increase with the concentrations of glucose 1-phosphate and vanadate used in the reaction

mixture. This indicates that both species together actively contribute to the inhibition at the free dephosphoenzyme. At high concentrations of glucose 1-phosphate, however, the apparent first-order rate constant was found to reach a limiting value of 7.9 ±0.5 x 10^{-2} s^{-1}. This has been explained in terms of a change of the rate limiting step at high inhibitor concentration, from the bimolecular association of the mixed diester to the rate limiting appearance of the free dephosphoenzyme arising from the dissociation of glucose-diphosphate off the mutase reaction path. From the limiting value determined for k_{obs} and the value of the turnover number (k_{cat}) for the phosphoglucomutase reaction of 10^3 s^{-1} it is estimated that the free dephosphoenzyme will appear once in every 1.3 x 10^4 catalytic cycles. Evidence supporting this interpretation based on a feature of the mechanism of the mutase reaction, as opposed to some rate limiting step in the enzyme-inhibitor complex, eg., a conformational change , is obtained from the results of the experiment which was conducted to determine the effect of glucose on vanadate inhibition. In this experiment the non-competitive inhibition detected as the effect on the vertical intercepts of the plots shown in Figure 18 was rationalized in terms of a glucose 6-vanadate ester acting as substrate for the phosphoenzyme (EP). The absence of a presteady-state phase in the glucose enhanced vanadate inhibition is taken as evidence against a rate-limiting conformational change. The results of this experiment suggest in favour of the rate-limiting step at high inhibitor concentration being a property of the mutase mechanism, namely an infrequent appearance of the free dephosphoenzyme. The same experiment also sheds light on another feature of the mutase mechanism ; specifically the reaction step that controls phosphoryl transfer in the complex of the dephosphoenzyme with glucose-diphosphate. It is possible to explain glucose 6-vanadate competitive inhibition at the phosphoenzyme in terms of the earlier "Exchange" hypothesis and the established presence of two phosphoryl group binding subsites which differ in their tendancy to transfer a phosphoryl group to and from the enzyme. The conclusion that can be drawn from the results is that partial dissociation and rearrangement of the glucose-diphosphate molecule on the dephosphoenzyme as proposed by the "Exchange" hypothesis is a feature of the catalytic mechanism of the normal mutase reaction. The phosphoryl group on the

substrate that becomes transferred to the enzyme is determined by the positioning of the glucose-diphosphate molecule with respect to the weak (high transfer potential) and strong (low transfer potential) phosphoryl group binding subsites present on the dephosphoenzyme.

APPENDIX I

Derivation of the rate equation for the model in Figure 1 describing the Ping-Pong mechanism of phosphoglucomutase in the absence of inhibition due to vanadate. The model of Figure 1 can be described by 4 open patterns of (n-1) sides, where n refers to the number of enzyme intermediates. Referring to Figure 1 the basic pattern is:

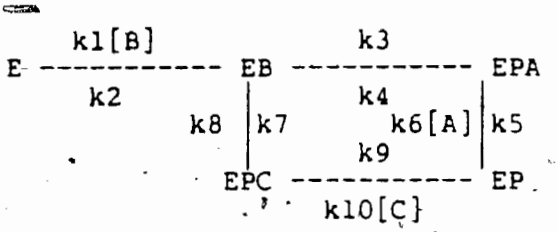

The four open patterns are as follows:

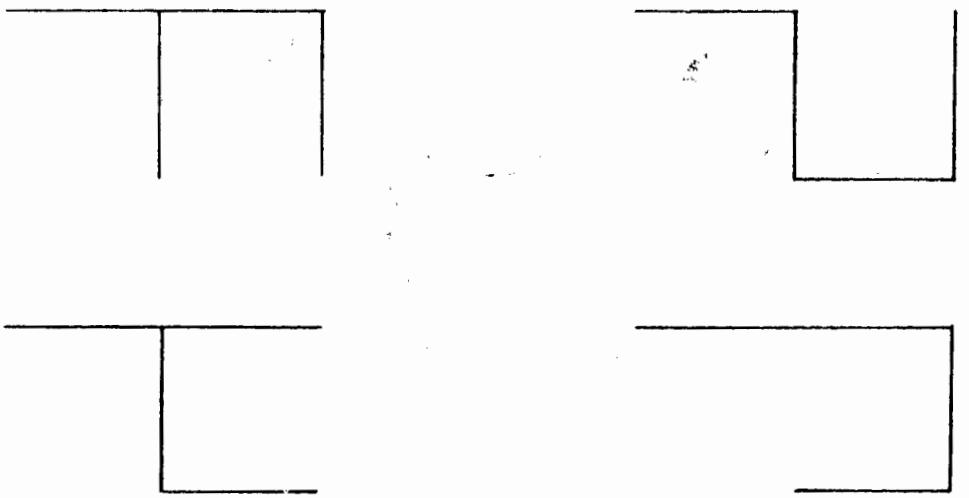

The distribution equations for the intermediates appearing in the model obtained using the four open patterns above are:

$$
\begin{aligned}
E/e &= k_6\,[A]\,k_4\,k_2\,k_8 \\
&\quad + k_5\,k_{10}\,[C]\,k_8\,k_2 \\
&\quad + k_9\,k_6\,[A]\,k_4\,k_2 \\
&\quad + k_{10}\,[C]\,k_8\,k_4\,k_2 \\
&= \mathrm{coef}_E\,[A]
\end{aligned}
$$

$$
\begin{aligned}
EB/e &= k_6\,[A]\,k_4\,k_8\,k_1\,[B] \\
&\quad + k_1\,[B]\,k_3\,k_5\,k_{10}[C]\,k_8 \\
&\quad + k_1\,[B]\,k_9\,k_6\,[A]\,k_4 \\
&\quad + k_{10}\,[C]\,k_8\,k_4\,k_1\,[B] \\
&= \mathrm{coef}_{EB}\,[A]\,[B]
\end{aligned}
$$

$$
\begin{aligned}
EPA/e &= k_1\,[B]\,k_3\,k_8\,k_6\,[A] \\
&\quad + k_1\,[B]\,k_7\,k_9\,k_6\,[A] \\
&\quad + k_1\,[B]\,k_3\,k_9\,k_6\,[A] \\
&\quad + k_1\,[B]\,k_3\,k_{10}\,[C]\,k_8 \\
&= \mathrm{coef}_{EPA}\,[A]\,[B]
\end{aligned}
$$

$$
\begin{aligned}
EPC/e &= k_1\,[B]\,k_7\,k_6\,[A]\,k_4 \\
&\quad + k_1\,[B]\,k_7\,k_5\,k_{10}\,[C] \\
&\quad + k_1\,[B]\,k_3\,k_5\,k_{10}\,[C] \\
&\quad + k_{10}\,[C]\,k_4\,k_8\,k_1\,[B] \\
&= \mathrm{coef}_{EPC}\,[A]\,[B]
\end{aligned}
$$

$$
\begin{aligned}
EP/e &= k_1\,[B]\,k_8\,k_3\,k_5 \\
&\quad + k_1\,[B]\,k_7\,k_9\,k_5 \\
&\quad + k_1\,[B]\,k_3\,k_5\,k_9 \\
&\quad + k_1\,[B]\,k_8\,k_9\,k_4 \\
&= \mathrm{coef}_B\,[B]
\end{aligned}
$$

Since the rate of the reaction is given by

$$v = k_9 [EPC]$$

and the conservation equation is

$$e = [E] + [EB] + [EPA] + [EPC] + [EP]$$

then

$$v/e = \frac{k_9 [EPC]}{[E] + [EB] + [EPA] + [EPC] + [EP]}$$

and therefore

$$v/e = \frac{k_9 \, coefEPC \, [A] \, [B]}{coef_E \, [A] + coef_{EB} \, [A] \, [B] + coef_{EPA} \, [A] \, [B] + coef_{EPC} \, [A] \, [B] + coef_{EP} \, [B]}$$

Dividing numerator and denominator by $coef_{EPC}$ the terms in the equation become:

$coef_{EPC}/coef_{EPC} = 1$

$coef_{EB}/coef_{EPC}$ = a constant (c')

$coef_{EPA}/coef_{EPC}$ = a constant (c")

$coef_E/coef_{EPC} = Kb$

$coef_{EP}/coef_{EPC} = Ka$

Substituting for these terms in the above equation gives:

$$v/e = \frac{k_9 [A] [B]}{Kb [A] + Ka [B] + [A] [B] (1 + c' + c")}$$

Dropping the terms that are constant in the bracket, the equation becomes:

$$v/e = \frac{k_3 [A] [B]}{Kb [A] + Ka [B] + [A] [B]}$$

Since $Vm = k_3 e$,

$$v = \frac{Vm [A] [B]}{Kb [A] + Ka [B] + [A] [B]}$$

where,

[A] = glucose 1-phosphate concentration

[B] = glucose diphosphate concentration

The above is the general form of the rate equation for an enzyme following a Ping-Pong reaction mechanism in the absence of inhibition. Rearranging this equation to show [B] as the varied substrate (glucose diphosphate):

$$v = \frac{Vm [B]}{Kb + Ka [B] / [A] + [B]}$$

$$= \frac{Vm [B]}{(1 + Ka /[A]) [B] + Kb}$$

Expressing this equation in the form of the double reciprocal plot it becomes:

$$\frac{1}{v} = \left(\beta + \frac{Ka}{[A]} \right) \frac{1}{Vm} + \frac{Kb}{Vm} \cdot \frac{1}{[B]}$$

This equation predicts that in the absence of competitive inhibitors, the slope of a double reciprocal plot for a Ping-Pong reaction mechanism will remain constant, equal to Kb/Vm, but the intercept on the 1/v axis will change with the concentration of the fixed substrate used (here glucose 1-phosphate or [A]). A characteristic feature of the plots will be parallel lines.

APPENDIX II

Derivation of the rate equation for the model in figure 8 describing the Ping-Pong mechanism of phosphoglucomutase in the presence of inhibition due to vanadate.

The model of Figure 8 can be described by 12 open patterns of (n-1) sides where 'n' refers to the number of enzyme intermediates. Referring to Figure 8 the 12 patterns from which the distribution equations for the intermediates in the scheme can be obtained are as follows:

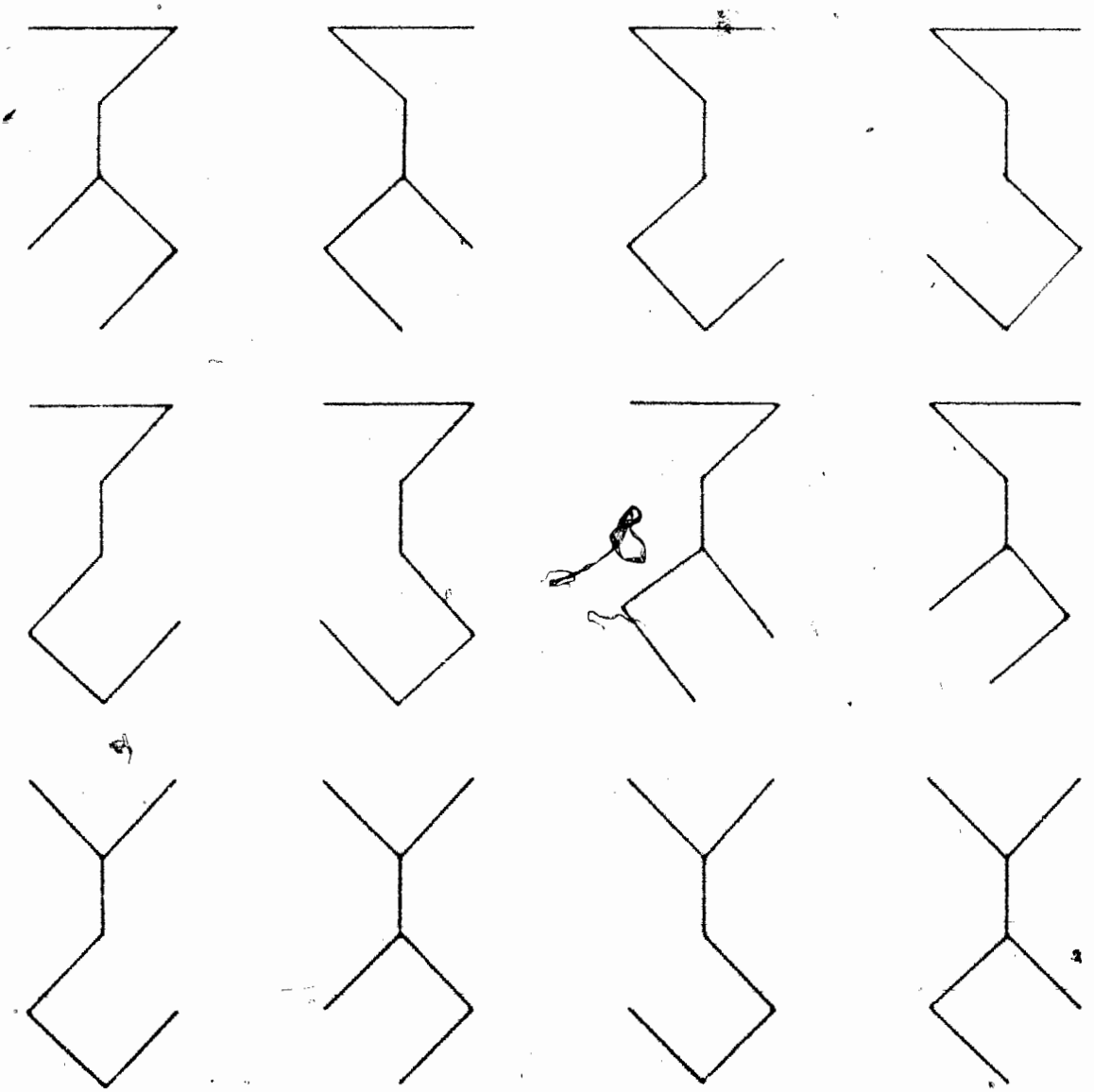

The distribution equations for the intermediates appearing in the model obtained using the twelve open patterns above are:

1) $$E/e = k_{14}\,k_{11}\,k_2\,k_3\,k_5[C]\,k_1 + k_{14}\,k_{11}\,k_2\,k_3\,k_4\,k_6[A] + k_{13}\,k_{11}\,k_2\,k_3\,k_4\,k_6[A] + k_{14}[A]\,k_{12}\,k_2\,k_3\,k_5[C] + k_{13}\,k_{11}\,k_2\,k_3\,k_5[C]\,k_1 + k_{13}\,k_{11}\,k_2\,k_4\,k_6[A]\,k_1 + k_{14}[A]\,k_{12}\,k_2\,k_3\,k_5[C]\,k_1 + k_{14}[A]\,k_{12}\,k_2\,k_4\,k_6[A]\,k_1 + k_{12}\,k_{11}\,k_2\,k_4\,k_6[A]\,k_1 + k_{12}\,k_{11}\,k_2\,k_4\,k_5\,k_7[C] + k_{13}\,k_{11}\,k_2\,k_4\,k_5\,k_7[C] + k_{14}[A]\,k_{12}\,k_2\,k_4\,k_5\,k_7[C] + k_{14}[A]\,k_{12}\,k_2\,k_4\,k_6[A]$$

when $[C] = 0$

$$E/e = [A]\,k_2\,k_4\,k_6\,k_{11}(k_3\,k_{12} + k_3\,k_{13} + k_5\,k_{13} + k_5\,k_{14}) + [A]^2\,k_2\,k_4\,k_6\,k_{12}\,k_{14}(k_3 + k_5)$$

$$E/e = coef_E[A] + coef_E[A]^2$$

2)

$$
\begin{aligned}
EB/e = {} & k_{16}\, k_{11}\, k_1[B]\, k_9\, k_7[C]\, k_5 \\
& + k_{16}\, k_{11}\, k_1[B]\, k_9\, k_4\, k_6[A] \\
& + k_{13}\, k_{11}\, k_1[B]\, k_9\, k_4\, k_6[A] \\
& + k_{14}[A]\, k_{16}\, k_1[B]\, k_9\, k_4\, k_7[C] \\
& + k_{13}\, k_{11}\, k_1[B]\, k_9\, k_7[C]\, k_5 \\
& + k_{13}\, k_{11}\, k_1[B]\, k_4\, k_6[A]\, k_5 \\
& + k_{14}[A]\, k_{16}\, k_1[B]\, k_9\, k_7[C]\, k_5 \\
& + k_{14}[A]\, k_{16}\, k_1[B]\, k_4\, k_6[A]\, k_5 \\
& + k_{16}\, k_{11}\, k_1[B]\, k_4\, k_6[A]\, k_5 \\
& + k_{16}\, k_{11}\, k_1[B]\, k_9\, k_4\, k_7[C] \\
& + k_{13}\, k_{11}\, k_1[B]\, k_4\, k_9\, k_7[C] \\
& + k_{14}[A]\, k_{16}\, k_1[B]\, k_9\, k_4\, k_6[A]
\end{aligned}
$$

when $[C] = 0$

$$
\begin{aligned}
EB/e = {} & [A][B]\, k_1\, k_4\, k_6\, k_{11}(k_9\, k_{16}\, k_9\, k_{13} + k_5\, k_{13} + k_5\, k_{16}) \\
& + [A]^2[B]\, k_1\, k_4\, k_6\, k_{14}\, k_{16}(k_5 + k_9)
\end{aligned}
$$

$$
EB/e = \mathrm{coef}_{EB}[A][B] + \mathrm{coef}_{EB}[A]^2[B]
$$

3)

$$
\begin{aligned}
EI/e = {} & k_{16}\, k_{12}[I]\, k_2\, k_9\, k_7[C]\, k_5 \\
& + k_{16}\, k_{12}[I]\, k_2\, k_9\, k_4\, k_6[A] \\
& + k_{13}\, k_{12}[I]\, k_2\, k_9\, k_4\, k_6[A] \\
& + k_{13}\, k_{15}[AI]\, k_2\, k_4\, k_9\, k_7[C] \\
& + k_{13}\, k_{12}[I]\, k_2\, k_9\, k_7[C]\, k_5 \\
& + k_{13}\, k_{12}[I]\, k_2\, k_4\, k_6[A]\, k_5 \\
& + k_{13}\, k_{15}[AI]\, k_2\, k_9\, k_7[C]\, k_5 \\
& + k_{13}\, k_{15}[AI]\, k_2\, k_4\, k_6[A]\, k_5 \\
& + k_{16}\, k_{12}[I]\, k_2\, k_4\, k_6[A]\, k_5 \\
& + k_{16}\, k_{12}[I]\, k_2\, k_4\, k_9\, k_7[C] \\
& + k_{13}\, k_{12}[I]\, k_{12}\, k_4\, k_9\, k_7[C] \\
& + k_{13}\, k_{15}[AI]\, k_2\, k_9\, k_4\, k_6[A]
\end{aligned}
$$

when $[C] = 0$

$$
\begin{aligned}
EI/e = {} & [A][I]\, k_2\, k_4\, k_6\, k_{12}(k_9\, k_{16} + k_9\, k_{13} + k_5\, k_{13} + k_5\, k_{16}) \\
& + [AI][A]\, k_2\, k_4\, k_6\, k_{13}\, k_{15}(k_5 + k_9)
\end{aligned}
$$

$$
EI/e = \mathrm{coef}_{EI}[A][I] + \mathrm{coef}_{EI}[AI][A]
$$

4)

$$
\begin{aligned}
EAI/e = {} & k_{15}[AI]\ k_{11}\ k_2\ k_9 - k_7[C]\ k_5 \\
& + k_{15}[AI]\ k_{11}\ k_2\ k_9\ k_4\ k_6[A] \\
& + k_{14}[A]\ k_{12}[I]\ k_2\ k_9\ k_4\ k_6[A] \\
& + k_{14}[A]\ k_{15}[AI]\ k_2\ k_9\ k_4\ k_7[C] \\
& + k_{14}[A]\ k_{12}[I]\ k_2\ k_9\ k_7[C]\ k_5 \\
& + k_{14}[A]\ k_{12}[I]\ k_2\ k_4\ k_6[A]\ k_8 \\
& + k_{14}[A]\ k_{15}[AI]\ k_2\ k_9\ k_7[C]\ k_5 \\
& + k_{14}[A]\ k_{15}[AI]\ k_2\ k_4\ k_6[A]\ k_8 \\
& + k_{15}[AI]\ k_{11}\ k_2\ k_4\ k_6[A]\ k_8 \\
& + k_{15}[AI]\ k_{11}\ k_2\ k_9\ k_4\ k_7[C] \\
& + k_{14}[A]\ k_{12}[I]\ k_2\ k_4\ k_9\ k_7[C] \\
& + k_{14}[A]\ k_{15}[AI]\ k_2\ k_9\ k_4\ k_6[A]
\end{aligned}
$$

when $[C] = 0$

$$
\begin{aligned}
EAI/e = {} & [AI][A]\ k_2\ k_4\ k_6\ k_{11}\ k_{15}(k_8\ k_9) \\
& + [A]^2[I]\ k_2\ k_4\ k_6\ k_{12}\ k_{14}(k_8 + k_9) \\
& + [A]^2[AI]\ k_2\ k_4\ k_6\ k_{14}\ k_{15}(k_8 + k_9)
\end{aligned}
$$

$$EAI/e = coef_{EAI}[AI][A] + coef_{EAI}[A]^2[I] + coef_{EAI}[A]^2[AI]$$

5)

$$EPC/e = k_{16}\, k_1[B]\, k_{11}\, k_{10}\, k_7[C]\, k_5 + k_{16}\, k_{11}\, k_1[B]\, k_{10}\, k_6[A]\, k_4 + k_{13}\, k_{11}\, k_1[B]\, k_{10}\, k_6[A]\, k_4 + k_{14}[A]\, k_{16}\, k_1[B]\, k_{10}\, k_4\, k_7[C] + k_{13}\, k_{11}\, k_1[B]\, k_{10}\, k_7[C]\, k_5 + k_{13}\, k_{11}\, k_1[B]\, k_3\, k_5\, k_7[C] + k_{14}[A]\, k_{16}\, k_1[B]\, k_{10}\, k_7[C]\, k_5 + k_{14}[A]\, k_{16}\, k_1[B]\, k_3\, k_5\, k_7[C] + k_{16}\, k_{11}\, k_1[B]\, k_3\, k_5\, k_7[C] + k_{16}\, k_{11}\, k_1[B]\, k_4\, k_{10}\, k_7[C] + k_{13}\, k_{11}\, k_1[B]\, k_4\, k_{10}\, k_7[C] + k_{14}[A]\, k_{16}\, k_1[B]\, k_{10}\, k_4\, k_6[A]$$

when $[C] = 0$

$$EPC/e = [A][B]\, k_1\, k_4\, k_6\, k_{10}\, k_{11}(k_{13} + k_{16}) + [A]^2[B]\, k_1\, k_4\, k_6\, k_{10}\, k_{14}\, k_{16}$$

$$EPC/e = coef_{EPC}[A][B] + coef_{EPC}[A]^2[B]$$

6)

$$EPA/e = k_{16}\, k_{11}\, k_1[B]\, k_{10}\, k_8\, k_6[A] + k_{16}\, k_{11}\, k_1[B]\, k_9\, k_3\, k_6[A] + k_{11}\, k_{13}\, k_1[B]\, k_9\, k_3\, k_6[A] + k_{14}[A]\, k_{16}\, k_1[B]\, k_3\, k_7[C]\, k_9 + k_{13}\, k_{11}\, k_1[B]\, k_{10}\, k_8\, k_6[A] + k_{13}\, k_{11}\, k_1[B]\, k_3\, k_8\, k_6[A] + k_{14}[A]\, k_{16}\, k_1[B]\, k_{10}\, k_8\, k_6[A] + k_{14}[A]\, k_{16}\, k_1[B]\, k_3\, k_8\, k_6[A] + k_{16}\, k_{11}\, k_1[B]\, k_3\, k_8\, k_6[A] + k_{16}\, k_{11}\, k_1[B]\, k_7[C]\, k_9\, k_3 + k_{13}\, k_{11}\, k_1[B]\, k_3\, k_7[C]\, k_9 + k_{14}[A]\, k_{16}\, k_1[B]\, k_9\, k_3\, k_6[A]$$

when $[C] = 0$

$$EPA/e = [A][B]\, k_1\, k_6\, k_{11}(k_8\, k_{10}\, k_{16} + k_3\, k_9\, k_{16} + k_3\, k_9\, k_{13} + k_8\, k_{10}\, k_{13} + k_3\, k_8\, k_{13} + k_3\, k_8\, k_{16}) + [A]^2[B]\, k_1\, k_6\, k_{14}\, k_{16}(k_8\, k_{10} + k_3\, k_8 + k_3\, k_9)$$

$$EPA/e = coef_{EPA}[A][B] + coef_{EPA}[A]^2[B]$$

7)

$$EP/e = k_{11}\,k_{16}\,k_1[B]\,k_{10}\,k_8\,k_5 + k_{16}\,k_{11}\,k_1[B]\,k_9\,k_3\,k_5 + k_{13}\,k_{11}\,k_1[B]\,k_9\,k_3\,k_5 + k_{14}[A]\,k_{16}\,k_1[B]\,k_4\,k_{10}\,k_8 + k_{13}\,k_{11}\,k_1[B]\,k_{10}\,k_8\,k_5 + k_{13}\,k_{11}\,k_1[B]\,k_3\,k_5\,k_8 + k_{14}[A]\,k_{16}\,k_1[B]\,k_{10}\,k_8\,k_5 + k_{14}[A]\,k_{16}\,k_1[B]\,k_3\,k_5\,k_8 + k_{16}\,k_{11}\,k_1[B]\,k_3\,k_5\,k_8 + k_{16}\,k_{11}\,k_1[B]\,k_4\,k_{10}\,k_8 + k_{13}\,k_{11}\,k_1[B]\,k_4\,k_{10}\,k_8 + k_{14}[A]\,k_{16}\,k_1[B]\,k_9\,k_3\,k_5$$

when[C] = 0

$$EP/e = [B]\,k_1\,k_{11}(k_5\,k_8\,k_{10}\,k_{16} + k_3\,k_5\,k_9\,k_{16} + k_3\,k_5\,k_9\,k_{13} + k_5\,k_8\,k_{10}\,k_{13} + k_3\,k_5\,k_8\,k_{13} + k_3\,k_5\,k_8\,k_{16} + k_4\,k_8\,k_{10}\,k_{16} + k_4\,k_8\,k_{10}\,k_{13}) + [A][B]\,k_1\,k_{14}\,k_{16}(k_4\,k_{10}\,k_8 + k_4\,k_{10}\,k_8 + k_5\,k_8\,k_{10} + k_3\,k_5\,k_8 + k_3\,k_5\,k_9)$$

$$EP/e = coef_{EP}[B] + coef_{EP}[A][B]$$

Since the rate of the reaction is given by

$$v = k_s[EPC]$$

and the conservation equation is

$$e = [E] + [EB] + [EI] + [EAI] + [EPC] + [EPA] + [EP]$$

then

$$v/e = k_s[EPC]/\ e$$

$$= \frac{k_s[EPC]}{[E] + [EB] + [EI] + [EAI] + [EPC] + [EPA] + [EP]}$$

$$v/e = \frac{k_s coef_{EPC}[A][B] + coef_{EPC}[A]^2[B]}{coef_E[A] + coef_E[A]^2 + coef_{EB}[A][B]}$$

$$+ coef_{EB}[A]^2[B]$$

$$+ coef_{EI}[A][I] + coef_{EI}[AI][A]$$

$$+ coef_{EAI}[AI][A] + coef_{EAI}[A]^2[I]$$

$$+ coef_{EAI}[A]^2[AI] + coef_{EPC}[A][B]$$

$$+ coef_{EPC}[A]^2[B] + coef_{EPA}[A][B]$$

$$+ coef_{EPA}[A]^2[B]$$

$$+ coef_{EP}[B] + coef_{EP}[A][B]$$

Dividing the terms of the numerator and denominator of the above equation by $coef_{EPC}$, where this equals, $coef_{EPC}[B][A](1 + [A])$, the terms become:

1) $$\frac{coef_E}{coef_{EPC}} = \frac{coef_E[A] + coef_E[A]^2}{coef_{EPC}[A][B] + coef_{EPC}[A]^2[B]}$$

rearranging,

$$= \frac{coef_E[A]\ (1 + [A])}{coef_{EPC}[B][A]\ (1 + [A])}$$

$$= \frac{coef_E}{coef_{EPC}[B]}$$

$$= \frac{Kb}{[B]}$$

2) $$\frac{coef_{EB}}{coef_{EPC}} = \frac{coef_{EB}[A][B] + coef_{EB}[A]^2[B]}{coef_{EPC}[A][B] + coef_{EPC}[A]^2[B]}$$

rearranging,

$$= \frac{coef_{EB}[A][B](1 + [A])}{coef_{EPC}[A][B](1 + [A])}$$

$$= \frac{coef_{EB}}{coef_{EPC}}$$

$$=$$ a constant

3) $$\frac{coef_{EI} + coef_{EAI}}{coef_{EPC}} = \frac{coef'[A][I] + [A]^2[I]}{coef_{EPC}[B][A]\ (1 + [A])}$$

rearranging,

$$= \frac{coef'[I][A]\ (1 + [A])}{coef_{EPC}[B][A]\ (1 + [A])}$$

$$= \frac{coef'[I]}{coef_{EPC}[B]}$$

$$= \frac{Kb[I]}{[B]K_V}$$

4) $$\frac{(coef_{EI} + coef_{EAI}) + coef_{EAI}}{coef_{EPC}}$$

$$= \frac{(coef_{EI} + coef_{EAI})[AI][A] + coef_{EAI}[A]^2[AI]}{coef_{EPC}}$$

Taking the term in brackets in the numerator as equal to, coef", the above equation can be rearranged as follows:

$$\frac{(coef'' + coef_{EAI})\ [AI][A]\ (1 + [A])}{coef_{EPC}[B][A]\ (1 + [A])}$$

$$= \frac{(coef'' + coef_{EAI})[AI]}{coef_{EPC}[B]}$$

$$= \frac{Kb[AI]}{[B]K_{VP}}$$

5) $$\frac{coef_{EPC} + coef_{EPC}}{coef_{EPC} + coef_{EPC}} = \frac{[B][A]\ (1 + [A])}{[B][A]\ (1 + [A])} = 1$$

$$6)\quad \frac{coef_{EPA}}{coef_{EPC}} = \frac{coef_{EPA}[A][B] + coef_{EPA}[A]^2[B]}{coef_{EPC}[B][A]\ (1 + [A])}$$

rearranging,

$$= \frac{coef_{EPA}[B][A]\ (\ 1 + [A])}{coef_{EPC}[B][A]\ (\ 1 + [A])}$$

$$= \frac{coef_{EPA}}{coef_{EPC}}$$

$$= \text{a constant}$$

$$7)\quad \frac{coef_{EP}}{coef_{EPC}} = \frac{coef_{EP}[B] + coef_{EP}[A][B]}{coef_{EPC}[A][B] + coef_{EPC}[A]^2[B]}$$

rearranging,

$$= \frac{coef_{EP}[B](1 + [A])}{coef_{EPC}[A][B](1 + [A])}$$

$$= \frac{coef_{EP}}{coef_{EPC}[A]}$$

$$= \frac{Ka}{[A]}$$

Taking the definitions 1) through 7) and substituting for them in the previous rate equation it becomes,

$$v = \frac{k_3 e}{\frac{Kb}{[B]} + \frac{Kb[I]}{[B]K_v} + \frac{Kb[AI]}{[B]K_{vp}} + \beta + \frac{Ka}{[A]}}$$

where e = the total enzyme concentration

since $Vm = k_t e$,

$$v = \frac{Vm}{\frac{Kb}{[B]}\left(1 + \frac{[I]}{K_v} + \frac{[AI]}{K_{vp}}\right) + \left(\frac{Ka}{[A]} + \beta\right)}$$

expressing this equation in the form of the double reciprocal plot, where glucose diphosphate [B]is the varied substrate, it becomes,

$$\frac{1}{v} = \frac{Kb}{Vm}\left(1 + \frac{[I]}{K_v} + \frac{[AI]}{K_{vp}}\right)\frac{1}{[B]} + \left(\frac{Ka}{[A]} + \beta\right)\frac{1}{Vm}$$

The terms in this equation are as defined earlier for the model of Figure 8 in the text. The rate equation predicts that in the presence of competitive inhibition due to vanadate acting at the free dephosphoenzyme (E) the slope of a plot of 1/v against 1/[B] will increase. At different vanadate and constant glucose 1-phosphate concentration the expected pattern of the double reciprocal plots should be a series of lines of varying slope converging to a common vertical intercept. The constants c' and c" that are incorporated into the constant β (= 1 + c' + c") have no influence on the values of the kinetic parameters K_v and K_{vp} determined in this study. β does not enter into the slopes of the plots but only into the intercepts.

APPENDIX III

Derivation of an expression for k_{obs}, i.e., the apparent first order rate constant of the time dependent inhibition, in terms of the reaction scheme shown in Figure 16. (After the methods of Strickland et al. 1975 (49) and Abeles et al. 1985 (50). The differential equations describing the reaction scheme are:

$$\frac{d[ES]}{dt} = k_1 [E][S] - k_2 [ES] \qquad \text{Eq. 1}$$

$$\frac{d[E]}{dt} = k_2 [ES] + k_4 [ET] - [E] (k_1 [S] + k_3 [T]) \qquad \text{Eq. 2}$$

$$\frac{d[ET]}{dt} = k_3 [E][T] - k_4 [ET] \qquad \text{Eq. 3}$$

$$[E_{total}] = [ET] + [E] + [ES] \qquad \text{Eq. 4}$$

It is assumed that subsequent to adding vanadate to the already initiated mutase reaction and prior to the attainment of steady-state, the concentration of the free dephosphoenzyme very rapidly reaches a low constant concentration such that

$$\frac{d[E]}{dt} = 0 \qquad \text{Eq. 5}$$

When this is the case the conservation Equation-4 above becomes equal to

$$[E_{total}] = [ES] + [ET] \qquad \text{Eq. 6}$$

Equations 2, 5 and 6 can be combined to provide an expression for [E], the concentration of free dephosphoenzyme in terms of $[E_{total}]$.

When $d[E]/dt = 0$

then

$$[E]\ (k_2\ [S] + k_3\ [T]\ ) = k_1\ [ES] + k_4\ [ET]$$

Upon rearrangement the concentration of free dephosphoenzyme is given by:

$$[E] = \frac{k_1\ [ES] + k_4\ [ET]}{(k_2\ [S] + k_3\ [T])}$$

and since

$$[ES] + [ET] = [E_{total}].$$

$$[E] = \frac{(k_1 + k_4)\ [E_{total}]}{(k_2\ [S] + k_3\ [T])} \qquad \text{Eq. 7}$$

Substituting for [E] above in Equation 3 and rearranging gives Equation 8 below:

$$\frac{d[ET]}{dt} + \left(\frac{k_2\ (k_3 - k_4)\ [T]}{k_2\ [S] + k_3\ [T]} + k_4 \right)\ [ET] - \frac{k_2\ k_3\ [T]\ [E_{total}]}{k_2\ [S] + k_3\ [T]} = 0$$

This equation has the form:

$$\frac{d[ET]}{dt} + \alpha[ET] - \beta = 0 \qquad \text{Eq. 9}$$

with solution

$$[ET] = \frac{\beta}{\alpha}\ e^{-\alpha t} + \frac{\beta}{\alpha} \qquad \text{Eq. 9a}$$

Rearranging Equation 9a and taking natural logs gives:

$$\ln(\beta/\alpha - [ET]) = -\alpha t \ln\beta/\alpha \qquad \text{Eq. 9b}$$

From Equation 8,

β/α = final equilibrium concentration of [ET]

and

$$\alpha = k_{obs} = \left(\frac{k_3 (k_2 - k_4)\,[T]}{k_1 [S] + k_2 [T]} + k_4 \right) \qquad \text{Eq. 10}$$

Equation 10 describes the apparent first order rate constant in terms of the concentrations of [S] = glucose diphosphate and [T] = the inhibitor glucose 1-phosphate 6-vanadate and the specific rate constants of the individual steps in the model of Figure 16. Equation 9b describes the form of the semi-log plots used in the progress curve analysis, i.e. $\ln (A_\infty - A_t) = -kt \ln A_\infty$, a plot of $\ln (A_\infty - A_t)$ against time yields a slope that gives the value of $-k_{obs}$. On rearrangement, Equation 10 becomes:

$$k_{obs} = \frac{k_3 (k_2 - k_4)\,[T] + k_4 (k_1 [S] + k_2 [T])}{k_1 [S] + k_2 [T]} \qquad \text{Eq. 11}$$

Working through the numerator of Equation 11 gives:

$$k_{obs} = \frac{k_2 k_3 [T] + k_1 k_4 [S]}{k_1 [S] + k_3 [T]} \qquad \text{Eq. 12}$$

Dividing the numerator and denominator of Equation 12 by $k_1[S]$, the equation becomes:

$$k_{obs} = \frac{\frac{k_2 k_3 [T]}{k_1 [S]} + k_4}{1 + \frac{k_3 [T]}{k_1 [S]}} \qquad \text{Eq. 13}$$

since

$\frac{k_2}{k_1}$ = K_{ds}, taken to be the Km of the dephosphoenzyme for glucose diphosphate,

the final expression for k_{obs} becomes:

$$k_{obs} = \frac{\frac{k_3 K_{ds} [T]}{[S]} + k_4}{1 + \frac{k_3 [T]}{k_1 [S]}} \qquad \text{Eq. 14}$$

where,

[T] = the inhibitor complex of glucose 1-phosphate 6-vanadate

[S] = glucose diphosphate

The form of Equation 14 will depend on the experimental conditions used to evaluate k_{obs} and the assumptions that can be made under these specific conditions.

In the experiment of Figure 14, k_{obs} was monitored as a function of increasing glucose 1-phosphate concentration i.e., a component of the inhibitor complex [T]. At the glucose diphosphate concentrations employed ≤ Km the apparent rate constant will be influenced by the inhibitor binding step in the model of Figure 16. As the inhibitor concentration increases the pseudo first order rate constant for the association step $k_3[T]$ becomes large with respect to k_4 (k_4 will be small by necessity to account for the low value of K_{vp}) and is assumed to form the major contribution overall to k_{obs}. Hence in the expression for k_{obs} used to analyse the data of this experiment k_4 is dropped, k_{obs} is then given by:

$$k_{obs} = \frac{\frac{k_3 K_{ds} [T]}{[S]}}{1 + \frac{k_3 [T]}{k_1 [S]}} \qquad \text{Eq. 15}$$

In reciprocal form Equation 15 becomes,

$$\frac{1}{k_{obs}} = \frac{1}{\frac{k_3 K_{ds} [T]}{[S]}} + \frac{1}{K_{ds} k_1} \qquad \text{Eq. 16}$$

since $K_{ds} = k_2/k_1$

$$\frac{1}{k_{obs}} = \frac{[S]}{k_3 K_{ds} [T]} + \frac{1}{k_2} \qquad \text{Eq. 17}$$

Equation 17 predicts that under the experimental conditions used here and taking account of the assumptions made that a plot of

$$\frac{1}{k_{obs}} \quad \text{against} \quad \frac{1}{[T]}$$

will be linear with the slope given by

$$\frac{[S]}{k_3 K_{ds}}$$

and an intercept on the vertical axis of,

$$\frac{1}{k_2}$$

where,

k_3 = specific rate constant for the step in the reaction scheme of Figure 16, involving the dissociation of glucose diphosphate from its complex with the dephosphoenzyme on the main mutase reaction path.

Intuitively this seems a reasonable result i.e., inhibition at high inhibitor concentrations limited by the rate of appearance of free dephosphoenzyme (E) off the main reaction path. This is also consistent with what is known of the phosphoglucomutase reaction in the literature, principally an infrequent dissociation of the complex of dephosphoenzyme with glucose diphosphate to the free components, estimated previously at around once every twenty catalytic turnovers (30).

APPENDIX IV

Derivation of the rate equation for the model shown in Figure 19 describing the Ping-Pong mechanism of phosphoglucomutase in the presence of inhibition due to vanadate and glucose 6-vanadate. The model of Figure 19 can be described by four open patterns of (n-1) sides, where 'n' refers to the number of enzyme intermediates. Referring to Figure 19 the four patterns from which the distribution equations for the intermediates in the scheme can be obtained are as follows:

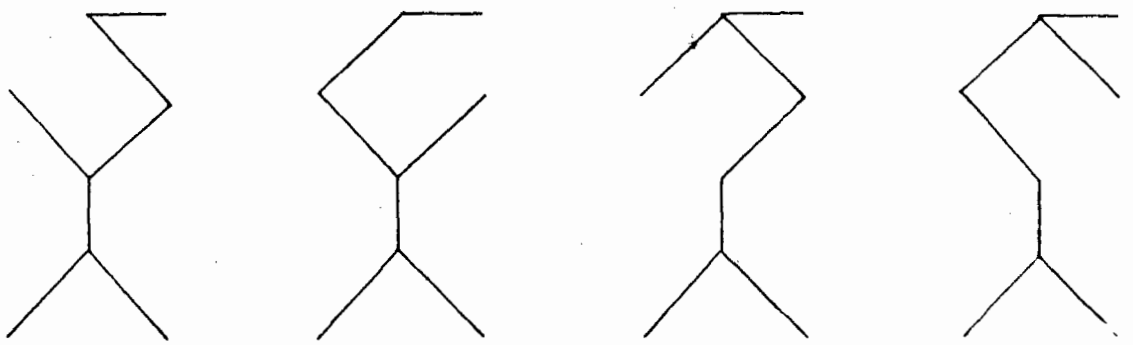

The distribution equations for the intermediates appearing in the model obtained using the four open patterns above are:

1) $$EP/e = k_{15}\, k_5\, k_3\, k_9\, k_1\, [B]\, k_{11}\, k_{13} + k_{15}\, k_4\, k_{10}\, k_8\, k_1\, [B]\, k_{13}\, k_{11} + k_{15}\, k_5\, k_6\, k_3\, k_2\, [B]\, k_{11}\, k_{14} + k_{15}\, k_5\, k_9\, k_{10}\, k_1\, [B]\, k_{13}\, k_{11}$$

$$EP/e = k_1\, [B]\, k_3\, k_5\, k_{11}\, k_{13}\, k_{15}\, (k_8 + k_9) + k_1\, [B]\, k_8\, k_{10}\, k_{11}\, k_{13}\, k_{15}\, (k_4 + k_5)$$

$$= k_1\, [B]\, k_{11}\, k_{13}\, k_{15}\, [\, k_3\, k_5\, (k_8 + k_9) + k_8\, k_{10}\, (k_4 + k_5)\,]$$

when [C] = 0

$$EP/e = coefEP\ [B]$$

2) $$EPC/e = k_{10}\, k_4\, k_6\, [A]\, k_{15}\, k_1\, [B]\, k_{11}\, k_{13} + k_{10}\, k_4\, k_7\, [C]\, k_{15}\, k_1\, [B]\, k_{11}\, k_{13} + k_7\, [C]\, k_{15}\, k_5\, k_3\, k_1\, [B]\, k_{11}\, k_{13} + k_{10}\, k_7\, [C]\, k_5\, k_{15}\, k_1\, [B]\, k_{11}\, k_{13}$$

when [C] = 0

$$EPC/e = k_1\, [B]\, k_4\, k_6\, [A]\, k_{10}\, k_{11}\, k_{13}\, k_{15} = \text{coefEPC}\ [A][B]$$

3) $$EPA/e = k_{15}\, k_4\, [A]\, k_3\, k_9\, k_1\, [B]\, k_{11}\, k_{13} + k_{15}\, k_7\, [C]\, k_9\, k_3\, k_1\, [B]\, k_{11}\, k_{13} + k_{15}\, k_8\, k_6\, [A]\, k_3\, k_1\, [B]\, k_{11}\, k_{13} + k_{15}\, k_6\, [A]\, k_8\, k_{10}\, k_1\, [B]\, k_{11}\, k_{13}$$

when [C] = 0

$$EPA/e = k_{15}\, k_6\, [A]\, k_3\, k_1\, [B]\, k_{11}\, k_{13}\, (k_8 + k_9) + k_{15}\, k_6\, [A]\, k_8\, k_{10}\, k_1\, [B]\, k_{11}\, k_{13}$$

$$EPA/e = k_1\, [B]\, k_6\, [A]\, k_{11}\, k_{13}\, k_{15}\, [\, k_3\, (\, k_8 + k_9) + k_8\, k_{10}] = \text{coefEPA}\ [A][B]$$

4) $$EB/e = k_{15}\, k_6\, [A]\, k_4\, k_9\, k_1\, [B]\, k_{11}\, k_{13} + k_{15}\, k_7\, [C]\, k_9\, k_4\, k_1\, [B]\, k_{11}\, k_{13} + k_{15}\, k_8\, k_6\, [A]\, k_4\, k_1\, [B]\, k_{11}\, k_{13} + k_{15}\, k_5\, k_7\, [C]\, k_9\, k_1\, [B]\, k_{11}\, k_{13}$$

when [C] = 0

$$EB/e = k_1\,[B]\,k_4\,k_6\,[A]\,k_{11}\,k_{13}\,k_{15}\,(k_8 + k_9)$$
$$= \text{coefEB}\,[A][B]$$

5)
$$E/e = k_{15}\,k_6\,[A]\,k_4\,k_9\,k_2\,k_{11}\,k_{13}$$
$$+ k_{15}\,k_7\,[C]\,k_9\,k_4\,k_2\,k_{11}\,k_{13}$$
$$+ k_{15}\,k_8\,k_6\,[A]\,k_4\,k_2\,k_{11}\,k_{13}$$
$$+ k_{15}\,k_5\,k_7\,[C]\,k_9\,k_2\,k_{11}\,k_{13}$$

when [C] = 0

$$E/e = k_2\,k_4\,k_6\,[A]\,k_{11}\,k_{13}\,k_{15}\,(k_8 + k_9)$$
$$= \text{coefE}\,[A]$$

6)
$$EAI/e = k_{16}\,[D]\,k_5\,k_3\,k_9\,k_1\,[B]\,k_{11}\,k_{13}$$
$$+ k_{16}\,[D]\,k_8\,k_{10}\,k_4\,k_1\,[b]\,k_{11}\,k_{13}$$
$$+ k_{16}\,[D]\,k_8\,k_5\,k_3\,k_1\,[B]\,k_{11}\,k_{13}$$
$$+ k_{16}\,[D]\,k_5\,k_8\,k_{10}\,k_1\,[B]\,k_{11}\,k_{13}$$

when [C] = 0

$$EAI/e = k_1\,[B]\,k_3\,k_5\,k_{11}\,k_{13}\,k_{16}\,[D]\,(k_8 + k_9)$$
$$+ k_1\,[B]\,k_8\,k_{10}\,k_{11}\,k_{13}\,k_{16}\,[D]\,(k_4 + k_5)$$
$$= k_1\,[B]\,k_{11}\,k_{13}\,k_{16}\,[D]\,[k_3\,k_5\,(k_8 + k_9) + k_8\,k_{10}\,(k_4 + k_5)]$$

$$EAI/e = \text{coefEAI}\,[B][D]$$

7)
$$EI/e = k_{15}\,k_6\,[A]\,k_4\,k_9\,k_2\,k_{13}\,k_{12}\,[I]$$
$$+ k_{15}\,k_7\,[C]\,k_9\,k_4\,k_2\,k_{13}\,k_{12}\,[I]$$
$$+ k_{15}\,k_8\,k_6\,[A]\,k_4\,k_2\,k_{13}\,k_{12}\,[I]$$
$$+ k_{15}\,k_5\,k_7\,[C]\,k_9\,k_2\,k_{13}\,k_{12}\,[I]$$

when [C] = 0

$$EI/e = k_2\, k_4\, k_6\, [A]\, k_{12}\, [I]\, k_{13}\, k_{15}\, (k_8 + k_9)$$
$$= \text{coefEI}\ [A][I]$$

8) $$ED/e = k_{15}\, k_6\, [A]\, k_4\, k_9\, k_2\, k_{11}\, k_{14}\, [D] + k_{15}\, k_7\, [C]\, k_9\, k_4\, k_2\, k_{11}\, k_{14}\, [D] + k_{15}\, k_8\, k_6\, [A]\, k_4\, k_2\, k_{11}\, k_{14}\, [D] + k_{15}\, k_5\, k_7\, [C]\, k_9\, k_2\, k_{11}\, k_{14}\, [D]$$

when [C] = 0

$$ED/e = k_2\, k_4\, k_6\, [A]\, k_{11}\, k_{14}\, [D]\, k_{15}\, (k_8 + k_9)$$
$$= \text{coefED}\ [A][D]$$

Since the rate of the reaction is given by

$$v = k_8\, [EPC]$$

and the conservation equation is

$$e = [EP] + [EPC] + [EPA] + [EB] + [E] + [EAI] + [EI] + [ED]$$

then

$$\frac{v}{e} = \frac{k_8\, [EPC]}{[EP] + [EPA] + [EPC] + [EB] + [E] + [EAI] + [EI] + [ED]}$$

Dividing the numerator and denominator by [EPC], the terms become:

a) $$\frac{\text{coefEP}}{\text{coefEPC}} \cdot \frac{[B]}{[A][B]} = \frac{\text{coefEP}}{\text{coefEPC}} \cdot \frac{1}{[A]} \left(\frac{\text{coefEP}}{\text{coefEPC}} \right) = Ka$$

$$\frac{\text{coefEP}}{\text{coefEPC}} \cdot \frac{[B]}{[A][B]} = \frac{Ka}{[A]}$$

b) $$\frac{coefEPC}{coefEPC} = 1$$

c) $$\frac{coefEPA}{coefEPC} \cdot \frac{[A][B]}{[A][B]} = \text{constant} = c'.$$

d) $$\frac{coefEB}{coefEPC} \cdot \frac{[A][B]}{[A][B]} = \text{constant} = c''.$$

e) $$\frac{coefE}{coefEPC} \cdot \frac{[A]}{[A][B]} = \frac{coefE}{coefEPC} \cdot \frac{1}{[B]}$$

$$\frac{coefE}{coefEPC} = \frac{k_2 (k_8 + k_9)}{k_1 k_{10}} = Kb$$

$$= \frac{coefE}{coefEPC} \cdot \frac{[A]}{[A][B]} = \frac{Kb}{[B]}$$

f) $$\frac{coefEAI}{coefEPC} \cdot \frac{[B][D]}{[A][B]} = \frac{coefEAI}{coefEPC} \cdot \frac{[D]}{[A]}$$

$$\frac{coefEAI}{coefEPC} = \frac{Ka}{Kgv^*}$$

$$\frac{coefEAI}{coefEPC} \cdot \frac{[D]}{[A]} = \frac{Ka\ [D]}{[A]\ Kgv^*}$$

g) $$\frac{coefEI}{coefEPC} \cdot \frac{[A][I]}{[A][B]} = \frac{coefEI}{coefEPC} \cdot \frac{[I]}{[B]}$$

$$\frac{coefEI}{coefEPC} \frac{[I]}{[B]} = \frac{Kb}{[B]} \cdot \frac{[I]}{Kv}$$

h) $$\frac{coefED}{coefEPC}\,\frac{[A][D]}{[A][B]} = \frac{coefED}{coefEPC}\,\frac{[D]}{[B]}$$

$$\frac{coefED}{coefEPC}\,\frac{[D]}{[B]} = \frac{Kb}{[B]}\cdot\frac{[D]}{Kgv}$$

Substituting for the terms a) through to h) in the previous rate equation, gives:

$$v/e = \frac{k_1}{\dfrac{[EP] + [EPA] + [EPC] + [EB] + [E] + [EAI] + [EI] + [ED]}{[EPC]}}$$

$$v = \frac{Vm}{\dfrac{Ka}{[A]} + \dfrac{Ka}{[A]}\dfrac{[D]}{Kgv^*} + \beta + \dfrac{Kb}{[B]} + \dfrac{Kb[I]}{[B]Kv} + \dfrac{Kb[D]}{[B]Kgv}}$$

Taking the reciprocals of this equation and expressing it in the form of the Lineweaver-Burke plot in which glucose-diphosphate is the varied substrate([B]) it becomes,

$$1/v = \left[\frac{Ka}{[A]}\left(1 + \frac{[D]}{Kgv^*}\right) + \beta\right]\frac{1}{Vm} + \frac{Kb}{Vm}\left(1 + \frac{[I]}{Kv} + \frac{[D]}{Kgv}\right)\frac{1}{[B]}$$

The rate equation predicts that in the presence of competitive inhibition at the free dephosphoenzyme (E) due to vanadate [I] and glucose 6-vanadate [D] the slope of a plot of 1/v against 1/[B] will increase. For glucose 6-vanadate [D] acting as a competitive inhibitor of the phosphoenzyme (EP), the effect of increasing glucose concentration will be to cause an increase in the value of the vertical intercept of the 1/v against 1/[B] plot. Although the constants c' and c" will appear in the intercept term, in the replot of the intercepts vs glucose concentration, they again enter only into the y-intercept of the replot and it is the slope that yields the desired information i.e. K_{gv^*} and are considered thus to have no influence upon the value of this parameter.

REFERENCES

1. Ramasarma, T., Crane, F.L., (1981) Current Topics in Cell. Reg. 20, p. 247.

2. Simons, T.J.B., (1979) Nature (London) 281, p. 337.

3. Macara, I.G., (1980) Trends Biochem. Sci. 5, p. 92.

4. Cotton, F.A., Wilkinson, A., (1972) Advanced Inorganic Chemistry 3rd Edition, John Wiley & Sons, New York

5. Nicholls, D., (1979) Complexes and First Row Transition Elements, Macmillan Press, London.

6. Clarke, R.J.H., (1968) The Chemistry of Titanium and Vanadium, An Introduction to the Chemistry of the Early Transition Elements, Elsevier Publishing Co., New York.

7. Lindquist, R.N., Lynn, J.L., and Lienhard, G.E., (1973) J. Am. Chem. Soc. 95, p. 8762.

8. Murmann, R.K., (1977) Inorg. Chem. 16, p. 46.

9. Pope, M.T., Dale, B.W., (1968) Chem. Soc. Lond. Quart. Rev. 22, p. 527.

10. Jameson, J.L., Cohen, H.J., and Rajagopalan, K.V., (1974) Biochem. Biophys. Res. Commun. 56, p. 940.

11. Cantley, L.C., Jr., and Aisen, P. (1979) J. Biol. Chem. 254, p. 1781.

12. Medda, P., Hasselbach, W., (1983). Eur. J. Biochem. 137, p. 7.

13. Willsky, A.R., White, D.A., McCabe, B.C., (1984) J. Biol. Chem. 259, p. 13273

14. Macara, I.G., Kustin, K., and Cantley, L.C., Jr., (1980) Biochem. Biophys. Acta 629, p. 95.

15. Harris, W.R., Friedman, S.B., Silberman, D., (1984) J. Inorg. Biochem. 20, p. 157.

16. Craig, M.C., (1986) MSc. Thesis, Simon Fraser University.

17. Lagunas, R., (1980) Arch. Biochem. Biophys. 225, p. 67

18. Long, J.W., Ray, W.J., (1973) Biochem. 12, p. 3932.

19. Gresser, M.J., Tracey, A.S., (1984) J. Am. Chem. Soc. 107, p. 4215.

20. Layne, P.P., Najjar, V.A., (1979) Proc. Natl. Acad. Sci. 107, p. 4215.

21. Ninfalli, P., Accorsi, A., Fazi, A., Palwa, F., Fornaini, G., (1983) Arch. Biochem. Biophys. 226, p. 441.

22. Carreras, J., Bartrons, R., Grisolia, S., (1980) Biochem. Biophys. Res. Commun. 96, p. 1267.

23. Lopez, V., Stevens, T., Lindquist, R.N., (1976) Arch. Biochem. Biophys. 175, p. 31.

24. Knowles, J.R., (1980) Ann. Rev. Biochem. 49, p. 877.

25. Ray, W.J., Peck, E.J., (1973) The Enzymes, 3rd Ed., P.Boyer, (Ed.) 6, Chapter 12, p. 407, Academic Press, New York.

26. Britton, H.G., Clark, J.B., (1968) Biochem. J. 110, p.161.

27. Lowe, G., Potter, B.V.L., (1981) Biochem. J. 199, p. 693.

28. Newman, L., LaFleur, W.G., Brousaides, F.J., Ross, A.M. (1958).

29. Lowry, O.H., Rosebrough, N.J., Farr, A.L., Randall, R.J.,(1951) J. Biol. Chem. 193 P. 265.

30. Ray, W.J., Roscelli, G.A., (1964) J. Biol. Chem. 239, p. 1228.

31. Walsh, C., (1979) Enzymatic Reaction Mechanism, Freeman, San Fransisco.

32. Segel, I.H. (1975) Behaviour and Analysis of Rapid Equilibrium and Steady State Enzyme Systems, John Wiley and Sons, New York.

33. Ray, W.J., Roscelli, G.A., Kirkpatrick, D.S. (1966) J. Biol. Chem. 241 p. 2603.

34. Ray, W.J., Roscelli, G.A. (1966) J. Biol. Chem. 241, p. 2596.

35. Carreras, J., Climent, F., Bartrons, R., Pons, G. (1982) Biochem. Biophys. Acta 705, p. 238.

36. Cha, S., (1975) Biochem. Pharmacol. 24, p. 2177.

37. Williams, J.W., Morrison, J.F., (1979) Methods in Enzymology 63, p. 437.

38. Hatfield, W.G., Ray, W.J., and Umbarger, E.H., (1970) J. Biol. Chem. 245, p. 1748.

39. Cha, S., (1976) Biochem. Pharmacol. 25, p. 2695.

40. Jencks, W.P., (1969) Catalysis in Chemistry and Enzymology, McGraw-Hill, New York.

41. Ferscht., A. (1977). Enzyme Structure and Mechanism, p. 250. W.H. Freeman and Co., New York.

42. Morrison, J.F., (1982) Trends. Biochem. Sci. 7, p. 102.

43. Baici, A., Gygermarazzi, M., (1982) Eur. J. Biochem. 129, p. 33.

44. Long, J.W., Ray, W.J., Jr., (1976). Biochem. 18, p. 3999.

45. Long, J.W., Ray, W.J., Jr., (1968). Biochem. 7, p. 152.

46. Ray, W.J., Jr., Mildvan, A.S., and Long, J.W., (1973). Biochem. 19, p. 3724.

47. Ray, W.J., Jr., Mildvan, A.S., (1973). Biochem. 19, p. 3733.

48. Frick, L., Wolfenden, R., Smal, E., Baker, D.C., (1985) Biochem. 25, p. 1616.

49. Strickland, S., Palmer, G., Massey, V., (1975). J. Biochem. 250, p. 4048.

50. Nakamura, C.E., Abeles, R.H. (1985). Biochem. 24, p. 1364.